Veröffentlichungen der Schweizerischen Meteorologischen Anstalt
Publications de l'Institut Suisse de Météorologie
Pubblicazioni della Centrale Meteorologica Svizzera

1991

49

ITAM-90

21. INTERNATIONALE TAGUNG FUER ALPINE METEOROLOGIE

Engelberg
Schweiz

17. - 21. September 1990

TAGUNGSBERICHT

2. Teil

551.5 (234.3) (06)
SZ ISSN 0080-7346

VERHANDLUNGEN DER EINUNDZWANZIGSTEN INTERNATIONALEN TAGUNG FÜR ALPINE METEOROLOGIE

COMPTES RENDUS DU VINGT ET UNIEME CONGRES INTERNATIONAL DE METEOROLOGIE ALPINE

ATTI DEL VENTUNESIMO CONGRESSO INTERNAZIONALE DI METEOROLOGIA ALPINA

PROCEEDINGS OF THE TWENTY-FIRST INTERNATIONAL CONFERENCE ON ALPINE METEOROLOGY

ENGELBERG
SCHWEIZ
17.-21. SEPT. 1990

2. TEIL

Contents / Inhaltsverzeichnis

Foreword

The Proceedings of the 21st International Conference on Alpine Meteorology in Engelberg (ITAM-90) from September 17 to 21, 1990, consists of two parts: The first volume was distributed to the participants at the beginning of the Conference and contains those texts of the oral and poster presentations which were submitted before the Conference. The second part which you are holding in your hands includes the texts which were turned in later, the Conference program, a short report of the Conference, as well as lists of participants and authors.

Both volumes are part of the Publication Series of the Swiss Meteorological Institute, and I hope that they will provide new incentives and will contribute to the solution of meteorological problems.

André Junod
Director of the SMI

Vorwort

Der Tagungsbericht der 21. Internationalen Tagung für Alpine Meteorologie in Engelberg (ITAM-90) vom 17. - 21. September 1990 besteht aus zwei Teilen. Während im ersten Band, welcher zu Beginn der Tagung an die Teilnehmer abgegeben wurde, die Texte der vor der Tagung eingereichten Vorträge und Poster veröffentlicht sind, enthält der nun vorliegende zweite Teil die später abgelieferten Arbeiten, das Tagungsprogramm, zusammenfassende Kurzberichte der Chairmen zu den sieben Tagungsteilen, einen kurzen Bericht über den Tagungsverlauf sowie die Teilnehmer- und Autorenverzeichnisse.

Ich hoffe, dass die beiden in die Reihe der Veröffentlichungen der Schweizerischen Meteorologischen Anstalt aufgenommenen Bände neue Anregungen vermitteln und zur künftigen Lösung meteorologischer Probleme beitragen werden.

André Junod
Direktor SMA

Préface

Le compte-rendu du 21e Congrès international de météorologie alpine (ITAM-90), qui s'est déroulé à Engelberg du 17 au 21 septembre 1990, se compose de deux parties. Distribué aux congressistes à l'ouverture de la manifestation, le premier volume contenait les textes des exposés et des affiches disponibles avant le congrès. Quant au second, objet de la présente publication, il comprend les résumés des travaux qui nous sont parvenus par la suite, le programme du congrès, de brefs rapports des présidents des sept groupes de travail, un court exposé sur le déroulement de la conférence, ainsi que la liste des adresses des auteurs et des participants.

Je forme le voeu que ces deux volumes, édités dans la série des Publications de l'Institut suisse de météorologie, incitent à de nouvelles recherches et contribuent à la résolution future des problèmes météorologiques actuels.

André Junod,
Directeur de l'ISM

Premessa

Gli Atti della 21a Conferenza Internazionale di Meteorologia Alpina (ITAM-90), tenutasi ad Engelberg il 17-21 settembre 1990, si compongono di due parti. Mentre nel primo volume, distribuito al Convegno, sono pubblicati i testi delle conferenze e delle sessioni poster ricevuti prima dell'inizio dell'ITAM, il secondo volume raccoglie i contributi consegnati solo più tardi, il programma del Convegno, un rapporto riassuntivo dei chairmen per le sette sezioni, un breve resoconto sullo svolgimento del Convegno, cosi come l'elenco dei partecipanti e degli autori.

Spero che i due volumi, ripresi nella serie delle pubblicazioni dell'Istituto Svizzero di Meteorologia, possano costituire uno spunto stimolante e contribuire a risolvere futuri problemi di meteorologia.

André Junod
Direttore dell'ISM

Tagungsverlauf

Die 21. Internationale Tagung für Alpine Meteorologie, welche vom 17. - 21. September 1990 in Engelberg, in den Voralpen der Zentralschweiz, abgehalten wurde, vereinigte über 300 Personen (231 wissenschaftliche Teilnehmer, 50 - 70 Begleitpersonen sowie 21 Mitarbeiterinnen und Mitarbeiter für Organisation, Technik und Betreuung) aus 15 Ländern (Belgien, Bulgarien, China, Deutschland, Frankreich, Israel, Italien, Jugoslawien, Neuseeland, Oesterreich, Polen, Rumänien, Schweiz, Ungarn, USA).

Zum vierten Mal, seitdem diese Veranstaltung im Jahre 1950 ins Leben gerufen wurde, war die Schweiz Gastgeberland und die SMA hauptverantwortlich für deren Organisation. An der Gestaltung wesentlich mitgearbeitet hat das Institut für Atmosphärenphysik der ETHZ: Prof. H. C. Davies war Programmchairman und Dr. H. Richner sorgte für einen reibungslosen technischen Ablauf.

Der Direktor der Schweizerischen Meteorologischen Anstalt, Dr. A. Junod, eröffnete die Tagung:

"Ladies and gentlemen,

On behalf of the Swiss Meteorological Institute, I have the great pleasure to welcome you warmly at the beginning of the 21st International Conference on Alpine Meteorology. It is very rewarding for the organizers to greet so many participants, whether faithful friends from previous conferences or likeable new-comers.

For the 4th time, the International Conference on Alpine Meteorology takes place in Switzerland, after Davos (1954), Brig (1966) and Grindelwald (1978). Now it is Engelberg in Central Switzerland which is proud to welcome you.

During the 12 years which passed since the 15th ITAM in Grindelwald, several significant events underlined the development of meteorology and climatology in our Alpine region:

- there was the Alpine Experiment ALPEX with its extensive observing campaign in 1981, analyses and verifications which followed and still continue, while results were presented in particular at the Conferences in Venice 1985 and Garmisch-Partenkirchen in 1989;

- a new european meteorological organization was born, EUMETSAT, which controls the operational meteorological geostationary satellite system in Europe since 1986;

- the 1st World Climate Conference which was organized in 1979 by WMO in Geneva defined the starting point for increased and better coordinated efforts in the frame of the World Climate Program as well as national climatological programs in several Alpine countries;

- also in the field of atmospheric pollution, the concern raised by the forest decline has initiated multi-disciplinary studies in which meteorology and climatology have proved to be indispensable disciplines.

However the pressing questions related to climate change and variability do not bannish the wide range of other problems, old and new, to which meteorologists devote their knowledge, as demonstrated by the broad diversity of about 150 contributions submitted to this conference.

The base conditions for fruitful exchanges of ideas and experiences being thus fullfilled, I wish to all participants the same mutual enrichment experienced in previous Conferences on Alpine Meteorology and a most pleasant stay while enjoying the late summer here in Engelberg."

Anschliessend an die Begrüssung durch Direktor Junod hielt der Generalsekretär der Weltorganisation für Meteorologie, Prof. G.O.P. Obasi, eine Ansprache. Sie ist anschliessend (siehe Seite 7) im Tagungsband abgedruckt.

Nach einem humorvollen, in fünf Sprachen vorgetragenen Grusswort durch den Landesstatthalter A. Höchli (Regierungsrat des Kantons Obwalden), wandte sich zum Abschluss der Eröffnungsveranstaltung der Tagungsleiter, Dr. Th. Gutermann, an die versammelten Teilnehmerinnen und Teilnehmer und an die Gäste:

"Sehr verehrte Damen und Herren,
Liebe Kolleginnen und Kollegen,

Im Namen des Organisationsstabes heisse ich Sie hier in Engelberg herzlich willkommen. Ein spezieller Gruss und Dank geht an Herrn Talammann von Holzen, den Vorsteher der Talschaft Engelberg sowie an die Direktion des Kurvereins Engelberg, speziell an Herrn Suter, welche uns die Durchführung unserer Tagung hier in Engelberg wesentlich erleichtert haben. Die Bedeutung der nicht im Auftrag einer offiziellen Organisation durchgeführten alpinmeteorologischen Tagung wird durch die Patronate unterstrichen, welche die Weltorganisation für Meteorologie mit Sitz in Genf sowie die Schweizerische Akademie für Naturwissenschaften übernommen haben: Es freut uns sehr, dass der Generalsekretär der WMO, Herr Professor Obasi, Zeit fand, persönlich zu Beginn der Konferenz unter uns zu sein und heute zu uns zu sprechen. Herr Dr. x.Du nimmt als Vertreter der WMO an der ganzen Tagung teil.

Die Organisation der 21. Tagung für Alpine Meteorologie wurde von der Schweizerischen Meteorologischen Anstalt übernommen, unter enger Mitarbeit des Instituts für Atmosphärenphysik der Eidgenössisch Technischen Hochschule in Zürich (ETHZ). Für diese grosse Unterstützung sei dem Institutsdirektor, Herrn Prof. Waldvogel , sowie dem Hauptverantwortlichen, Herrn Dr. Richner, bestens gedankt.

Einer, zwar ab und zu unterbrochenen, Tradition folgend wird die Tagung mehrsprachig und ohne Simultanübersetzung durchgeführt. Damit soll, neben dem finanziellen Vorteil, parallel zur wissenschaftlichen Arbeit auch ein sprachkultureller Beitrag geleistet werden. Wenden Sie sich bei Sprachproblemen an Kolleginnen und Kollegen oder an das Organisationsteam.

Das wissenschaftliche Programm wurde Ihnen vor der Tagung zugestellt. Herr Professor H.C. Davis, ebenfalls vom Institut für Atmosphärenphysik der ETHZ, hat sich spontan bereit erklärt, den Vorsitz des Programmkomitees zu übernehmen. Auch ihm gilt unser herzlicher Dank. Die eingereichten 157 Vorträge decken auch in diesem Jahr einen breiten alpinmeteorologischen und klimatologischen Themenbereich ab. Zusammen mit sechs weitern Fachspezialisten verschiedener Hochschulen der Schweiz sowie der SMA hat Herr Davies ein, wir hoffen auch nach Ihrer Beurteilung, interessantes Programm für die kommenden fünf Tage zusammengestellt: 66 mündliche Vorträge und über 50 Poster werden in sieben Themengruppen präsentiert. Sechs davon werden durch einen eingeladenen Uebersichtsvortrag eingeleitet. Im hochaktuellen Themenkreis "Untersuchungen des Klimas und seiner Elemente sowie Studien über kurz- und langfristige Klimaschwankungen" ist eine Plenumsdiskussion mit dem Titel "Schlüsselfragen der Alpinen Klimatologie" vorgesehen. Wir danken den eingeladenen Vortragenden sowie den Panelmitgliedern der Klimadiskussion für ihre speziellen, die Tagung bereichernden Beiträge. Im vorliegenden Tagungsprogramm sind die Arbeiten im Kapitel "Diagnose und Interpretation mesoskaliger Systeme und lokaler Phänomene" besonders zahlreich vertreten. Das 1982 durchgeführte internationale Feldexperiment ALPEX hat sich zusätzlich zur Wettervorhersage auch auf die Arbeiten im Diagnose- und Interpretationsbereich synoptischer und mesoskaliger Systeme wesentlich ausgewirkt. Verhältnismässig wenige Arbeiten gingen zum Kapitel " Energieaustausch an der Erdoberfläche über Strahlungsvorgänge und mikrophysikalische Prozesse" ein und mit nur vier Vorträgen ist der Themenkreis "Biometeorologie" hier in Engelberg leider nur am Rande vertreten.

Auch hier in Engelberg wird auf Parallelsitzungen verzichtet, was für das Vortragsprogramm eine Auswahl aus den eingereichten Arbeiten bedingte. Die Beurteilung erfolgte durch das Programmkomitee. Mit den ausgewählten etwa 115 Arbeiten ist das viereinhalbtägige wissenschaftliche Programm stark belastet.

Um Ihnen Gelegenheit zu geben, parallel zum Vortragsprogramm auch das aktuelle Wetter zu verfolgen und dessen Entwicklung für die nächsten Tage abzuschätzen, sind im Nebenraum verschiedene Informationssysteme aufgebaut. Ich will hier nicht auf Einzelheiten eingehen. Zwei Prognostiker des Schweizerischen Wetterdienstes, die Herren Hächler und Kappenberger, werden jedoch täglich eine kurze Wetterübersicht geben und Ihnen für die Beantwortung von Wetterdienstfragen zur Verfügung stehen. Zudem wird durch Mitarbeiter des Instituts für Atmosphärenphysik täglich mit der mobilen Radiosondieranlage ein Aufstieg hier im Engelbergtal ausgeführt, welcher Ihnen näheren Aufschluss über den Aufbau der Talatmosphäre und über die Strömungsverhältnisse über den Alpen geben wird.

Wenden wir uns noch kurz dem Klima in Engelberg zu: In der regionalen Klimauntersuchung der Alpennordseite der Schweiz von Frau Urfer wird Engelberg, wo Klimabeobachtungen seit 1864 durchgeführt werden, folgender Stationskategorie zugeordnet:
" Eher schmale, meist V-förmige Voralpentäler, in die der Föhn selten hinabsteigt, z.T. schon deshalb, weil das

Tal nicht in seiner Hauptströmungsrichtung liegt (Typ IIIc)".
Die Föhnhäufigkeit ist entsprechend deutlich geringer als in den bekannten Süd-Nord orientierten Föhntälern. Dies wirkt sich in einer, für Tallagen im Voralpenraum, höhern Nebelhäufigkeit, aber auch, dank der Höhenlage, in geringerer Bewölkung und höherer Sonnenscheindauer in den Wintermonaten aus. Die Niederschläge sind, auch als Folge des Höheneinflusses, etwa 200 bis 400 mm höher als in den eigentlichen Föhntälern und im Alpenvorland.

Lassen wir es bei diesen wenigen Klimahinweisen bewenden. Das aktuelle Wetter der kommenden Woche wird, sofern die Prognosen zutreffen, vom klimatologischen Mittel für die dritte Septemberwoche in Richtung "Konferenzwetter" etwas abweichen.

Gestatten Sie mir, sehr verehrte Damen und Herren, zum Abschluss noch einige organisatorische Hinweise:

Kongressbegleitend geben wir ein Informationsblatt, das "TITLIS-ECHO", heraus; die erste Nummer ist mit der Tagungsmappe bereits in Ihren Besitz gelangt. Dieses Bulletin enthält jeweils das bereinigte Vortragsprogramm für den folgenden Tag sowie Hinweise und Mitteilungen, die Exkursionen, das Programm für Begleitpersonen sowie weitere Anlässe betreffend. Das Mitteilungsblatt wird im Vorrraum bei der Information aufgelegt, wo auch allfällige weitere Unterlagen bezogen werden können.

Es bleibt mir noch, Sie auf den kleinen Empfang aufmerksam zu machen: Die Schweizerische Meteorologische Anstalt lädt alle Tagungsteilnehmerinnen und -teilnehmer mit Begleitung morgen Dienstagabend um 18.30 Uhr ein zu einem Aperitif im Barocksaal des Klosters von Engelberg. Vorgängig findet, vom Kur- und Verkehrsverein für Sie organisiert, ein kurzes Orgelkonzert in der Klosterkirche statt.

Damit danke ich für Ihr Zuhören und wünsche Ihnen allen eine interessante und angenehme Tagung hier in Engelberg:

Die 21. Internationale Tagung für Alpine Meteorologie ist eröffnet."

Das anschliessende fünftägige wissenschaftliche Programm umfasste 114 wissenschaftliche Beiträge (63 Vorträge und 51 Poster). Die Chairmen der sieben Konferenzteile erarbeiteten eine Zusammenfassung der wichtigsten Aussagen für den hier vorliegenden zweiten Teil des Tagungsberichtes (Seiten 97 - 107).

Aus dem Rahmenprogramm der Tagung seien erwähnt: Die speziell von Andreas Walker für den Begrüssungsabend der ITAM-90 geschaffene Tonbildschau, das Orgelkonzert in der Klosterkirche von Engelberg, die Titlisexkursion, welche am Mittwochnachmittag bei sonnigem Wetter und guter Sicht von gegen 200 Teilnehmern besucht wurde sowie eine Tagesexkursion am Samstag über Brünig, Grimsel und Furka. Besichtigungen und Kurzvorträge (Felslabor der Nagra, Talkessel von Gletsch/Rhonegletschervorfeld, Elektrizitätswerk Göschenen und Föhnstation Altdorf im Reusstal) lockerten die teilweise regnerische Dreipässefahrt auf.

An der Schlusssitzung fasste Prof. H.C. Davis die wesentlichen Beiträge der Tagung zusammen. Im Namen der Teilnehmer dankte anschliessend Dr. M.E. Reinhardt für die gute Organisation der Veranstaltung. Mit diesem Dank an den Programmchairman Prof. H.C. Davis und die Mitglieder des Programmkomitees sowie an die zahlreichen Organisationsmitarbeiter, insbesondere an den administrativen Leiter P. Morscher, an die Damen des Tagungsbureaus E. Simmen, R. Spaar und E. Wildberger sowie an die Betreuerin des Programms für die Begleitpersonen, Frau A. Junod, konnte die erfolgreich abgelaufene Tagung pünktlich geschlossen werden.

Th. Gutermann

Statement by Professor G.O.P. Obasi, Secretary-General of the World Meteorological Organization, at the Opening of the 21st International Conference on Alpine Meteorology

Engelberg, Switzerland, September 17, 1990

Mr. A. Höchli, Vice-President of the Governing Council of the Canton of Obwalden,

Mr. E. von Holzen, Mayor of Engelberg,

Dr. A. Junod, Director of the Swiss Meteorological Institute and Permanent Representative of Switzerland with WMO

Dr. Th. Gutermann, Chairman of the Organizing Committee,

Distinguished guests,

Ladies and Gentlemen,

May I first take this opportunity to thank our hosts for inviting me to address you at this Twenty-first International Conference on Alpine Meteorology. It gives me great pleasure to meet many of the scientists involved in studies of alpine and mountain meteorology, especially as the Conference takes place in the country which hosts the headquarters of the World Meteorological Organization (WMO).

This important conference seeks to bring together many of the world's internationally renowned research workers and experts in mountain meteorology for a review of the progress achieved in this field since the last conference two years ago. Also, it will serve to identify relevant key problems, where more research efforts could be focused on in the future. I am confident that the excellent facilities placed at the Conference's disposal in this beautiful setting will be most conducive to constructive recommendations and conclusions.

The subject of this Conference is indeed a major concern to many scientists. The topics you will discuss, while relating primarily to Alpine meteorology, will also have a bearing on weather prediction on all time scales and other related problems in many mountain areas elsewhere. While features of mountain ranges such as their orientation and topography vary, some of the findings in the Alpine experience will have relevance to other mountain chains such as the Himalayas, the Andes and the Rocky Mountains. This additional knowledge will lead to a further advance of the science of meteorology on a worldwide basis. It will also facilitate appropriate meteorological and hydrological applications at national, regional and international levels, particularly in the context of integrated mountain area development that is now being pursued in various countries.

Furthermore, we are becoming more fully conscious of the strong linkage between the prevailing meteorological situation in the mountain ranges at a particular time, and the livelihood as well as leisure of their population and those nearby. We are aware of the effect of the Himalayas on the occurence and intensity of monsoon rains in the region, which could determine crop yield. We note the effect on the ski industry and the people who depend on it of the recent mild winters in the European mountain resorts. There are also socio-economic repercussions in the Mediterranean countries due to the higher frequency of Alps-related cyclogenesis in the region.

The World Meteorological Organization is continuously putting attention to the relevant areas of concern. For instance, since the field phase in March/April 1982, the data from the mountain sub-programme (ALPEX) of the Global Atmospheric Research Programme (GARP), together with those from the other GARP programmes, have been and continue to be fully exploited as a foundation and an inspiration for research. The use of ALPEX data has been given very high priority within the WMO Weather Prediction Research Programmes. These data are also being widely used in the WMO limited-area modelling study project, Mediterranean cyclones studies and other numerical simulations activities.

Recently at the tenth session of the WMO Commission for Atmospheric Sciences (CAS), held in Offenbach in April 1990, as well as at the tenth session of RA VI, held in Sofia in May 1990, the importance of the use of the

ALPEX data in weather prediction research was further stressed. In these meetings, it was noted that the use of the ALPEX data has formed the basic for a range of studies on mountain effects in weather prediction. These include those on lee cyclogenesis and the boundary layer over complex topography which have led to improved understanding of the flow over mountainous terrain, as well as further insight into the thermal and dynamic structure of frontal surfaces over elevated areas.

Not surprisingly, a wide interest has been expressed by many scientists, limited-area modelling groups and Mediterranean cyclone investigators in analyses based on ALPEX data. Through the auspices of WMO, substantial effort is being made to prepare a global merged data set covering the ALPEX Special Observing Period as well as the required global and regional analyses. The availability of these final ALPEX analyses would stimulate a great deal of further numerical experimentation on mountain effects in weather prediction research.

For its part, WMO will continue to stimulate the further use of ALPEX data and to promote workshops, seminars and studies in Alpine meteorology. WMO would be prepared to assist scientists and institutions in meeting their Alpine data requirements. WMO will also encourage in every possible way related improvements in operational models and the advancement of Members' forecasting services.

Furthermore, it is noteworthy to refer to the human dimension of the importance of the scientific work relating to the Alps. This could be better appreciated if we note that, apart from its own population, about 100 million visitors come annually to the 200,000 square-kilometre expanse of the Alps which extend over seven countries. The Alpine ranges and their users are affected by weather conditions which unfortunately, on some occasions, have led to disasters such as flooding, landslides and avalanches. These phenomena are part of those being addressed in connection with the United Nations International Decade for Natural Disaster Reduction (IDNDR) in which WMO is taking a leading role.

Also to be borne in mind is the fact that the situation in the Alps and other mountain areas will affect and be affected by potential climate change. The related comprehensive assessment on this subject has recently been finalized by the Intergovernmental Panel on Climate Change (IPCC) which was established by WMO and the United Nations Environment Programme (UNEP).The climate change issue will also be the focus of the forthcoming Second World Climate Conference which will take place in Geneva, 29 October to 7 November 1990. It is expected that negotiations towards an international framework convention on climate change will proceed in earnest thereafter. It is praiseworthy that this Conference is devoting a section of its program to the examination of short- and long-term variation of climate and climate elements.

Looking towards the future, I see a continuing need to co-ordinate and encourage national and regional activities related to mountain meteorology. WMO will continue to give active support to this aspect through the activities which I have indicated. I therefore look forward to the results of the present 21st International Conference in Alpine Meteorology whose outcome will surely contribute greatly to the progress in this field.

I wish you all a most successful and fruitful session.

Thank you.

Section 1:

Observational Methods and Instrument Technology

UNA RETE DI STAZIONI AUTOMATICHE PER LA PREVISIONE DELLE VALANGHE

di Anselmo CAGNATI e Alberto LUCHETTA

Centro Sperimentale Valanghe e Difesa Idrogeologica
32020 Arabba BL Italia

RIASSUNTO

La previsione delle valanghe a breve termine secondo il metodo convenzionale si basa in buona parte sulla raccolta di dati meteorologici e nivologici. Nei servizi valanghe dei paesi alpini questi dati provengono normalmente da reti di stazioni tradizionali che richiedono la presenza giornaliera di un osservatore sul campo. Sul territorio montano della Regione Veneto (Dolomiti meridionali e Prealpi venete) a partire dal 1984 funziona una rete di stazioni automatiche che sostituisce i rilievi manuali giornalieri. Le stazioni sono ubicate nella fascia altimetrica compresa tra i 1500 e 2500 m di quota dove si trovano la maggior parte delle zone di distacco di valanghe. Esse sono alimentate a celle solari e la trasmissione dei dati alla centrale di acquisizione avviene via radio. I parametri misurati sono: altezza della neve, temperature della neve, temperatura dell'aria, velocita' e direzione del vento, radiazione incidente e riflessa, umidita' relativa. La possibilita' di ottenere i dati in tempo reale e con qualsiasi scadenza consente di prevedere il verificarsi di situazioni di rischio da valanghe, in particolar modo quelle determinate da nuovi apporti nevosi. La gestione della rete presenta altresi' una serie di problemi dovuti soprattutto a cause di natura climatica.

A NEIWORK OF AUTOMATIC STATIONS FOR THE FORECASTING OF AVALANCHES

by Anselmo CAGNATI and Alberto LUCHETTA

Avalanches and Hydrogeological Defence Experimental Centre
32020 Arabba BL Italy

ABSTRACT

The short-term forecasting of avalanches according to the conventional method is based mostly on the gathering of meteorological and nivological data. In the avalanche services of Alpine countries these data usually come from networks of traditional stations which require the day-by-day presence of on site observers. In the mountain territory of the Veneto Region (Southern Dolomites and Veneto Pre-Alps) a network of automatic stations has been in function since 1984 which has substituted the day-by-day manual surveys. The stations are situated at a height betwen 1500 and 2500 metres, which is the zone where most avalanches begin. They are powered by solar cells and the data are trasmitted to the centre by radio. The parameters measured are the following: depth of the snow, temperature of the snow, temperature of the air, speed and direction of the wind, incidental and reflected radiation, relative humidity. The fact that can be obtained at once and at any moment makes it possible to forecast situations where there is a risk of avalanches, in particular those determined by new snowfalls. The running of the network presents likewise a series of problems due above all to causes of a climatic nature.

UNA RETE DI STAZIONI AUTOMATICHE PER LA PREVISIONE DELLE VALANGHE

di Anselmo CAGNATI e Alberto LUCHETTA

Centro Sperimentale Valanghe e Difesa Idrogeologica
32020 Arabba BL Italia

1. Introduzione

Una delle principali attivita' dei servizi valanghe dei paesi alpini e' previsione delle valanghe a breve termine ovvero una stima, sul territorio di competenza, della probabilita' di distacco di valanghe in un arco di tempo che va dalle 24 fino alle 168 ore successive. Il metodo correntemente usato, chiamato metodo convenzionale, e' un insieme di trattamento deterministico dei dati nivometeorologici e di logica induttiva in cui l'esperienza del previsore gioca ancora un ruolo fondamentale. Esso richide una vasta raccolta di informazioni e dati che riguardano il manto nevoso al suolo, il tempo atmosferico in atto e previsto e l'attivita' valanghiva.
Accanto a sistemi di rilevamento tradizionali che si basano su misure e osservazioni eseguite giornalmente o periodicamente e che richedono l'intervento dell'uomo, si sono andati sviluppando in questi ultimi anni reti di stazioni automatiche che consentono di disporre in continuo e in tempo reali di dati relativi ad alcuni parametri che influiscono sulle condizioni di stabilita' del manto nevoso. In Italia, sul territorio montano della Regione Veneto (Dolomiti e Prealpi venete), a partire dal 1984 e sulla base delle precedenti esperienze francesi (stazioni NIVOSE), e' stata sviluppata una rete di stazioni nivometeorologiche automatiche che ha permesso di sostituire i rilievi manuali giornalieri. Le stazioni sono alimentate a celle solari e la trasmissione dei dati alla centrale di acquisizione di Arabba presso il Centro Sperimentale Valanghe e Difesa idrogeologica, avviene via radio.

2. Caratteristiche della rete e sviluppi previsti

Attualmente la rete di stazioni nivometeorologiche automatiche della montagna veneta e' composta di 15 unita' collegate alla centrale di acquisizione di Arabba mediante 7 ripetitori (fig.1). La dotazione di sensori e' differenziata a seconda della rappresentativita' dei siti in relazioni alla misura dei vari parametri (vento, altezza neve, precipitazione ecc.)
Considerando il territorio regionale al di sopra dei 500 m di quota, la densita' della rete e' di 1 stazione ogni 330 kmq, ben al di sopra quindi della densita' media relativa all'arco alpino italiano per questo tipo di stazioni che e' di 1 stazione ogni 1660 kmq. I programmi di completamento della rete prevedono l'installazione di altre 7 unita' e cio' porterebbe la densita' della rete ad 1 stazione ogni 250 kmq.
Per quanto riguarda la dislocazione altimetrica, le stazioni sono ubicate tra i 1400 e i2600 m con la seguente distribuzione:
- 12,5% nella fascia al di sotto dei 1500 m di quota;
- 62,5% nella fascia compresa tra i 1500 e i 2000 m di quota;
- 25,0% nella fascia al di sopra dei 2000 m di quota.

I siti sono generalmente accessibili durante la stagione estiva con normali mezzi fuoristrada e durante la stagione invernale con gli sci utilizzando gli impianti di risalita. Nella totalita' dei casi sono sprovvisti di energia elettrica.

3. Caratteristiche delle stazioni

Ciascuna stazione nivometeorologica e' costituita da due strutture a palo sulle quali sono disposti i diversi sensori, la periferica di acquisizione e trasmissione dei dati e il pannello solare per la ricarica delle batterie. I pali sono collegati ad un loculo sotterraneo, opportunamente drenato, dove sono alloggiate le batterie. I sensori nivologici (nivometro, termometri neve, pluviometro) si trovano ad una certa distanza dal resto della stazione al fine di limitare le perturbazioni al manto nevoso (fig.2). Il palo principale, di 10 m, e' cosi' equipaggiato:
- sensori: termoigrometro

anemometro
anemoscopio
albedometro

- periferica di acquisizione, archiviazione e trasmissione dati
- pannello solare
- antenna

Il secondo palo, di 6 m, e' cosi' equipaggiato:

- sensori: nivometro (ad ultrasuoni)
  12 termometri neve

Alcune stazioni sono inoltre dotate di un pluviometro totalizzatore "a filo vibrante" e liquido anticongelante particolarmente adatto per la misura della precipitazione nevosa in siti remoti.

L'alimentazione e' a celle solari mediante un pannello da 20 watt con tensione a vuoto di 19,5 volt e una corrente di 1,3 ampere a 13,8 volt.

La periferica di gestione e' alloggiata in 2 contenitori di alluminio pressofuso montati uno internamente all'altro con elevato grado di protezione (IP 55 e IP 43).

Controlli e verifiche di funzionamento avvengono mediante terminale incorporato munito di tastiera protetta e display a 2 righe LCD per 40 caratteri. Esso consente 3 diversi livelli di interazione a seconda della capacita' dell'utente.

Il programma di gestione della stazione risiede su memoria EPROM da 64 Kbyte. La stazione e' inoltre dotata di memoria locale su modulo asportabile da 256 Kbyte (128.000 dati) e cio' consente la possibilita' di recuperare fino a 6 mesi di dati in caso di mancata trasmissione.

La misura dell'altezza del manto nevoso avviene mediante una coppia di trasduttori ultrasonici tipo SODAR uno dei quali invia sul manto nevoso un impulso a 331,4 m/s a 18°C (la precisione media complessiva della misura, una volta effettuata la correzione in base alla temperatura dell'aria, e' +0,7% dell'altezza del manto nevoso).

I termometri neve sono disposti su un palo in vetroresina a distanze fisse di 20 o 40 cm l'uno dall'altro e sono dotati di supporti in acciaio per resistere alle sollecitazioni determinate dall'assestamento del manto nevoso.

Le tarature dei vari sensori avvengono in loco con possibilita' di

autotaratura.
La protezione contro le scariche atmosferiche e' assicurata da un impianto di messa a terra in pozzetto.
L'intervallo termico di funzionamento della stazione e' compreso tra i -30 e +60°C, mentre le strutture sono collaudate per resistere a raffiche di vento fino a 160 km/h.

4. Vantaggi e svantaggi legati all'uso di una rete di stazioni automatiche.

Il vantaggio principale risiede nella maggior frequenza di rilevamento. Mentre con le stazioni di tipo tradizionale sono possibili 1 o al massimo 2 rilevamenti al giorno, con le stazioni automatiche vengono normalmente utilizzati intervalli di interrogazione di 30 min o 20 min. Cio' consente di avere a disposizione, per ciascun parametro 48 o 72 dati al giorno con possibilita' quindi di costruire serie temporali molto dettagliate anche su brevi periodi di tempo. Possono cosi' essere facilmente individuati fenomeni meteorologici locali molto importanti per la previsione delle valanghe quali l'inizio e la fine di una precipitazione nevosa, l'intensita' della stessa, improvvisi riazi termici dovuti ad effetto fhoen, fenomeni locali di inversione termica, attivita' del vento nel corso di un certo periodo ecc.
Il secondo vantaggio, altrettanto importante, risiede nella possibilita' di effettuare misure sui parametri nivometeorologici alle quote elevate, al di fuori delle aree antropizzate nella fascia altimetrica compresa tra i 2000 e i 3000 m dove si trovano la maggior parte delle zone di distacco di valanghe.
Un'ultimo lato positivo e' la bonta' delle misure dovuta sia alla maggior precisione degli strumenti elettronici, sia all'eliminazione degli errori accidentali commessi dall'uomo nell'esecuzione delle letture.
Un aspetto negativo e' legato alla impossibilita', con le stazioni automatiche, di misurare parametri interni del manto nevoso (resistenze, coesione dei vari strati, tipo e dimensione dei grani) ,di effettuare valutazioni qualitative (caratteristiche dello strato superficiale) o osservazioni (attivita' valanghiva) ritenute ancora fondamentali nell'applicazione del metodo convenzionale per la previsione delle valanghe.

Nel settore della previsione delle valanghe, allo stato attuale delle conoscenze e della tecnologia, non e' quindi ancora realizzabile una completa automatizzazione della fase di rilevamento dei dati. Per questo motivo la rete di stazioni automatiche del Veneto e' integrata da una serie di punti di rilevamento manuale dove vengono eseguite settimanalmente i rilievi delle caratteristiche interne del manto nevoso (prova penetrometrica e prova stratigrafica) nonche' il controllo dell'attiviat' valanghiva.
Un'altro aspetto negativo risiede negli elevati costi di installazione, di manutenzione e di gestione di una rete di stazioni automatiche in alta quota. Forse oggi la sola previsione delle valanghe non giustifica simili investimenti se la rete non viene studiata in un'ottica multisettoriale (meteorologia, climatologia, scienze ambientali) e come fonte di dati per diverse attivita' economiche (produzione di neve) o del tempo libero (alpinismo, volo libero ecc.)

5. Problemi legati all'uso operativo di una rete di stazioni automatiche in alta quota.

L'uso operativo di una rete di stazioni automatiche di alta quota abilitate per la trasmissione dei dati in tempo reale via radio comporta una serie di problemi legati alle particolarita' orografiche e climatiche dei siti.
Il problema principale e' senza dubbio legato alla trasmissione dei dati dalla bonta' della quale dipende l'utilizzo degli stessi ai fini previsionali. Per quanto riguarda la rete del Veneto, considerando un intervallo di interrogazione di 30 min, la percentuale di collegamento fra le stazioni periferiche e la centrale di acquisizione varia tra il 70 e il 96% a seconda dei siti e delle condizioni meteorologiche. Con condizioni di tempo buono, la media generale si aggira intorno al 90%, mentre scende all'84% in caso di tempo perturbato (con precipitazioni in atto).
Rotture di tipo meccanico alle strutture e ai sensori sono dovute al peso della neve nella fase di assestamento, alla forza del vento e a sovraccarichi determinati da formazioni di ghiaccio e galaverna. Le parti piu' colpite sono le antenne, i parafulmini e i sensori di temperatura della neve. I sensori di velocita' e direzione del vento, anche se temporaneamente

bloccati nel loro funzionamento, non subiscono generalmente danni strutturali.
Per quanto riguarda l'elettronica, i danni sono limitati. Possono verificarsi nel periodo estivo in seguito a temporali (stazioni colpite da fulmini), specialmente in quei siti dove il terreno roccioso non ha consentito la realizzazione di una messa a terra efficente e nel periodo invernale nel caso di periodi prolungati di freddo intenso (temperature inferiori a -30°C) e scarso innevamento (periferica di gestione fuori del manto nevoso)
Escludendo le periodiche visite di controllo sostituzione dei moduli di registrazione e di ritaratura dei sensori, ogni stazioni richiede mediamente per guasti, rotture ecc. 1,5 interventi all'anno. Il costo delle manutenzioni e' tuttavia elevato, aggirandosi intorno al 10% del valore delle stazioni.
La gestione dei dati e' particolarmente complessa, soprattutto nella fase di controllo della qualita' dei dati. Gli errori piu' frequenti sono dovuti a cause climatiche e riguardano i parametri altezza del manto nevoso e precipitazione nevosa (nel caso di forti venti), temperature della neve (nel caso di circolazione di aria esterna attorno i sensori), velocita' e direzione del vento (nel caso di ghiaccio o galaverna) e radiazione incidente (nel caso di neve umida depositata sul radiometro).

Bibliografia

CAGNATI A. (1988)
Prevedere e informare: i bollettini valanghe
Rassegna della Protezione Civile, anno V, No.9, pp.38-44

CAGNATI A., VALT M. (1990)
Il rilevamento dei dati nivometeorologici
Neve e Valanghe, No.9, pp.72-75

LA CHAPELLE R. (1980)
The fundamental processes in conventional avalanche forecasting

Journal of Glaciology, Vol.26, No.94

LAFEUILLE J. (1982)
Nivose
Neige et Avalanches, No.28, pp.7-13

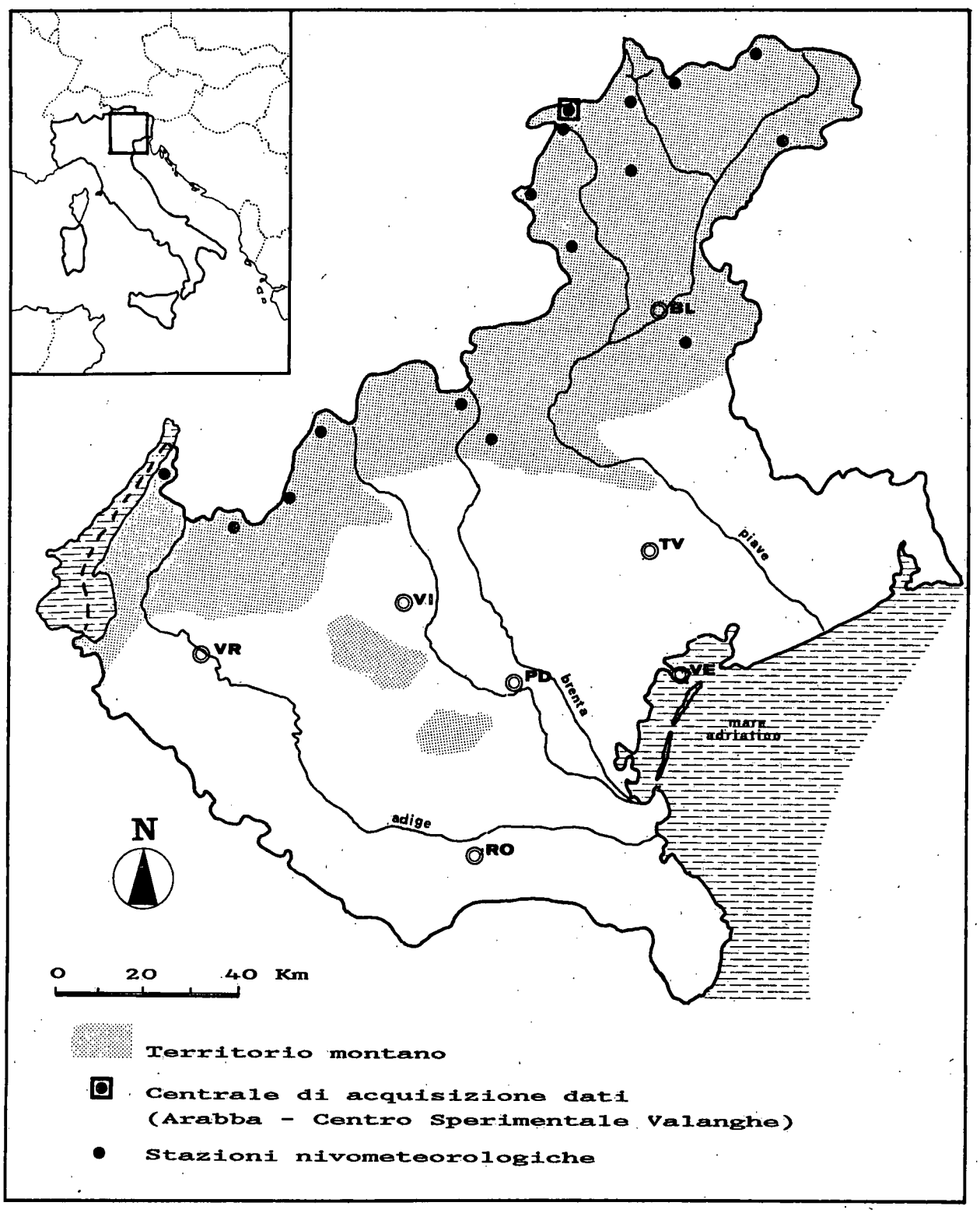

Fig. 1 Rete di stazioni nivometeorologiche della montagna veneta

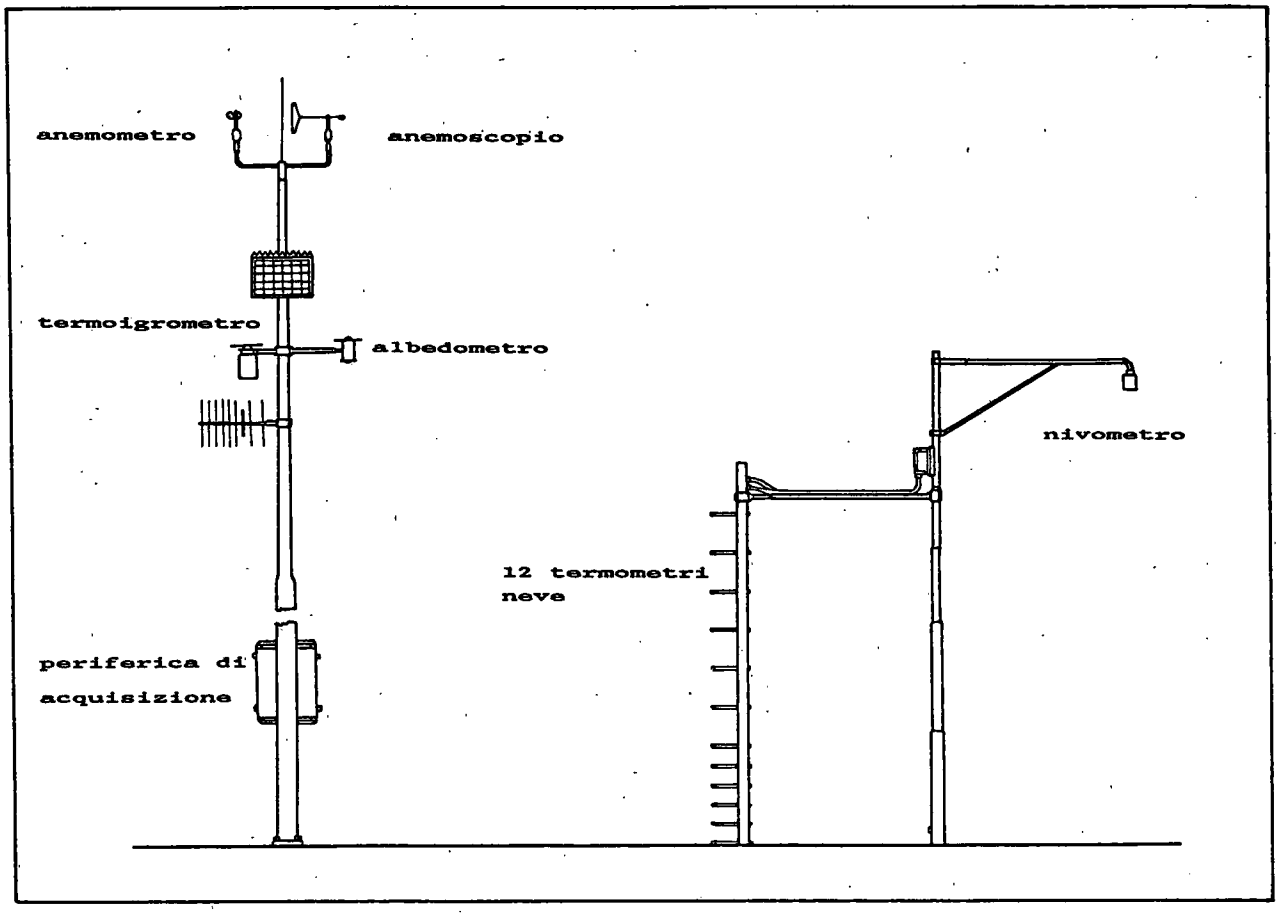

Fig. 2 Schema di una stazione tipo (senza pluviometro)

Correction of Atmospheric Masking as a Prerequisite of Ecological Mapping with Satellite Data

Hartmut Graßl and Waltraud Jahnen
Max-Planck-Institut für Meteorologie, Hamburg

Introduction

Satellite remote sensing of the earth surface becomes more and more important in different branches of science. The major advantage is the objective observation of large areas nearly simultaneously. A considerable disadvantage of satellite observation systems, however, is the extinction of solar radiation by the atmosphere first on its path downward to the earth surface and after reflection or scattering on its path to the satellite.
An immediate interpretation of measured data - the common case- introduces considerable errors from atmospheric masking. Therefore, the correction of the atmosphere's influence is the prerequisite for making full use of satellite data for remote sensing of the earth surface.
Our goal is to produce an ecological map of the Nationalpark Berchtesgaden with the help of Landsat 5 Thematic Mapper data. The atmospheric correction relies above all on the use of the spectral properties of lakes in different altitudes.

Thematic Mapper

For ecological mapping Landsat 5 Thematic Mapper is at present the instrument suited best. It measures the spectral radiance in seven bands, three of them in the visible (ch. 1 centered at 0.49 µm, ch. 2 at 0.57 µm, ch. 3 at 0.66 µm), one in the near infrared (ch. 4 at 0.84 µm), two in the middle infrared (ch. 5 at 1.68 µm, ch. 7 at 2.22 µm) and one in the thermal infrared (ch. 6 at 11.04 µm). Each picture element for channels, 1, 2, 3, 4, 5 and 7 has a size of approximately 30 * 30 m^2 and for channel 6 of 120 * 120 m^2.

Calibration

For the conversion of digital numbers (DN) into spectral radiances (L) the linear equation $L = a_0 + a_1 * DN$ is used, where a_0 is the offset and a_1 the gain. Unfortunately there is no valid standard calibration for Thematic Mapper. If one uses the values distributed by NASA and ESA, negative radiances occur in channels 4, 5 and 7 over rather dark surfaces like lakes, slopes in shadow or cloud shadows. *Price* (1989) mentions, that the offsets of all channels are too low and should be positive rather than negative. New calibrations by *Richter* (1990) show, that prelaunch gain data are not too bad, but offsets are too low. During our application even his new offset values were found to be too low. So we had to determine new offsets.
Our approach as well as the atmospheric correction lateron are based on the spectral properties of water in the near and middle infrared. While in the visible channels a considerable part of the signal at the satellite comes from below the water surface, the penetration depth at higher wavelengths is virtually zero (ch. 4: 36 cm, ch. 5: 1.5 mm, ch. 7: 0.6 mm). Therefore, for clear, oligotrophic water there should be no underlight observable even for channel 4.
All radiances measured over water by satellite should be only due to the influence of the atmosphere as long as the wind speed is low and the zenith-angle of the sun is above 10°. Such a minimum radiance measured over a water surface without underlight is still composed of three parts (cf. Fig. 1):

A) Light scattered backwards from the incident solar beam by atmospheric molecules and aerosol particles.
B) Forward scattered incident solar light specularly reflected at the water surface towards the satellite.
C) Light scattered forward towards the satellite after specular reflection of the direct solar beam at the water surface.

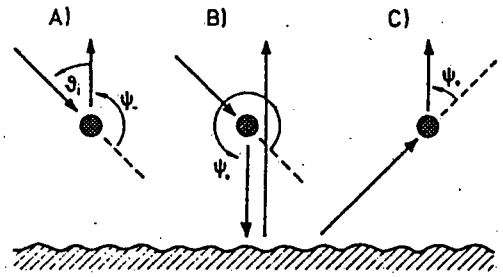

Fig. 1: Components of scattered and/or reflected sun light at satellite altitude; taken from Krüger (1989).

If the digital number of a pixel over water is zero, at least this above mentioned radiance should have arrived at the satellite. As this is indeed the case over some of the lakes in our satellite scene, this radiance is used as the new offset. We calculated these offsets (table 1) for August, 9, 1986, a rather clear scene, but they should be valid for the whole year.

Table 1: New offset values a_0 of the TM calibration curve in W/(m² sr µm).

channel 4	0.29810
channel 5	0.01719
channel 7	0.00392

Atmospheric correction

The following steps were taken to correct the atmosphere's influence:

1. First we had to find homogeneous surfaces such as lakes or plane snow. In our case only lake surfaces were suitable.
2. Second we averaged DN over cloudless lake centers, thereby even using small lakes. Plotting these values for channels 4, 5 and 7 as a function of height we expected a stronger atmospheric signal over low-lying lakes. But no height dependence could be recognized. Even two neighbouring lakes (Waginger See and (x) Tachinger See (*)) had a significantly different averaged signal (cf. Fig. 2).

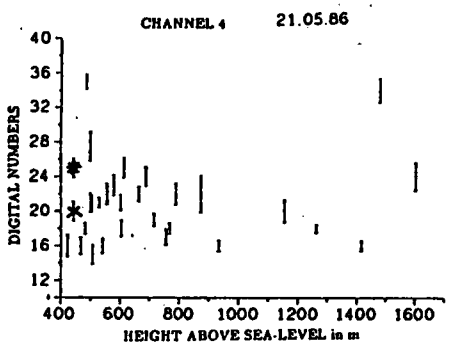

Fig. 2: Averaged DN of all lakes together with their standard deviation versus height above sea level.

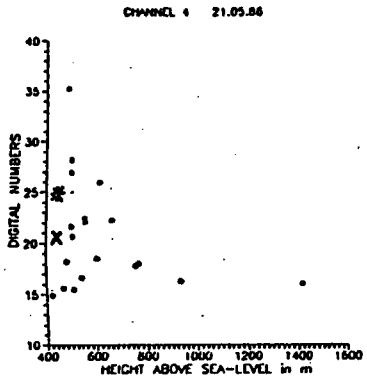

Fig.3: Average DN of darkest pixels for all larger lakes versus height above sea level.

We tried to improve the height dependence by omitting the smaller lakes, which might be influenced by surrounding highly reflective areas. But we did not get better results. Next we thought, the radiance differences might be due to the satellite's scan direction, which could have a great influence in our case, because most lakes are extended vertical to the scan direction. After examination of the Attersee we could exclude this possibility, too.

The most likely explanation left then was the existence of surface microlayers covering the lakes, which reflect more strongly than a water surface.

3. We hoped to find clear water areas by just using the darkest pixels of channels 4, 5 and 7, thereby accounting for radiometric noise. But even these averages over darkest values showed no height-dependence. It seems, that most of the lakes are covered rather unifomly by surface films (cf. Fig. 3) of different thickness and properties. If an aerosol difference would have been the cause a stronger decline of the difference towards infrared wavelengths should have been visible.
4. In order to confirm the hypothesis of surface microlayers, we examined the wavelength dependence of the signal. In the case of the two above mentioned neighbouring lakes we could show, that the spectral radiance over the Tachinger See in May is higher in all six channels (cf. Fig. 4), thus pointing to microlayers with constantly higher reflection (higher refractive index) on top of this lake.
5. After all these unsuccessful attempts to correct for the atmosphere's influence we tried to make the atmospheric correction with the help of all visible channels because the influence of aerosols and molecules is highest in these channels. By using only the darkest lake pixels the influence of underlight should be minimized. This method seems to be successful as long as the surface films are not too stong. In a spring scene (May 21, 1986)

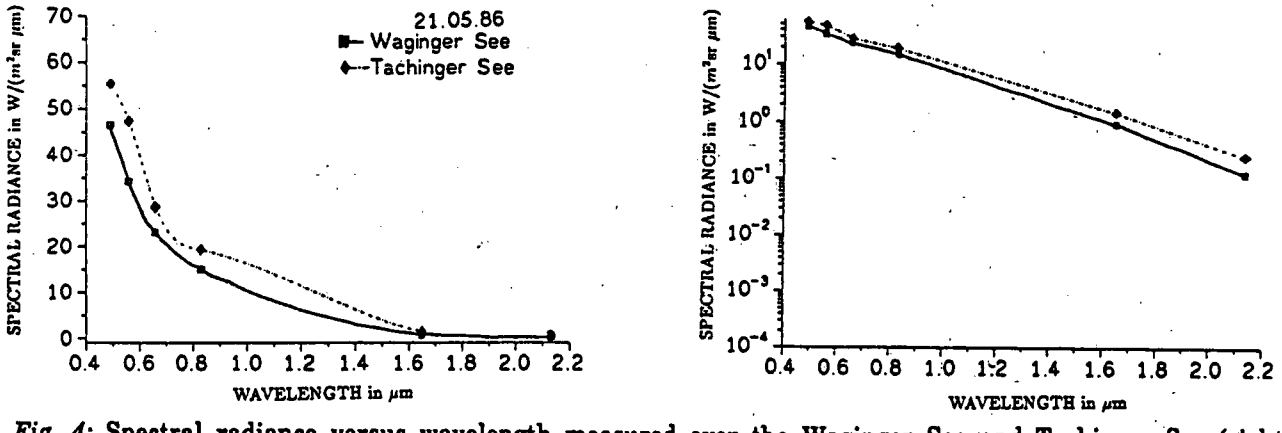

Fig. 4: Spectral radiance versus wavelength measured over the Waginger See and Tachinger See (right: logarithmic ordinate).

we cannot detect a height dependence, but for summer and autumn it looks promising. To exclude the influence of molecular scattering we subtracted Rayleigh-scattering from the measured radiance. The results are shown in figure 5.

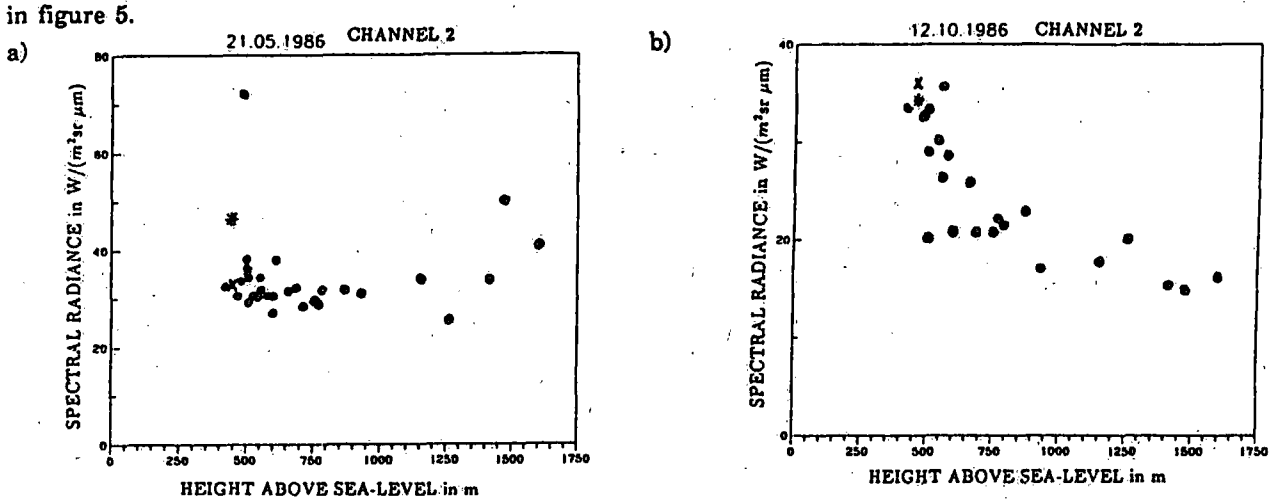

Fig. 5: TM radiances over all lakes minus molecular scattering, i.e. aerosol path radiance, in spring (a) and autumn (b).

In order to roughly assess the validity of the aerosol path radiance height profile we have to compare it to a standard atmosphere with different aerosol types. For a first comparison we have used tables given by *McClatchey* (1972) and calculated values for a standard atmosphere which agreed very well to the satellite measured radiances over lakes for the October case.

The correction valid over water has to be adapted to all other parts of the scene reflecting more strongly. Here we follow *Krüger* (1989), who has modified the radiative transfer model of (1983) to correct the atmosphere over near-ocean land surfaces. Since the satellite signal only allows the derivation of an apparent reflectance before correction, an algorithm using the apparent reflectance is necessary. Simulations with a radiative transfer model for many surface reflectance values have shown, that a simple linear relation between satellite measured radiance L_{SAT} and upwelling radiance at the surface L_{SURF} exists. Knowing the coefficients a and b of a regression of the form $L_{SURF} = a\, L_{SAT} + b$ the corrected L_{SURF} can be calcuated. *Krüger* was able to show, that the amount and sign of this correction is not only dependent on the aerosol type, but also on the reflection factor of the surface (cf. Fig. 6) and on wavelength.

The lower the reflection the higher is the relative correction, thus increasing the relative radiance differences in a corrected scene. Depending on the reflection factor of a surface, the necessary correction for a small optical thickness may be larger than for a high optical thickness. As shown in figure 6 for channel 4 it is even possible, that the satellite measured spectral radiance is too low, because the absorption by aerosol particles is higher than backscattering. For a reflection of 75% (fresh snow) and a high optical thickness of urban aerosols this effect may amount up to 12% of the signal, which corresponds to about 13 W/(m^2 sr µm). In this case they have to be added to the satellite radiance.

Outlook

The wavelength dependent reflection of soils, vegetation, rocks, snow and other surfaces is the basis of thematic mapping. But, as shown by *Krüger* (1989) and others this reflection is masked by the atmosphere in a rather complicated way. There must be big errors by using the unmodified satellite radiances. As shown by *Krüger* (1989) by two classifications, one with and one without an atmospheric correction for a coastal area the improvement is considerably. Even *Richter* (1990), who uses only a standard atmosphere and radiosonde data to correct, was able to improve the data set. We hope to do even better by using the in-scene information over water surfaces and applying it in a height-dependent fashion to an alpine scene. Only after this when ever possible height dependent correction the scene will contain the maximum information on surface types, facilitating thematic mapping. We will apply the correction established now to four scenes in the course of a year soon.

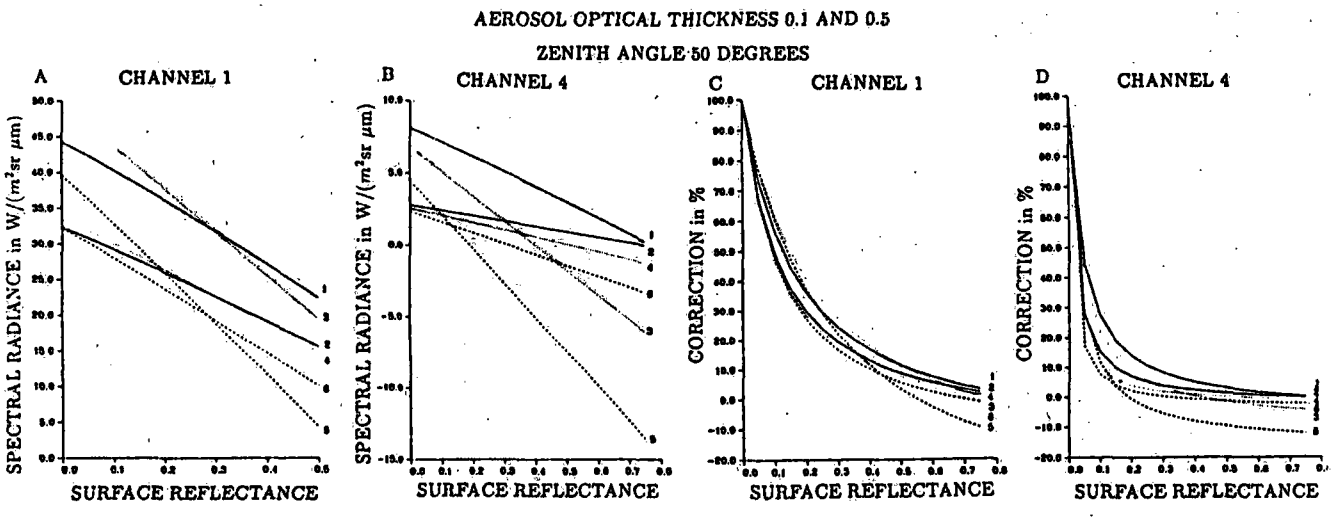

Fig. 6: Spectral radiances to be corrected [W/(m^2 sr µm)] [A, B], in per cent of the satellite measured radiance [C, D], for channels 1 and 4 of TM depending on surface reflectance for three different aerosol types, each with an optical thickness of 0.1 or 0.5
1), 2) maritime aerosols; 3), 4) continental aerosols; 5), 6)

Literature

Fischer, J. (1983): Fernerkundung von Schwebstoffen im Ozean. Dissertation, Universität Hamburg.

Krüger, O. (1989): Atmosphärenkorrektur von Thematic-Mapper-Messungen über Wattengebieten der Deutschen Bucht. Diplomarbeit, Universität Hamburg.

Price, J. (1989): Calibration comparison for the Landsat IV and V multispectral scanners and thematic mappers. in: Applied Optics, Vol. 28, No.. 3, 465-471.

Richter, R. (1990): A fast atmospheric correction algorithm applied to Landsat TM images. in: Int. J. of Remote Sensing, Vol. 11, No. 1, 159-166.

First results of tracer experiments over complex Alpine terrain: TRANSALP

R. Lamprecht
Paul Scherrer Institute, CH-5232 Villigen PSI

Abstract-Within the frame of the TRANSALP project in Switzerland tracer release studies were performed in prealpine valleys in the Canton Ticino at two selected days during October 1989. The objectives of these experiments were to investigate the behavior of pollutant dispersion in drainage flows during daytime and to test the performance of computer models for predicting pollutant immission concentrations in such complex terrain. An astonishingly good agreement between measured and calculated ground level concentrations was achieved even with the simple Gaussian plume formula expecting flat terrain. The assumption of channeled flow in these valleys could be confirmed by the experiments under the meteorological condition of thermally induced valley breeze in autumn.

1. Introduction

TRANSALP, a subproject of TRACT within the frame of EUROTRAC, intends to investigate the transport and diffusion properties of airborne material within the Planetary Boundary Layer over Swiss Alpine terrain in order to identify the main transport channels, including an estimate of flow rates, leading from the western Po Valley to the Swiss Plateau and vice versa.
Atmospheric dispersion processes are usually investigated by releasing tracers. Such an experiment was performed by Paul Scherrer Institute, Switzerland together with the European Joint Research Center at Ispra, Italy, in the Canton Ticino near the Italian-Swiss frontier in October 1989. This experiment was intended to be the starting point for a series of future experiments performed in order to prepare for a full-scale trans-Alpine tracer experiment, tentatively anticipated for 1993.
The scientific objectives of the initial experiment described in this paper were to investigate the structure of drainage flows and the behavior of tracer gases released in a valley during daytime.
In addition to allowing direct predictions of impacts of pollutants emitted within this region, these data can be used to test the validity of numerical models.

2. Experimental Details

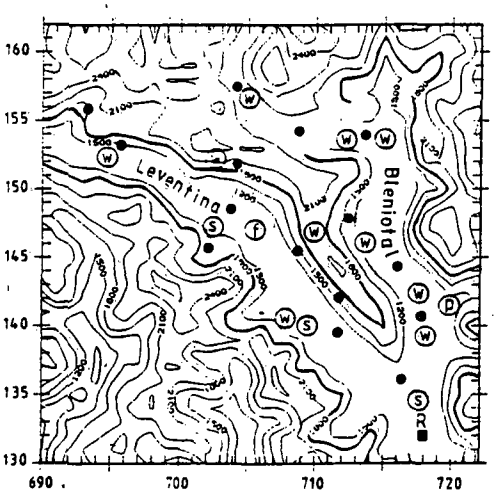

Fig. 1 Outline of the experimental area and locations of the operated instruments.

- *w*: Mast for wind and temperature measurements
- *s*: SODAR
- *f*: Tethered balloon
- *p*: Pilot balloon
- *R*: Tracer release point
- ●: Typical sampler locations

The experimental area for the initial experiment of TRANSALP was restricted to the Leventina and Blenio valleys, north-west of Bellinzona due to the assumption that north-south directed valleys are expected to represent one of the main entrances for air pollutants originating from the western Po Valley leading to the Swiss Plateau.
The Leventina bifurcates at Biasca where the smaller Blenio valley branches out. This latter valley leads to the Lucomagno pass, whereas the Leventina ends at Airolo with the beginning of the San Gottardo alpine barrier in the north. In the south, the Leventina bifurcates with the Mesolcina valley before joining the Magadino plain at Bellinzona.
Thanks to the supplemental instrumental assistance of different Italian institutes, we could finally operate three SODAR, 10 meteorological ground stations equipped with anemometers and temperature and humidity sensors, one tethered balloon, a pilot balloon system and one sonic anemometer-thermometer at the tracer release point for measurements of atmospheric turbulence parameters. The region of investigation and the location of the different instruments is depicted in Figure 1.
Two tracer experiments were carried out on October 5th and 19th, 1989. The tracer release took place at both times in the morning between 10 am and 11 am, with the development of the valley breeze.

Due to the low detection limit and the very low background of perfluorocarbon tracers, the chemical C_7F_{14} was released. The release point was located at Iragna south of Biasca. The release height was 8 m a.g.l. and the rate of emitted tracer 4 g/s. The immission of this species was registered with 60 sampler units at several locations along the bottom of the valleys and upslope the hills. Each sampler station contained 8 sampling bags which were filled consecutively with an integration time of 30 minutes. The recordings of the tracer plume at higher levels were performed with a motorglider.

3. Meteorological Analyses

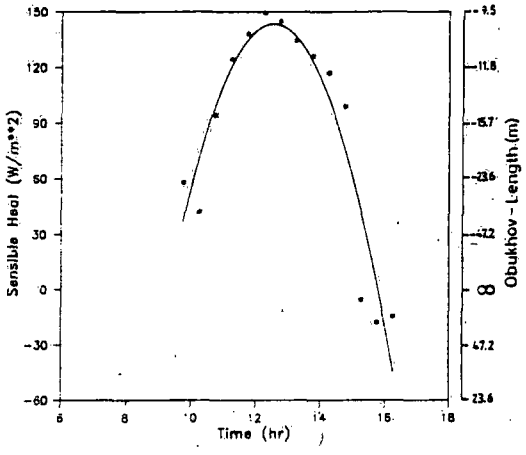

Fig. 2 Measured sensible heat flux.

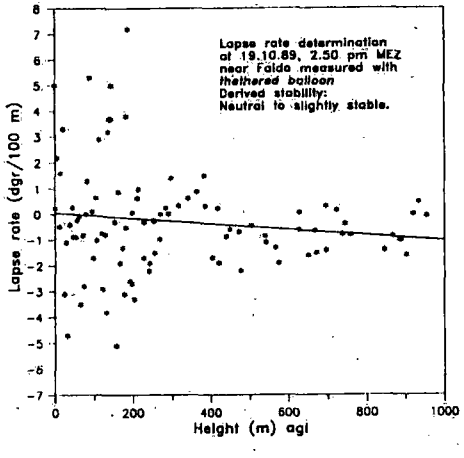

Since the analyses in section 4 are focused on the second experiment performed on October 19th, the following characterizations of the meteorological conditions shall also be restricted to this period. A first analysis revealed a better reliability of the data acquired during the second experiment.

The meteorological conditions chosen for the experiments were thermally induced local wind regimes called Inverna. The synoptic weather conditions showed a flat pressure distribution over the Central Alps with north foehn aloft.

Some supporting meteorological data from the continuously working 12 m high masts and echo sounders distributed over the area of concern are summarized in Table 1.

For the determination of the sensible heat flux and hence the atmospheric stability at ground level a Kaijo-Denki sonic anemometer-thermometer was used. The results of these measurements are mainly representative for sunny regions of the experimental area, since the instrument was measuring under sunny conditions during the execution of the tracer experiment. The time dependence of the measured sensible heat flux is presented in Fig. 2. In addition to stability estimations at ground level for sunny conditions, hourly tethersonde profiles of the vertical temperature and humidity distribution for the determination of the lapse rate in shady regions were performed. The result of these measurements revealed a neutral to slightly stable atmosphere in the absence of irradiation as can be seen from Fig. 3. A further vertical distinction of the derived stability, particularly near ground level, is due to the poor quality of the data not possible.

Fig. 3 Tethersonde lapse rate determination for shady regions.

Type of Instrument	Location (Swiss Coordinates)	Height of measurement [m] asl, agl	Wind velocity [m/s]	Wind direction [dgrs] Ann.
1) SODAR	718.1, 131.8	347, 60	1.3	148
		587, 240	4.3	155
2) SODAR	711.3, 138.8	400, 50	4.5	168
		600, 250	5.3	160
3) SODAR	702.5, 148.4	1300, 60	2.7	86
		1480, 240	3.1	97
3) Mast	702.8, 151.6	1862, 12	1.4	146
3) Mast	694.9, 152.5	1019, 12	2.2	124

Wind conditions over the experimental area at October 19th between 1) 10 to 11 am, 2) 0.30 to 1 pm and 3) 1 to 2 pm.

Table 1

Ann.: The azimuth of the outgoing wind was defined with respect to the south axis.

4. Tracer Plume Analysis

The analysis of the data concentrates mainly on a comparison of the measured downwind, crosswind and vertical tracer concentrations with immission calculations based on simple bi-Gaussian plume estimations and calculations performed with a particle trajectory model. A short outline of the applied trajectory model is given in [1]. Our aim of applying dispersion models to the measured tracer concentrations is to analyze the experimental data in order to get a better understanding of the dispersion characteristics under these particular topographical conditions. In the present case the most interesting question was to evidentiate to which extent air pollutants were trapped and channeling occurred in the considered valleys under the meteorological conditions of up-valley breeze in autumn.

On the other hand the application of models to dispersion experiments particularly if performed in complex terrain allows to test the performance of a model in dependence of a certain amount of measured meteorological information.

Figure 4 now depicts the time integrated tracer concentrations measured in the Leventina and Blenio valleys. As the Figure shows, most of the tracer entered the Leventina valley. The ratio of the time integrated concentrations measured in the two valleys is approximately between 1:4 to 1:5. The measurements in the upper Leventina were not used for this consideration since the plume had arrived this area before the sampling was started.

In section 3 we have already seen that the atmosphere over sunny area in the early afternoon yielded an Obukhov-Length of approximately -15 m according to the sonic anemometer measurements. On the other hand the lapse rate determination from tethered balloon soundings delivered a neutral to slightly stable atmosphere in shady regions up to a height of 1000 m. From these two stability measurements a slightly convective atmosphere for both valleys was estimated. This assumption is further supported by the relative strong wind situation that occurred particularly in higher altitudes. Strong advection lowers the unstability of the atmosphere. For the bi-Gaussian plume calculations stability class C according to Pasquill was used in combination with the parameterization scheme recommended by Briggs [2]. The random walk model produced the best results with an Obukhov-Length of -65 m.

Estimates of concentrations based upon the Gaussian model require the knowledge of the mean wind velocity. In accordance to the measured wind fields in the two valleys the magnitude of the mean up-valley wind was determined to be 4 m/s.

On the basis of these assumptions characterizing the meteorological situation we primarily performed simple Gaussian dispersion calculations. The results obtained therefrom for the considered valleys downwind of the tracer source are depicted in Fig. 5 and Fig. 6, respectively. Furthermore a comparison with the measured maximum downwind concentrations is presented.

In the case of the Blenio valley the Gaussian model slightly overrates the measured concentrations at ground level for the assumptions met. The samplers located in the Blenio valley were lined up along the bottom of the valley up to the Lucomagno pass. In the Leventina the samplers were mainly distributed along the sunny south-west slope up to Quinto, 7 km north-west of Faido. Some samplers must have been located on the lee side of obstacles in order to explain the extraordinary low concentrations detected at certain points. The

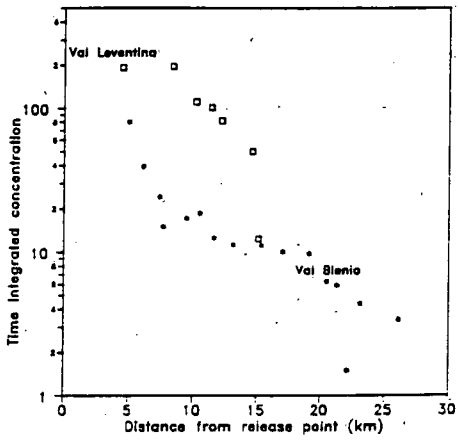

Fig. 4 Time integrated tracer concentrations measured in the considered valleys.

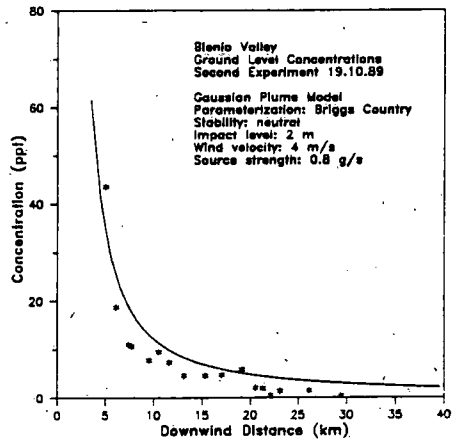

Fig. 5 Alongwind ground level concentrations in the Blenio valley.

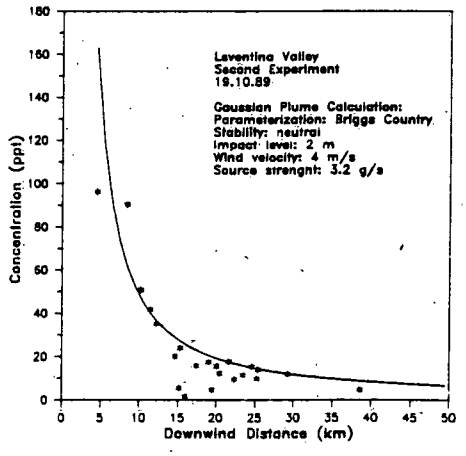

Fig. 6 Alongwind ground level concentrations in the Leventina valley.

scattering of the concentration levels is also caused by location deviations perpendicular to the plume centerline.

The most distant sampler was located on a serpentine of the Gotthard pass road. The maximum tracer concentration measured at this point was 5 ppt, slightly less than the predictions from the Gaussian formula for a ground level station at this distance. Apart from measurement and calculation uncertainties a possible explanation for this observation might be due to the height of the regarded sampler station of 380 m above the bottom of the valley, whereas the calculation refers to ground level concentrations.

Uphill the south-west slope above Faido, the most critical area in the Leventina where tracer overflow to the Blenio valley was expected, a vertical concentration profile was measured by motorglider.

The result of this measurement is depicted in Fig. 7 together with the predictions of the Gaussian formula again using the same parameters discussed above. The discrepancy between measured and calculated concentrations is due to bad time synchronization of the measurement. The tracer sampling during this flight took place approximately 1 hour after the maximum of the tracer plume passed by. According to calculations the estimated maximum flow rate of tracer traversing the regarded mountain crest at 2700 m a.s.l. has not exceeded 1/5 of the maximum flow rate measured in the valley at the same source distance. Therefore no upslope transport removed significant quantities of tracer-laden air before it reached the upper valley. This may account for the rather well agreement between observed and expected tracer concentrations in the upper Leventina valley.

In order to determine the crosswind concentration of the tracer plume in the vicinity of Faido, perpendicular to the valley axis a line consisting of 4 samplers was created. The outermost sampler west of the valley was exposed at Gribbio nearly on the top of a slope building a sort of channel leading down to the Leventina valley. The measured crosswind profile is depicted in Figure 8 including again the results obtained from the Gaussian plume formula. The maximum of the concentration distribution was measured at Campello on the sunny south-west slope, 1.5 km apart from the valley axis. This observation suggests that the plume centerline was located above the south-west slope of the valley. Further confirmation for this suggestion was obtained from constant density balloons which were always lost on the Leventinas south-west slope.

The regular arrangement of the samplers along the bottom of the Blenio valley favorites a comparison of the measured ground level concentrations in this area with a corresponding particle trajectory model calculation. Since the Blenio valley is aligned quite precisely from north to south, differential heating at the valley slopes should not occur in the early afternoon. Thus the maximum tracer concentration is assumed to be found in the middle of the valley at this time. For that purpose a Monte Carlo simulation was performed on a mass consistent windfield obtained from the diagnostic wind model CONDOR [3]. The input data for that model was supplied by the meteorological network which was measuring permanently during October 1989.

In contrast to the Gaussian model the trajectory model considers terrain features indirectly through the interpolated windfield. One result obtained with the particle model is depicted in Fig. 9. The employed parameters are indicated in the graphics plot. The stars denote the measured and the triangles the calculated ground level concentrations.

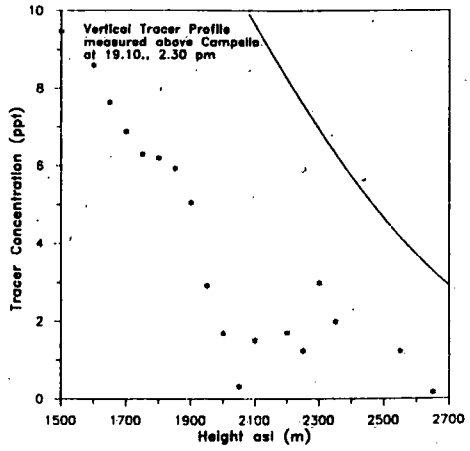

Fig. 7 Measured time delayed vertical tracer profile compared with Gaussian plume predictions for the maximum concentrations.

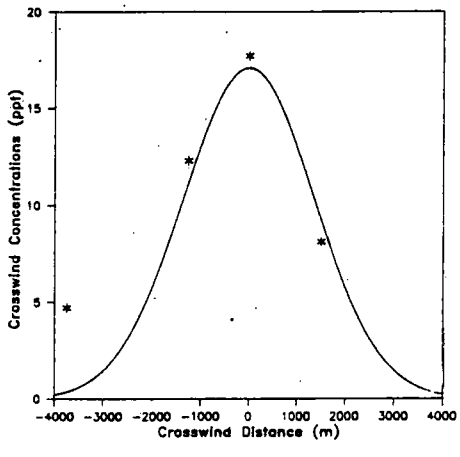

Fig. 8 Measured and calculated crosswind concentration profile near Faido.

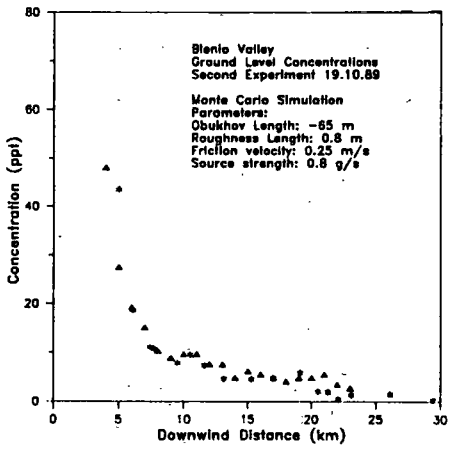

Fig. 9 Result of a trajectory model run for the Blenio valley along with the measured concentration levels.

5. Discussion

The available data set provides estimates of tracer dilution in the prealpine valleys Blenio and Leventina along with sufficient meteorological data to perform model calculations.
Apart from an expected shift of the plume centerline towards the south-west slope of the Leventina due to differential heating, the plume dispersion characteristics at ground level were obviously not unlike than over flat terrain which is rather surprising at first sight. This conclusion can be drawn according to the rather consistent agreement between the results obtained from the simple Gaussian plume formula and the measured downwind and crosswind concentrations.
The principal difference between homogeneous flows over flat terrain and channeled valley breezes consists in the different turbulence structure within these different flows. Thus the particular terrain features of a north to south directing broad valley are assumed to influence the dispersion characteristics of a plume in the early afternoon only by additional large scale eddies. Specifically at the bottom of the valley, additional terrain induced eddies give rise to an enlargement of the lateral dispersion parameter, i.e. a plume is assumed to disperse faster than over flat terrain under similar atmospheric stability. In the most extreme case, significant amount of tracer gets entrained by the up-slope flow layer out of the valley. This mechanism was reported by Willson et al. [4] for the narrow San Miguel valley, Colorado. A similar observation was not confirmed for the Blenio and Leventina valleys due to the rather good agreement between measured and calculated downwind ground level concentrations in both valleys which strongly evidentiates the conclusion of channeled flow without significant loss of tracer. But an increased lateral dispersion in relation to flat terrain must also be taken into account. A direct verification of this suggestion however has not been tried since plume dispersion specifically at ground level is strongly influenced also by other reasons than only due to atmospheric stability. A separation of all these effects might be challenging.
The predictive power of more refined models for dispersion calculations over complex terrain is limited as long as detailed turbulence and wind data had not been measured or an input from a boundary layer model is not available. Thus the application of a particle trajectory model to interpret the measured data did not produce significantly different results than the simple Gaussian formula. The introduction of the measured windfield which considers certain terrain features and thus velocity and direction irregularities of the flow slightly improved the accuracy of the dispersion predictions. This was shown in the case of the Blenio valley.

Acknowledgements-The author wishes to thank the Italian tracer group under the leadership of Dr. P. Gaglione from the Joint Research Center at Ispra for their participation in the experiments. Without their support, these tracer experiments would never have been possible. I am also indebted to Mr. G. Merki from PSI for his analyses of the meteorological data as well as for calculating mass consistent windfields as input for the random walk model.

References:

[1] Lamprecht, R. (1989): Modelling of air pollution dispersion with a Monte Carlo diffusion model. Newsletter in PSI annual report 1989 for General Energy Technology.

[2] Pasquill, F; Smith, F.B. (1983): Atmospheric Diffusion. Publisher: Ellis Horwood Ldt. Chichester. 3rd edition pp. 339.

[3] Moussiopoulos, N; Flassak, Th; Knittel, G. (1988):A refined diagnostic wind model. Environmental Software, Vol. 3, No. 2.

[4] Willson, R. et al. (1983): Characterisation of the transport and dispersion of pollutants in a narrow mountain valley region by means of an atmospheric tracer. Atmospheric Environment, Vol. 17, No 9, pp. 1633-1647.

Section 2:

Weather Prediction: Analysis and Forecasting of Synoptic and Mesoscale Systems

What Did We Learn From ALPEX?

Joachim Kuettner
National Center for Atmospheric Research
Boulder, Colorado, U.S.A.

The answer to this question can only be a subjective one as it depends on the degree of one's ignorance. It will also be incomplete in the sense that it cannot cover the whole ALPEX literature which now has reached many hundreds of papers. I, therefore, arbitrarily have selected four major scientific subjects: Lee Cyclogenesis; flow splitting and blocking; mountain drag, and Bora. The major deficiency of this selection is the foehn problem, however, this is due to a lack of cooperation by Mother Nature who preferred to bless us, during the special observing periods (SOP) with many lee cyclones rather than a good case of south-foehn.

1. Lee Cyclogenesis

There were about 8-10 such events -- perhaps not all genuine mountain induced depressions -- resulting in an unprecedented observational material on lee cyclones.

Pichler and Steinaker (1990) have analyzed 8 of the ALPEX SOP cyclones and produced a beautiful Atlas that has just appeared. In addition, they have studied all lee cyclones during the full ALPEX year, a total of 40 (Pichler and Steinacker, 1987), and have arrived at two main types of lee cyclogenesis, the "Vorderseiten" (frontside) type with prevailing southwest upper flow (Fig. 1) and the "Überströmungs" (overflow) type with northwesterly upper flow (Fig. 2). This is probably the most comprehensive study of alpine lee cyclogenesis available today.

A series of careful case studies has resulted in some remarkable conceptual or, one may say, "phenomenological" models. These are, in my opinion, among the most important results of ALPEX, as they elucidate the common physical mechanisms underlying lee cyclogenesis. According to Bleck (1990), Tafferner (1990), McGuinley and Zupanski (1989) and their co-workers, lee cyclogenesis is due to the interaction of a traveling upper-level IPV (Isentropic Potential Vorticity) center approaching the Alps and a low-level vorticity center locked on the lee side.

The upper center is a large 3-D perturbation of external origin that travels jointly with a cold dome beneath towards the Alps. The mountain barrier stops the cold dome, but the upper-vorticity center continues its travel. The associated jetstreak is suddenly out of thermal equilibrium. In the meantime, a low-level vorticity center forms on the leeside coincidental with the upstream blocking action. This represents the first phase of lee cyclogenesis. The second phase of deepening occurs when the two IPV centers get into the proper vertical phase (Fig. 3 after Bleck, 1990).

What is most interesting is that this is precisely the mechanism of cyclogenesis postulated by Hoskins, McIntyre, and Robertson in their classical 1985 paper. The severe cyclones on the east coast of the North American continent, recently explored in the GALE and ERICA Projects, show the same organization of upper and lower IPV centers, the lower one being generated by diabatic heating over the Gulf stream. As soon as the upper and lower centers come into the proper vertical phase, explosive cyclogenesis takes place. (Hibbard et. al., 1989). The two steps of pressure-fall were already discovered by v. Ficker in 1920 who called them "primary and secondary pressure waves". Now their physical role has become clear.

ALPEX has also stimulated the development of new theories of lee cyclogensis. Only three shall be mentioned here: the theory of the Bologna group (Speranza, Buzzi, Trevisan, Malguzzi, 1985 to 1987); that of Pierrehumbert (1985); and the theory of Smith (1984, 86). All three are linear, quasi-geostrophic theories of a baroclinic flow crossing an idealized mountain, whereby the mountain generates or deepens a baroclinic wave. By introducing a negatively sheared flow with a critical (zero wind) level, Smith asserts that the deepening wave remains stationary.

Egger (1988), in a quite sophisticated study, has tried to verify these theories by comparing them with a "generic", but realistic numerical simulation of lee cyclogenesis. None of the theories was capable of explaining the cyclogenetic process. After the forementioned conceptual results we cannot be too surprised: The crucial IPV centers are large 3-dimensional disturbances that can not be treated by linear theory. One must hope that an analytical model of the observed mechanisms may be achieved in the future. Because of its highly non-linear nature this will not be easy.

2. Flow Splitting and Blocking.

Occasionally, if rarely, one encounters something totally unexpected in a field project. That happened to some extent in ALPEX on 9 April 1982 when two long-range aircraft were sent on a circumferential flight track around the Alps in the hope to penetrate somewhere a fast moving cold front. They did not accomplish that, but instead got something more interesting, namely, a precise picture of flow splitting. That in itself is not new: every child knows that water will rather flow around a stone than over it. What surprised us were two things: the one aircraft flying at about 2.8 km altitude encountered the described split-flow; the other aircraft flying only 600 to 1,000 meters higher saw nothing of that kind (Fig. 4). While the lower air masses managed to avoid the Alps by circumventing them, the upper flow seemed to ignore them and to be totally de-coupled from the lower flow. The second surprise was that the split point (or stagnation point) did not change during these long flights. After seven hours it was still near Lake Geneva.

Most course-grid models let the air masses flow over the mountains rather than around them because the mountain ranges are flat and shallow in these models. To preserve the steepness and height of the obstacle one uses tricks like the "envelop orography"; but the time is close where even global models will have mesoscale grids that will reproduce the mountain and the flow around them properly. However, the thin de-coupling layer is still surprising. Once the lower-level flow spills over the mountains and runs down the lee side, the de-coupling of the upper and low flows is well known, Smith (1985). Apparently, it can happen already upstream.

Closely related to the split flow is the upstream blocking of cold air. How far upstream is the flow decelerated? An interesting theoretical study by Pierrehumbert and Wymann (1985) has shown that, without Coriolis force, the flow can be blocked farther upstream than with it, depending only on the Froude number. In rotational flow it also depends on the Rossby number, actually on the ratio of the two numbers, and the typical blocking distance is of the same order as the Rossby radius of deformation, i.e., a few hundred kilometers in the case of the Alps. ALPEX observations bear that out. The deformation of an air parcel by blocking and flow splitting is impressively described by Pichler and Steinacker (1987) during 48 hours of cyclogenesis as seen in Fig. 5.

3. Mountain Drag.

Blocked cold air is also an important contributor to the mountain drag. The determination of the drag of the Alps was one of the scientific objectives of ALPEX. We are interested here in the effect of mountains on the atmosphere, not vice versa. Therefore, by definition, the drag exerted by the obstacle on the air is a vector directed against the flow (not with the flow as is common in aircraft studies, in case that surprises anybody). The definition of drag used here refers to 3 components: the surface (frictional) draft, the form drag, and the wave drag. The sum of the latter two is often called pressure drag, but the total pressure drag must also include the hydrostatic drag due to blocked air masses.

If one neglects the frictional surface drag, which is usually done, one can derive the pressure drag directly by measuring the pressure field at the mountain surface (if this can be done!). Several of the ALPEX scientists have tried that and it is interesting that all arrive at the same order of magnitude of the drag exerted by the Alps on the atmosphere, namely about 5 to 10 x 10^{11}N. I am referring to Hafner and Smith (1985), and Carrisimo, Pierrehumbert, and Pham (1988). If one extrapolates the measurements of Davis and Phillips (1985) on the Gotthard Pass to the total mountain range of the Alps, one finds a similar but slightly higher magnitude of the drag.

How much of this drag is wave drag? It is generally assumed that the wave drag is a small part of the total drag (see for example Emeis, 1990). Is that true?

A new study by Hoinka and Clark (1990) computes the drag values from a non-hydrostatic numerical model based on observed initial conditions for a strong foehn event in November 1982. Interestingly enough it yields values of the vertical momentum flux (that is the wave drag) which are a large percentage, say about half, of the total drag (Fig. 6). However, if one compares the computed value with that measured by aircraft it turns out that the computed value is about 6 times larger than the observed. Nevertheless, there are reasons why the observed values may not be representative of the total Alps as they were conducted on a marginal flight track. This remains an unresolved problem.

Why is it important to know the mountain drag? The net pressure due to mountains is an important consideration in the large-scale momentum budget. The horizontal and vertical distribution of the sub-grid contribution of this drag is a necessary component of gravity wave drag parameterization for General Circulation Models. With gravity wave lengths between 10 and 20 km. one has to use parameterization as long as this scale is not resolved in the model.

A new critical investigation by Clark and Miller (1990) using varying grid scales from 5 to 80 km for the forementioned south foehn case shows that "envelop orography" produces indeed realistic drag and momentum flux values and that, surprisingly, hydrostatic treatment is sufficient to describe the basic dynamics. The effects of model resolution and of hydrostatic treatment on the drag are shown in Fig. 7. Again, wave drag appears to be a fairly large fraction of the total drag.

4. Bora.

I come now to the last subject of my talk, the Bora. It's investigation was one of the scientific objectives of ALPEX. The Bora is generally known as a cold, severe downslope wind. It occurs everywhere in the world, but its name comes from the classical Bora of the Adriatic coast of Yugoslavia.

Four extended periods of three to five days each occurred during ALPEX over this coast. For the first time it was possible to explore the Bora thoroughly by instrumented aircraft. In a beautiful paper, Ron Smith (1987), who directed most of the flights, has described some of results.

The typical Yugoslavian Bora has a wind reversal in the mid-troposphere. This critical layer limits the height of the phenomenon. In the only case without wind reversal (25 March 82) lee waves propagated vertically throughout the troposphere, made visible by high wave clouds.

It has been suspected, for example by Pettré (1984) and by the Yugoslavian authors of this conference (Jurec, Bajic, and others) that the Bora is a hydraulic phenomenon,

whereby the fall winds reach critical velocity (that is the maximum phase speed of long waves) over the mountain crest and accelerate to a super critical "shooting flow" over the downslope. Further downwind they reverse back to subcritical flow in a severely turbulent hydraulic jump. Certainly some of the investigated cases resemble such hydraulic flow (Fig. 8-9). If there is a pronounced inversion over the cold air a simple relation of hydraulic theory between layer height, mountain height, and Froude number should hold: That seems indeed to be the case for the Bora.

But is there really a basic difference between Bora and Foehn or are they essentially the same flow phenomenon? Does it matter that the Bora is cold and Foehn warm? In, what I consider one of the most enlightening papers resulting from ALPEX, Klemp and Durran (1987) have shown that there is no basic distinction between the two. Even without an inversion, shooting flow occurs because of wave breaking aloft (Fig. 10). The severe downslope winds at low levels are surprisingly insensitive to variations in the upwind condition aloft.

If we consider the work done -- and being done by our Yugoslavian colleagues on "their Bora" -- we must conclude that the Bora studies of ALPEX have given an important impetus to fundamental research on air flow over mountains.

Conclusion

Having picked out only a few raisins from the large pie called "ALPEX" I feel that everybody should judge for himself what the answer is to the topic of this talk: "What did we learn from ALPEX?"

There is however, something else we learned, even if it is not strictly scientific. The organizer of this conference, Thomas Gutermann, was also the Operations Director of ALPEX. He, together with Hans Wanner, as his deputy, recognized early how important it is that young people participate in such an interesting venture and they arranged that these students could all live, cook, and sleep together in an air shelter (bunker) in Geneva while they spent their days with prominent scientists. This international "bunker gang", as it was called, became a crucially important part of ALPEX. They are now scattered throughout the world and many of them have already made fine careers as researchers, aviation experts, forecasters, artists, or even astronauts; and they still keep contact with each other. I hope, that they too have learned something from ALPEX, namely that science is not only serious business, but that it can be (and should be) fun. More importantly, they may have learned -- like we have -- that tolerant and enjoyable human relations are as important in such a large undertaking as science and technology. In fact, without this human dimension, the best science and technology turn out to be nearly useless.

References

Bleck, R., 1990: Personal communication, see also Bleck (1990a).

Bleck, R. 1990a: Depiction of upper/lower vortex interaction associated with extratropical cyclogenesis. *Mon. Wea. Rev.*, 118, 573-585.

Buzzi, A., A. Speranza, S. Tibaldi, and Tosi: A unified theory of orographic influences upon cyclogenesis. *Meteorol. Atmos. Phys.*, 36, 91-107.

Carissimo, B.C., R.T. Pierrehumbert, and H.L. Pham, 1988: An estimate of mountain drag during ALPEX for comparison with numerical models. *J. Atmos. Sci.*, 45, 1949-1960.

Clark, T.L. and M. Miller, 1990: Pressure Drag and momentum fluxes forced by the Alps. Part II: Representation in large-scale atmospheric models. Submitted to *Quart. J.R. Met. Soc.*.

Davies, H.C. and P. D.Phillips, 1985: Mountain drag along the Gotthard section during ALPEX. *J. Atmos. Sci.*, 42, 2093-2109.

Egger, J., 1988: Alpine lee cyclogenesis: verification of theories. *J. Atmos. Sci.*, 45, 2187-2203.

Emeis, S., 1990: Surface pressure distribution and pressure drag of mountains. *Meteorol. Atmos. Phys.*, 43, 173-185.

Hafner, T.A. and R.B. Smith, 1985: Pressure drag on European Alps in relation to synoptic events. *J. Atmos. Sci.*, 42, 562-575.

Hibbard, W., L. Uccellini, D. Santec, and K. Brill, 1989: Application of the 4-D McIDAS to a model diagnostic study of the President's Day cyclone. *Bull. Amer. Meteor. Soc.*, 70, 1394-1403.

Hoinka, K.P., and T.L. Clark, 1990: Pressure drag and momentum fluxes forced by the Alps. Part I: Comparison between numerical simulations and observations (submitted to *Quart. J. Roy. Meteor. Soc.)*.

Hoskins, B., M. McIntyre, W. Robertson, 1985: On the use and significance of isentropic vorticity maps. *Quart. J. Roy. Met. Soc.*, 111, 877-945.

Klemp, J. and D. Durran, 1987: Numerical modeling of bora winds. *Meteor. Atmos. Phys.*, 36, 215-227.

Kuettner, J., 1959: The rotor flow in the lee of mountains. GRD Research Notes No. 6, Geophysical Research Directorate, Air Force Cambridge Research Center, Bedford, Massachusetts, U.S.A..

Kuettner, J., 1986: The aim and conduct of ALPEX. *GARP Publications*, Series No. 27, WMO, Geneva, Switzerland.

Lanzinger, A., H., Pichler, R. Steinacker, 1990: *ALPEX Atlas*, Inst. of Met. and Geoph., University of Innsbruck, Austria.

McGinley, J., and M.Zupanski, 1990: Numerical analysis of the influence of jets, fronts, and mountains on alpine lee cyclogenesis. *Meteor. Atmos. Phys.*, 43, 7-20.

Pettrè, P., 1984: Contributions to the hydraulic theory of Bora wind using ALPEX data. *Beitr. Phys. Atmosph.*, 57, 536-545.

Pichler, H. and R. Steinacker, 1987: On the synoptics and dynamics of orographically induced cyclones in the Mediterranean. *Meteorol. Atmos. Phys.*, 36, 108-117.

Pierrehumbert, R., 1985: A theoretical model of orographically modified cyclogenesis. *J. Atmos. Sci.*, 42, 1244-1258.

Pierrehumbert, R. and B. Wyman, 1985: Upstream effects of mesoscale mountains. *J. Atmos. Sci.*, 42, 977-1003.

Smith, R., 1984: A theory of lee cyclogenesis. *J. Atmos. Sci.*, 41, 1159-1168.

Smith, R.B., 1985: On severe downslope winds. *J. Atmos. Sci.*, 42, 2597-2603.

Smith, R.B., 1986: Further development of a theory of lee cyclogenesis. *J. Atmos. Sci.*, 43, 1582-1602.

Smith, R.B., 1987: Aerial observations of the Yugoslavian Bora. *J. Atmos. Sci.*, 44, 269-297.

Speranza, A., A. Buzzi, A. Trevisan, P. Malguzzi, 1985: A theory of deep cyclogenesis in the lee of the Alps. Part I: Modification of baroclinic instability by localized topography. *J. Atmos. Sci.*, 42, 1521-1535.

Tafferner, A, 1990: Lee cyclogenesis resulting from the combined outbreak of cold air and potential vorticity against the Alps. *Meteorol. Atmos. Phys.*, 43, 31-47.

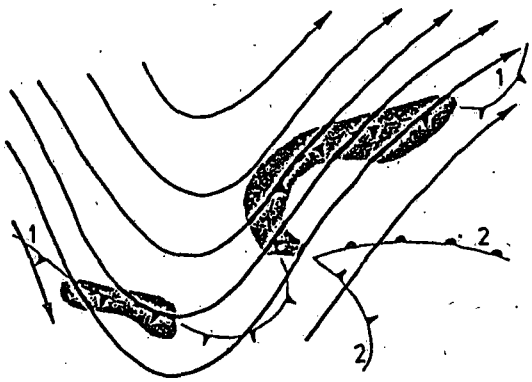

Fig. 1: Frontside ("Vorderseiten") type of Alpine lee cyclogenesis. Upper-level flow across Alps from southwest. (After Pichler and Steinacker, 1987.)

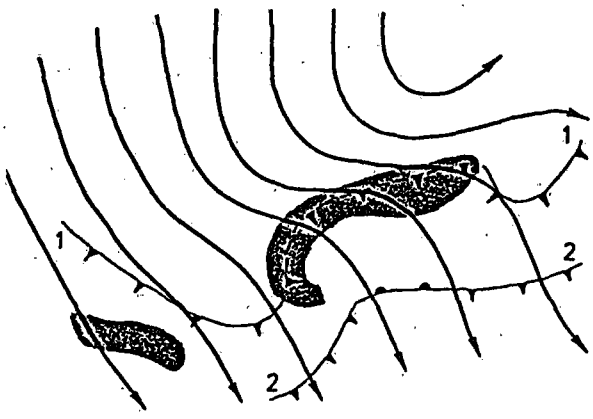

Fig. 2: Overflow ("Überströmungs") type of Alpine lee cyclogenesis. Upper-level flow across Alps from northwest. (After Pichler and Steinacker, 1987.)

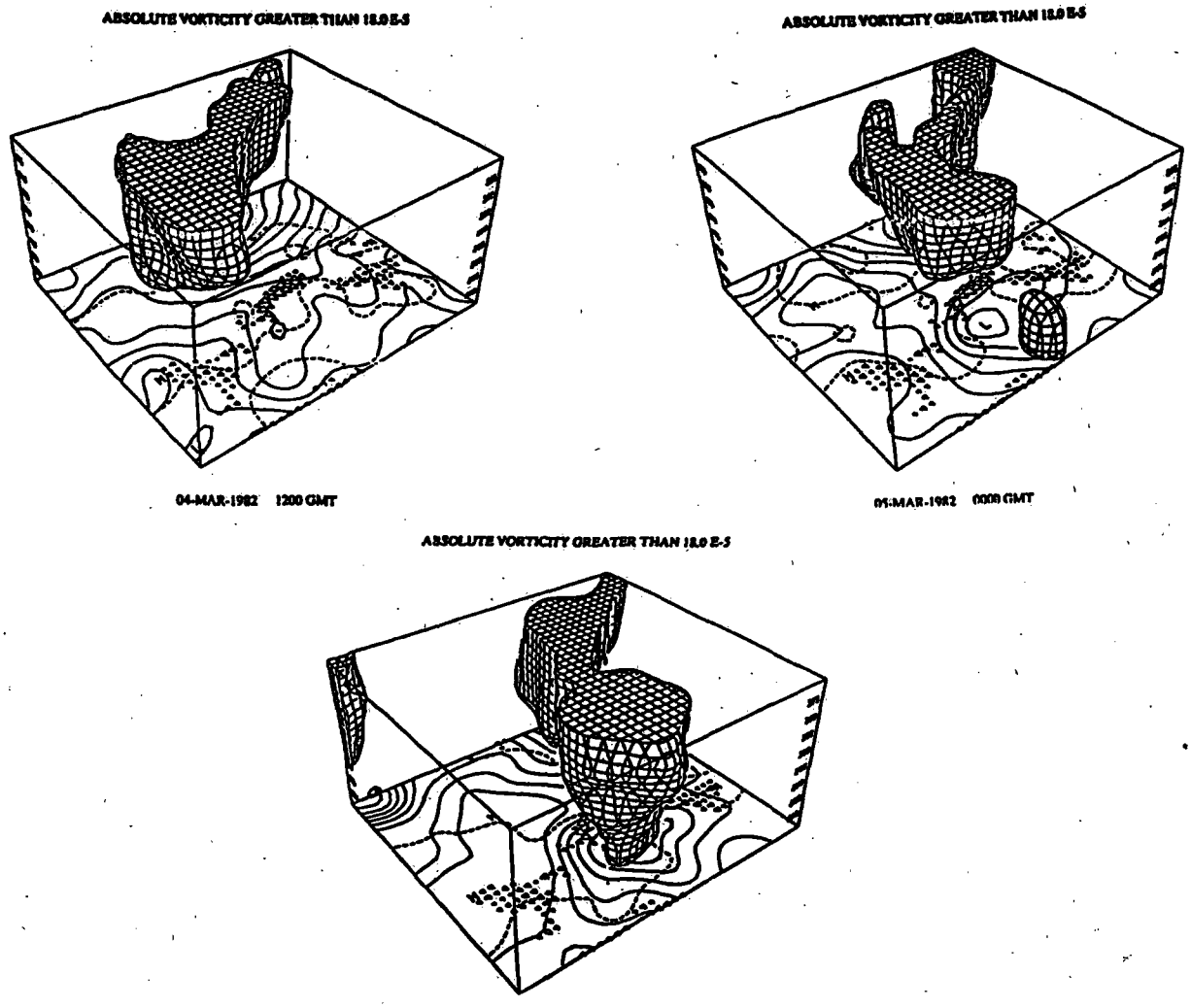

Fig. 3: Lee cyclogenesis (12-hour intervals, 4 to 5 March 1982) associated with the approach of an upper vorticity center north of the Alps (upper left) and a lower vorticity center developing south of the Alps (upper right). The mature stage is reached when the two centers join vertically (lower figure). (After Bleck, 1990.)

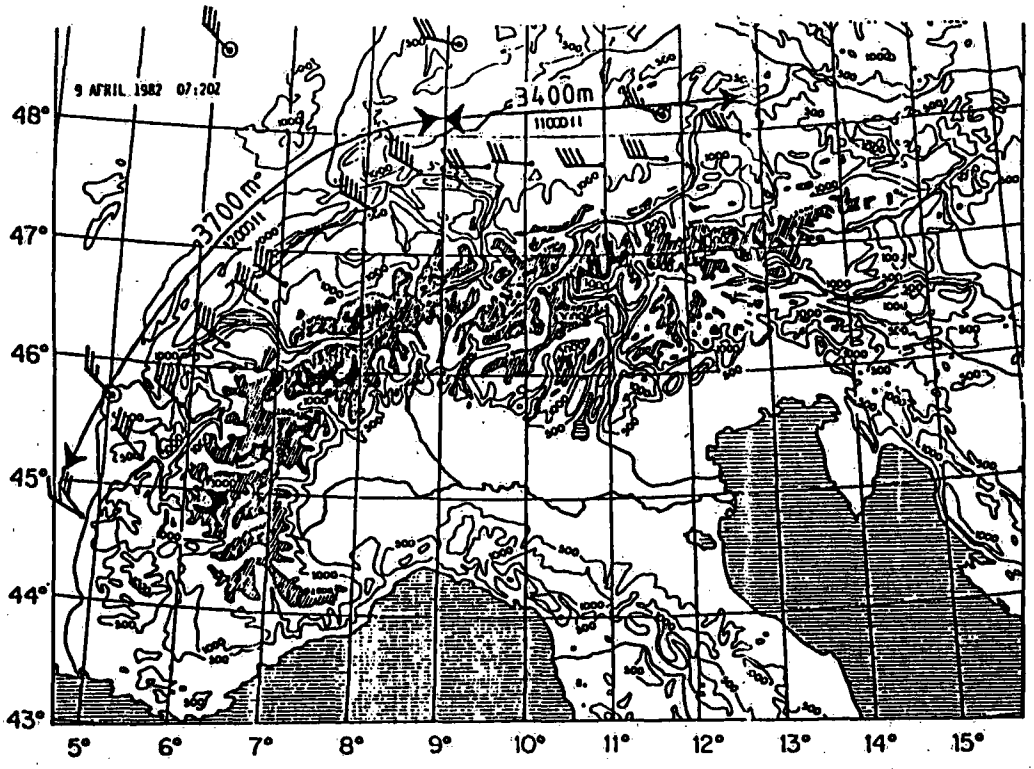

Aircraft measurements on 9 April 1982 at 3400 to 3700 m - Electra flight

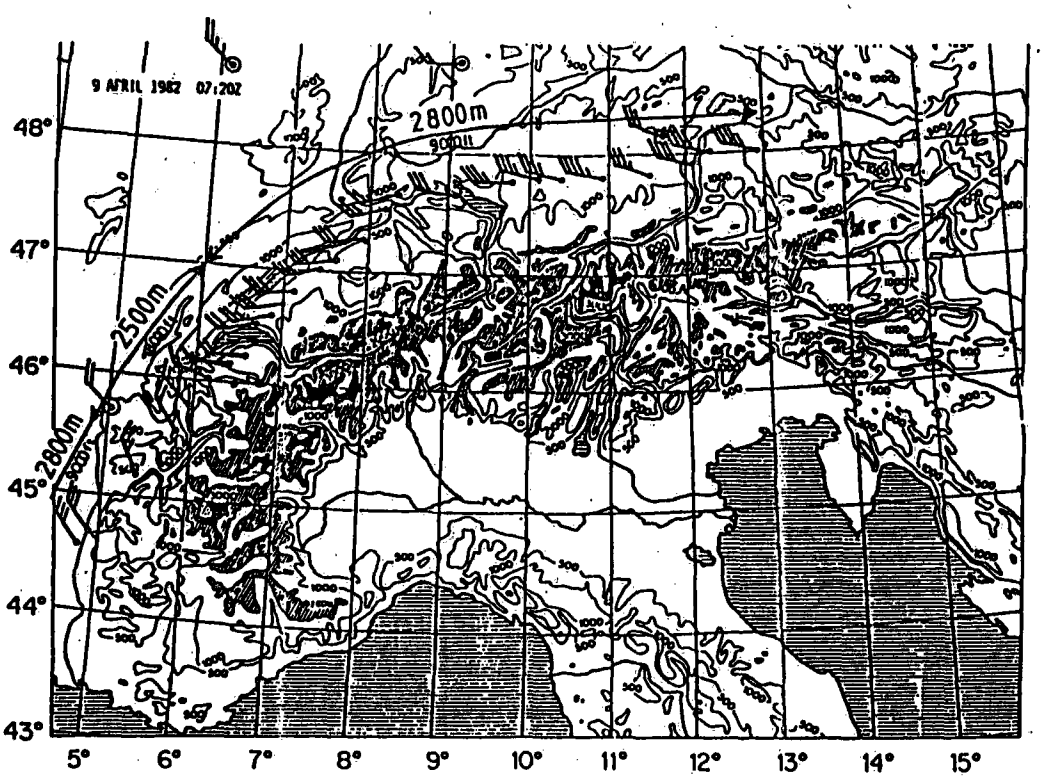

Aircraft measurements on 9 April 1982 at 2500 to 2800 m - P-3 flight

Fig. 4: Flow splitting at the 2.5 to 2.8 km level on the northwest side of the Alps (lower figure) apparently decoupled from undisturbed, straight flow at 3.7 km (upper figure) as measured by two vertically stacked aircraft on 9 April 1982. (After Kuettner, 1986.)

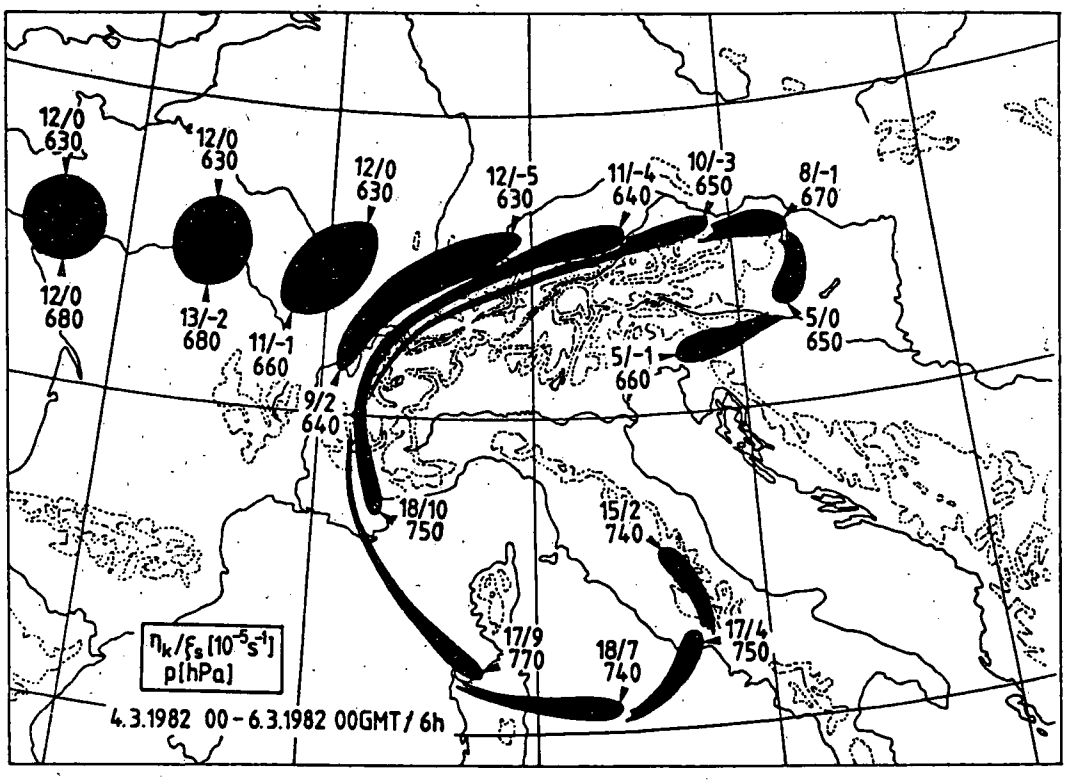

Fig. 5: Deformation of an isentropic material surface in the lower troposphere during alpine lee cyclogenesis. 6-hour intervals; 4 to 6 March 1982. (After Pichler and Steinacker).

Fig. 6: Meridional and zonal components of total drag (D) and wave drag (M = vertical momentum flux) as a function of time during alpine south foehn event of 8 November 1982. Note that, according to this numerical simulation by Hoinka and Clark (1990), wave drag is roughly half of total drag.

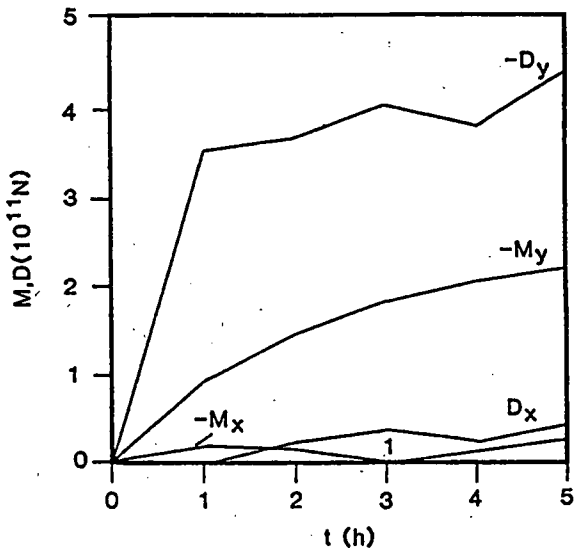

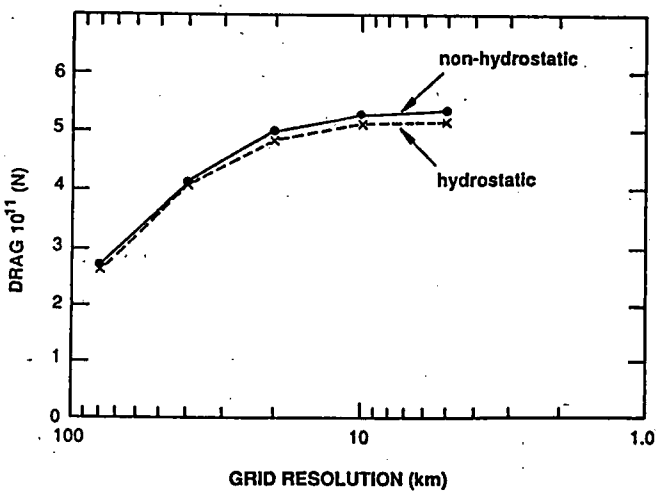

Fig. 7: Pressure drag versus grid resolution for non-hydrostatic and hydrostatic numerical simulations of Alpine foehn case of Fig. 6. After Clark and Miller (1990).

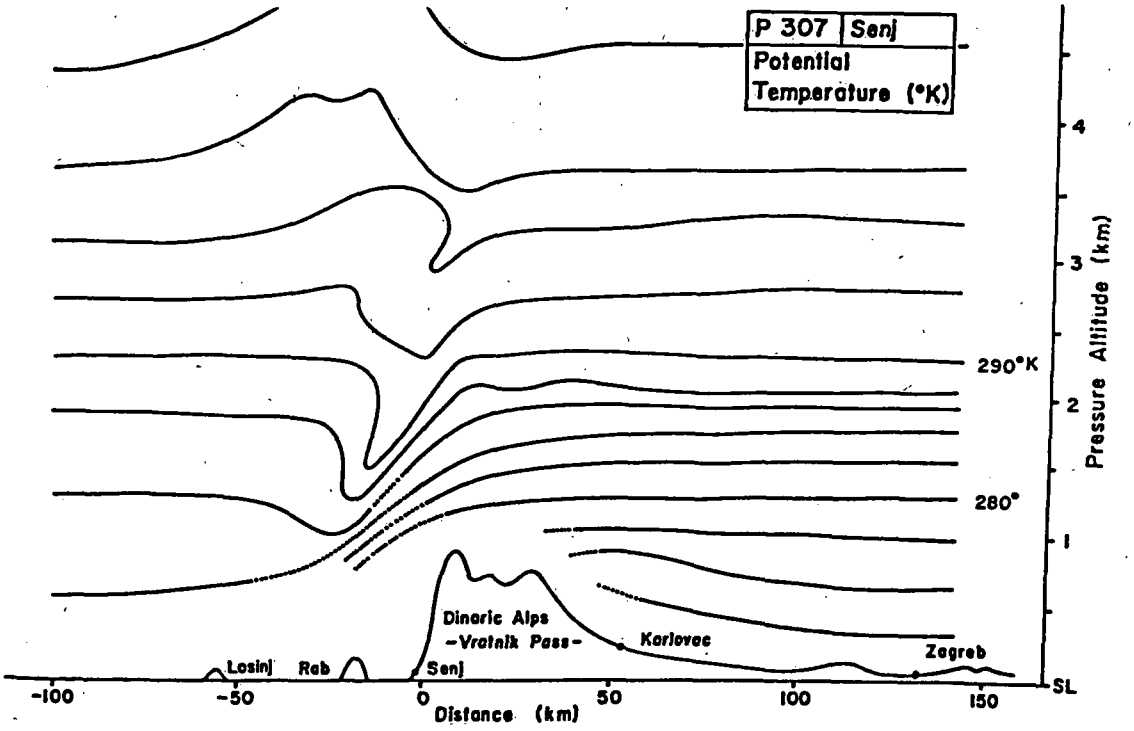

Fig. 8: Potential temperature field during Bora over the Dinaric Alps on 7 March 1982. Flow is from right to left (After Smith, 1987)

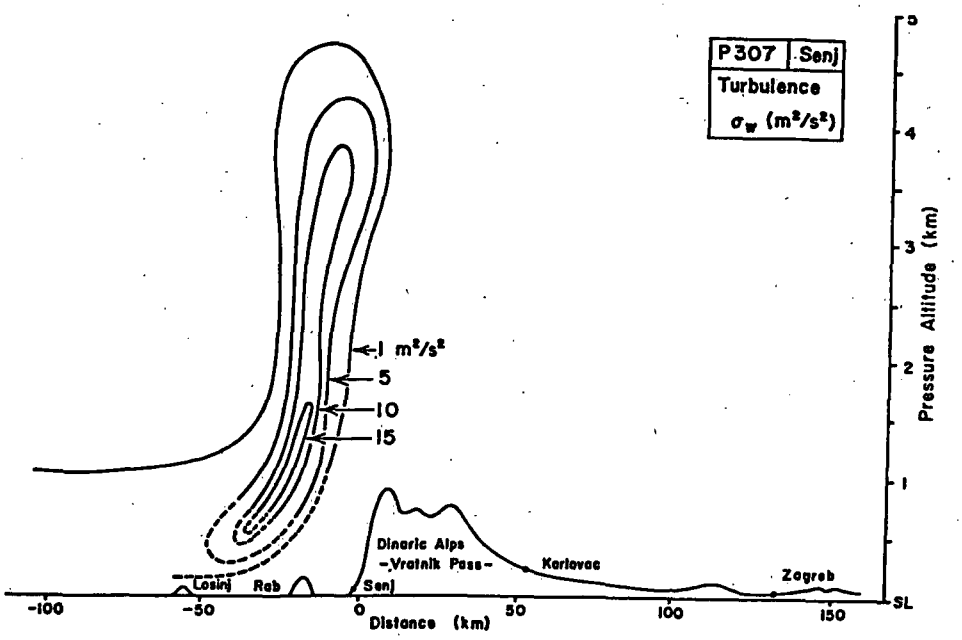

Fig. 9: Region of intense turbulence in the lee of Dinaric Alps during same Bora case as Fig. 8. (After Smith, 1987.)

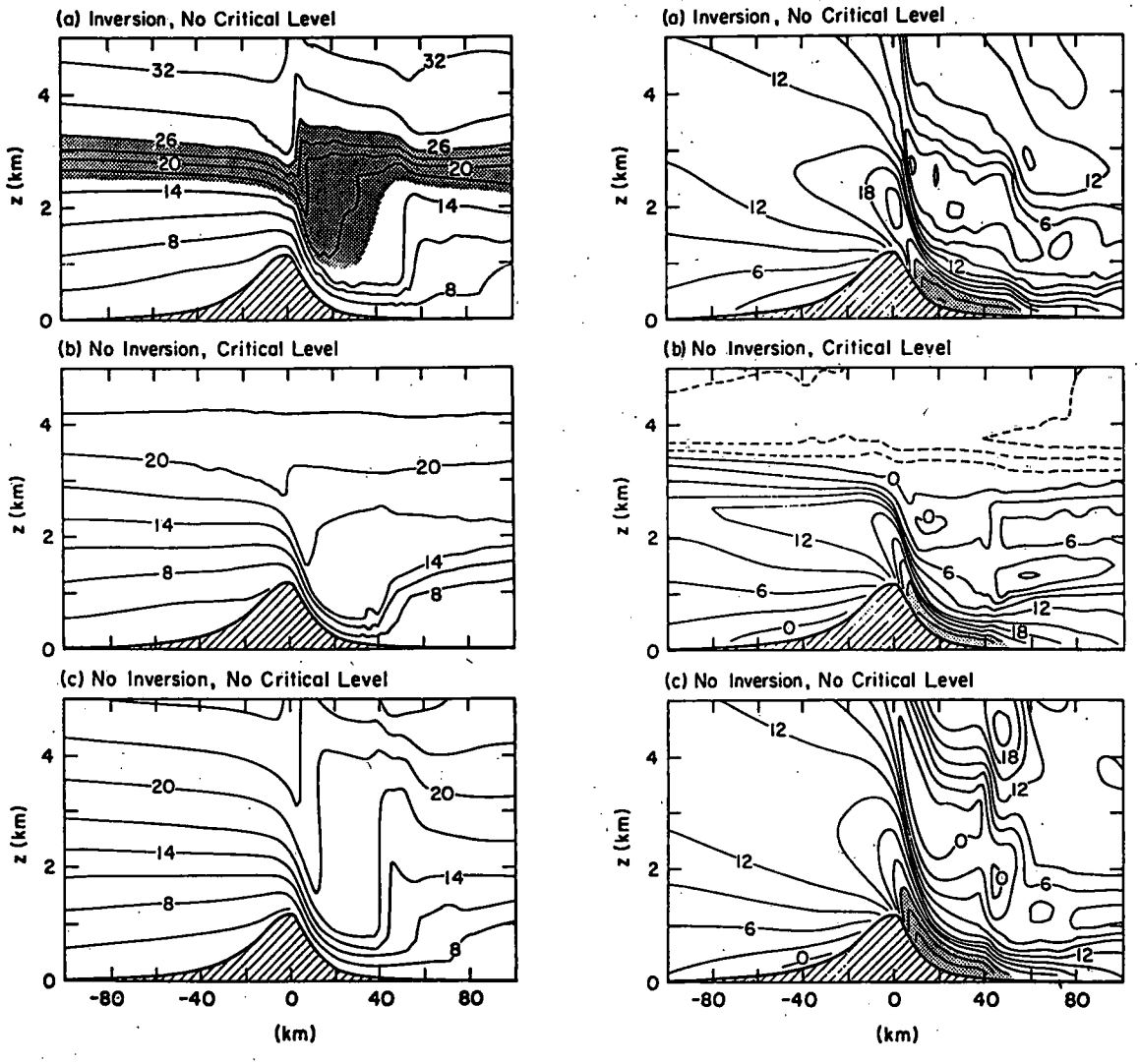

Fig. 10: Influence on Bora flow of presence or absence of inversion layer (shaded) and critical level (flow reversal at 3 km altitude). Left side: potential temperature contour in (C). Right side: contours of horizontal velocity field (in m/s). Down slope velocities over 24 m/s are shaded. Numerical simulation by Klemp and Durran (1987).

Section 3:

Diagnosis and Interpretation of Mesoscale Systems and Local Phenomena

FINE MESH ISENTROPIC ANALYSIS OF FRONTS IN THE ALPINE REGION

Reinhold Steinacker

Institut für Meteorologie und Geophysik
Universität Innsbruck

Summary:

An objective isentropic analysis scheme designed for ALPEX-analyses is used to investigate the frontal structure in the vicinity of the Alps. A new tool is introduced to analyse objectively the fronts position and intensity. It is shown that fronts may be extremely complex three dimensional phenomena which become significantly modified by orography.

1. Introduction

Atmospheric fronts, with a few exceptions (e.g. Renard and Clarke, 1965; Huber-Pock and Kress, 1989) are still analysed manually and hence subjectively by most weather services on an operational basis. Even for scientific investigations of real fronts their location is plotted manually which often leads to differences between the individual analysts opinion.

Several qualitative or climatological/quantitative definitions of fronts are found in literature (e.g. Bergeron, 1928; Taljaard et al. 1961; Palmen and Newton, 1969; Geb, 1971) and every textbook on synoptic meteorology contains a descriptive outline of what a front is. Nevertheless no definition is generally accepted, which is easy to understand, as all definitions are valid only for a certain scale (e.g. polar front), or for a specified parameter (e.g. thermal front) or for one part of the phenomenon (e.g. warm air boundary of a hyperbaroclinic zone).

2. Mathematical approach to the front definition

A general and liberal definition of a front in the sense of a working hypothesis with respect to any arbitrary variable of a fluid may be given with a minimum of 2 mathematical conditions:

"Each volume bounded on two sides by surfaces of opposite extreme values of the second derivative (perpendicular to the surface) of an arbitrary scalar variable Ψ may be called a front if for both surfaces

$$\left|\frac{\partial^2\psi}{\partial n^2}\right| \gg \overline{\left|\frac{\partial^2\psi}{\partial n^2}\right|} \qquad (1)$$

and

$$A \gg \left(\overline{\Delta_3 n}\right)^2 \qquad (2)$$

where A represents the area of the bounding surface and $\Delta_3 n$ is the normal distance of the two bounding surfaces" (see fig. 1).

This rather abstract definition has the advantage to be scale independent and applicable to any scalar atmospheric or oceanographic variable. It further implies a magnitude of the gradient of Ψ within the volume which is significantly larger than the mean value over the whole domain and tells us that a front (volume) is strongly anisotropic (layer-like). Although a front should be always seen as threedimensional structure, the above defintion may be reduced to two dimension as well:
"Each area bounded on two sides by lines of opposite extreme values of the second derivative (perpendicular to the line) of an arbitrary scalar variable Ψ may be called a front if for both lines

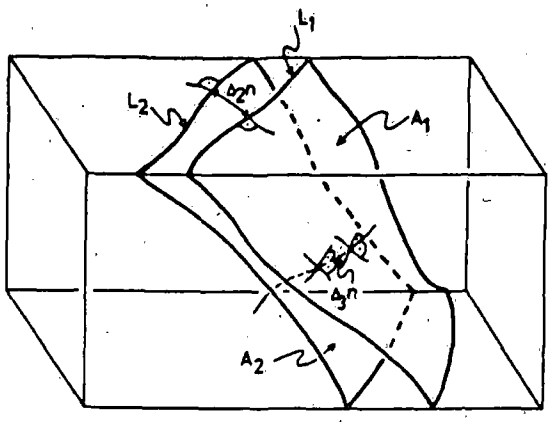

Fig. 1: Schematic view of a front volume (area) and its limiting surfaces A_1, A_2 (lines L_1, L_2).

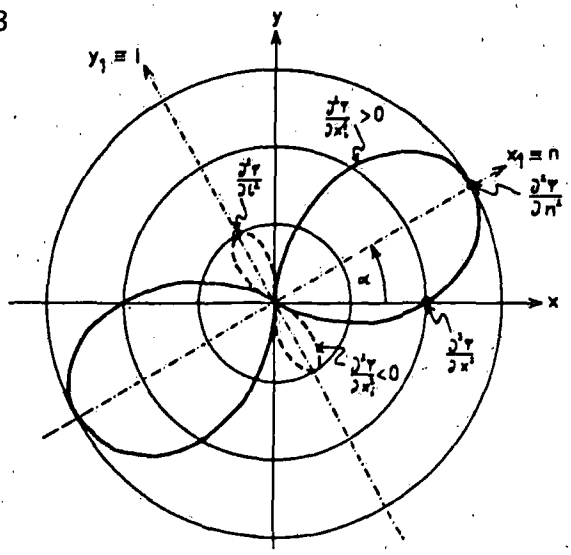

Fig. 2: Example for a 2-D distribution of $\frac{\partial^2\psi}{\partial x_1^2}$ with $\frac{\partial^2\psi}{\partial n^2}$ being the maximum value, further explanations see text.

$$\left|\frac{\partial^2\psi}{\partial n^2}\right| \gg \overline{\left|\frac{\partial^2\psi}{\partial n^2}\right|} \qquad (3)$$

and

$$L \gg \overline{\Delta_2 n} \qquad (4)$$

where L represents the length of the bounding lines and $\Delta_2 n$ is the normal distance between the two bounding lines" (see fig. 1).

This definition implies a magnitude of the 2D-gradient of Ψ within the area which is significantly larger than the mean value over the whole domain and tells us that the area must be strongly anisotropic (bandlike).

By this way all possible fronts including exotic types like humidity fronts, (oceanographic) salinity fronts, sea breeze fronts[1] or even valley wind fronts[1] may be analysed objectively, provided a sufficient resolution of data is available over the domain in view.

3. Determination of the second derivatives

We will restrict ourselves to the 2-D case here. The Laplacian of Ψ on two dimensions consists of two parts

$$\nabla^2\psi = \frac{\partial^2\psi}{\partial x^2} + \frac{\partial^2\psi}{\partial y^2} \qquad (5)$$

A transformation (rotation) of the coordinate system does not change the Laplacian but it changes the two parts. According to our definition we have to rotate the coordinate system until the two parts are extreme values

$$\nabla^2\psi = \frac{\partial^2\psi}{\partial n^2} + \frac{\partial^2\psi}{\partial l^2} \qquad (6)$$

where furthermore

$$\left|\frac{\partial^2\psi}{\partial n^2}\right| \geq \left|\frac{\partial^2\psi}{\partial l^2}\right| \qquad (7)$$

1) Vectorial quantities (e.g. wind velocity) may be used as variables if they are divided into cross front and along front components.

The angle of rotation α (see fig. 2) can be obtained by the condition

$$\frac{\partial}{\partial \alpha}\left(\frac{\partial^2 \psi}{\partial x_i^2}\right) = 0 \tag{8}$$

which yields

$$\alpha = \frac{1}{2}\, a\tan\left[\frac{\partial^2 \psi}{\partial x \partial y} \Big/ \left(\frac{\partial^2 \psi}{\partial x^2} - \frac{\partial^2 \psi}{\partial y^2}\right)\right] \tag{9}$$

and hence the solution for $\frac{\partial^2 \psi}{\partial n^2}$.

The classic paper on objective front analysis of Renard and Clarke, 1965, in contrast, uses the second derivative along the gradient of Ψ, which says that no alongfront gradient is permitted. This is clearly a severe restriction especially with regard to occluded frontal systems.

4. Application to a 850 hPa-surface

As an example the "airmass fronts" ($\Psi = \Theta_e$) have been analysed objectively for 850 hPa on November 11, 1987, 00 UTC (the second event of the German Fronts Experiment, see e.g. Zwatz-Meise and Kress, 1988). Fig. 3 shows the Θ_e-analysis with maximum and minimum lines of $\partial^2\Theta_e/\partial n^2$, where the grid distance was 45 km.

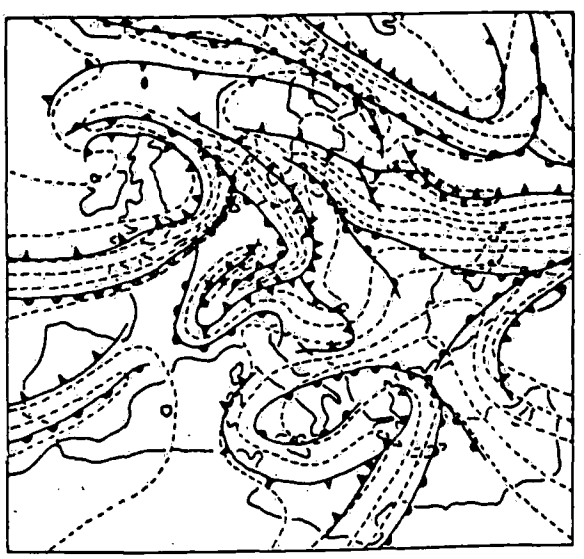

Fig. 3: Objective analysis of the "airmass fronts" on Nov. 12, 1987, OO UTC. Dashed lines are isotherms of equivalent potential temperature with 4 K interval. Minimum lines of $\partial^2\Theta_e/\partial n^2$ are indicated with warm front symbols in the sense of the warm side boundary of the front, maximum lines are plotted with cold front symbols in the sense of the cold side boundary of the front.

It comes out clearly that the bands of concentrated gradients are bounded by the lines of extreme values of $\partial^2\Theta_e/\partial n^2$ and thus can be seen as the "airmass fronts". Comparing a conventional front analysis (e.g. Berliner Wetterkarte) with fig. 3 an excellent agreement between the location of the minimum line of $\partial^2\Theta_e/\partial n^2$ (except for mesoscale features) and the hand drawn "front lines" may be observed.

In the Alpine region a complicated frontal structure appears which is caused by a weak S-foehn flow, producing stationary "orographic fronts".

5. Application to an isentropic cross section

Cross sections are often used to investigate the details of a frontal structure. They however suggest a two dimensional front which is hardly found in nature. Even if the section is exactly perpendicular to the jet streak flow it will not be so over the whole troposphere,

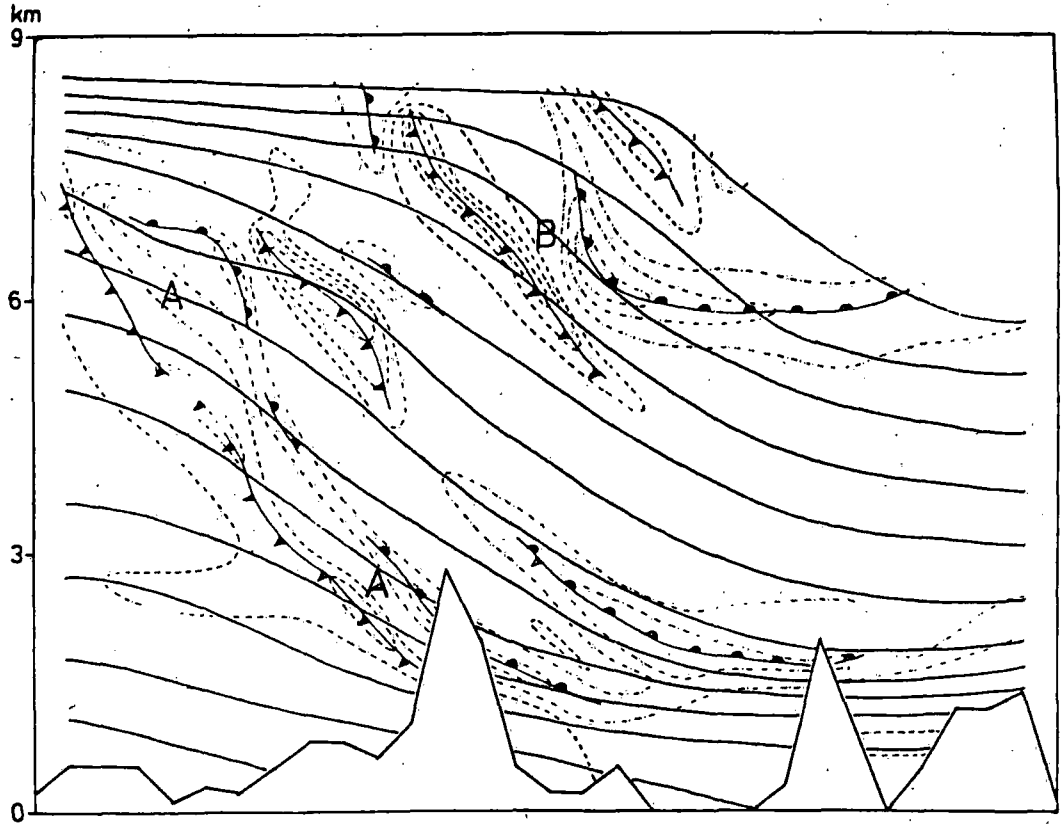

Fig. 4: Isentropic (N-S) cross section from northern Germany (left side) to Sardinia. Isentropes with 2.5 K interval are continuous lines, isolines of horizontal $\partial^2\theta/\partial n^2$ are plotted dashed (positive value) and dash-dotted (negative values) with an interval of 1×10^{-10} K m^{-2}, zero line is omitted. The maximum and minimum lines of $\partial^2\theta/\partial n^2$ are plotted with cold front symbols (maximum = cold side boundary of front) and warm front symbols (minimum = warm side boundary of front).

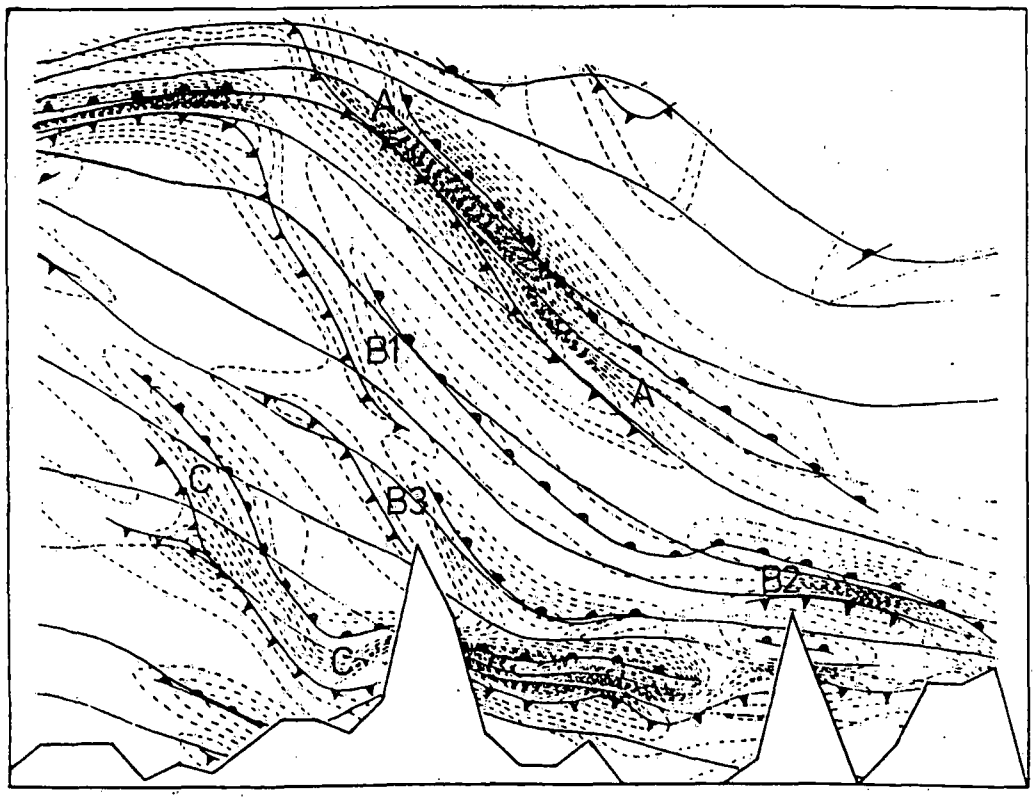

Fig. 5: Same as fig. 4 but for fine mesh analysis (see text).

furthermore the curvature of the flow is neglected. If we choose our front intensity and locating parameter $\partial^2\Psi/\partial n^2$ we are able to overcome this problems and obtain a more realistic impression about fronts.

Fig. 4 shows a N-S section along 9 deg. east (through Genoa) on March 2, 1982, 00 GMT, at the beginning of the first ALPEX front and Genoa cyclogenesis case. It is based on the ECMWF operational analyses, which show a broad but moderate baroclinic troposphere over the whole width of the cross section from N-Germany to Sardinia.

The analysis of $\partial^2\theta/\partial n^2$ (which was derived from a grid with 45 km distance) shows a rather weak front north of the Alps (A) and an indication of a tropospause folding over and just south of the Alps (B). It is not surprising that a broad scale analysis does not show spectacular frontal structures.

A fine mesh analysis with the ECMWF fields as first guess (see Lanzinger and Steinacker, 1990) in contrast gives us an excellent information on the complex nature of fronts (fig. 5). A triple structure can be seen where the first (A) is very sharp at upper tropospheric levels over and south of the Alps. A second front is well pronounced at mid tropospheric levels just north of the Alps (B1) and again over Corsica and Sardinia (B2). Over and just south of the Alps an "orographic front" appears (B3) which is caused by the NW-flow over the Alps. This orographic deformation of the isentropes seems to be the cause for the splitting of the second front into two parts.

The third front (C) finally is restricted to the lower troposphere north of the Alps. This front was the so called first ALPEX front and shows here a deformation on the north side of the Alps due to a blocking effect. A strong nearly horizontal low level front south of the Alps (D) would probably be classified as inversion from this cross section. The large values of $\partial^2\theta/\partial n^2$ however indicate that there must be an inclination perpendicular to the section shown.

6. Conclusion

For a meaningful investigation of the frontal structure of the atmosphere a fine mesh analysis is necessary. The analysis scheme used here, which takes special care of the anisotropy over and around mountains seems to be capable to resolve orographic modifications of fronts.

The objective front analysis scheme - which may be completely automatized - promises to become a powerful task in future. Further investigations are necessary to test the scheme also with other variables and three dimensionally.

References

Bergeron, T., 1928: Über die dreidimensional verknüpfende Wetteranalyse. Geof. Publ. 5, 1-117.

Berliner Wetterkarte, 12.11.1987: Institut f. Meteor. Freie Universität Berlin.

Geb., M., 1971: Neue Aspekte und Interpretationen zum Luftmassen und Frontenkonzept. Met. Abh. Freie Univ. Berlin 109, 1-138.

Huber-Pock, F.; Ch. Kress, 1989: An operational Model of objective frontal analysis based on ECMWF products. Meteor. Atmos. PHys. 40, 170-180.

Lanzinger, A.; R. Steinacker, 1990: A fine mesh analysis scheme designed for mountainous terrain. Met. Atm. Phys. 43, 213-219.

Palmen, E.; C.W. Newton, 1969: Atmospheric circulation systems. Acad. Press, 603 pp.

Renard, R.J.; L.C. Clarke, 1965: Experiments in numerical objective frontal analysis. Mon. Wea. Rev. 93, 547-556.

Taljaard, J.J.; W. Schmitt, H. van Loon, 1961: Frontal analysis with application to the southern hemisphere. Notos 10, 25-58.

Zwatz-Meise, V.; Ch. Kress, 1988: Frontexperiment 1987; Diagnosis with satellite images and derived meteorological parameters. DFVLR Frontexperiment Mitt. 13, 45 pp.

Density and Pressure Changes during the Passage of a Frontal System over the Alps

Gerd Ragette

Zentralanstalt für Meteorologie und Geodynamik, Wien

ABSTRACT
On October 20, 1974, an occluding frontal system crossed central Europe. Considerable pressure changes were observed during the frontal passage. From the pressure tendency equation which relates temporal density changes to spatial variations of wind and density it is found that horizontal density advection, though it contributed least, was of decisive importance for them. It is shown that in the lowest 3 km above ground the vertical wind divergence is of greater magnitude than the horizontal wind divergence. For the mass divergence this relation was in general not fulfilled except for the frontal zones.

1. Introduction

With the introduction of pressure as vertical coordinate the use of geometric height as independant variable has become somewhat obsolete in meteorology. Nevertheless the surface pressure is one of the most accurately measured observables and for the synoptician of invaluable importance. Using the continuity equation and assuming hydrostatic equilibrium we obtain

$$\frac{\delta p}{\delta t} = -\int_z^\infty g\nabla\ (\rho\vec{v})\, dz^* = -g\int_z^\infty \rho\,(\nabla\vec{v}_h)\, dz^* - g\int_z^\infty (\vec{v}_h\nabla\rho)\, dz^* + g\rho w \qquad (1)$$

which allows an easy interpretation as all terms in (1) are readily understood. For the surface pressure in particular we obtain

$$\frac{\delta p_s}{\delta t} = -g\int_z^\infty \nabla\,(\rho\vec{v}_h)\, dz^* \qquad (2)$$

If we use pressure as vertical coordinate a similar expression as equation (2) can be derived for the surface pressure tendency with the approximation

$\frac{\delta p_s}{\delta t} \approx \omega_s$ (Pichler, 1984). From $\frac{\delta\omega}{\delta p} = -\nabla\vec{v}_h$ we obtain

$$\frac{\delta p_s}{\delta t} = -\int_0^{p_s} \nabla\vec{v}_h dp \qquad (3)$$

However, in the p-system the height tendency represents the equivalent to the pressure tendency. The tendency equation for the geopotential can be written in the form (Pichler, 1984)

$$\nabla^2\left(\frac{\delta\Phi}{\delta t}\right) + \frac{f^2}{\sigma}\frac{\delta^2}{\delta p^2}\left(\frac{\delta\Phi}{\delta t}\right) = J\left(\frac{1}{f}\nabla^2\Phi + f, \Phi\right) + \frac{f}{\sigma}\frac{\delta}{\delta p}\left(J\left(\Phi_p, -\frac{\delta\Phi}{\delta t}\right)\right)$$

which does not permit an interpretation as straightforward as (1). Thus it seems justified to use (x, y, z)-coordinates for this type of problem as it facilitates its discussion and solution. Equations (2) and (3) indicate the well-known fact that for the surface pressure tendency the horizontal mass divergence at constant height or the horizontal wind divergence at constant pressure, respectively, is decisive. Both equations are, however, somewhat misleading, as they apply only for the surface pressure whose tendency is determined by the mean divergence over the whole atmosphere. Thus it is not permissible to con clude that a convergent layer gives a contribution to pressure rise or a divergent layer one to pressure fall. This would be the case if convergence were always associated with increasing density, divergence with decreasing density. For density changes, however, also the vertical part of the divergence, which has cancelled out for the surface pressure tendency, needs to be considered. Principally then a convergent layer may as well be a layer where the density diminishes, if vertical divergence outbalances horizontal convergence, as one with rising density. A similar argument holds for a divergent layer. In order to clarify the situation a real case - the storm of 20 October 1974 - , whose frontal passages were accompanied by considerable pressure changes, has been studied using (x, y, z)-coordinates.

2. Data and data analysis

Synoptic data and chart records form several central European stations were used together with soundings and winds from Stuttgart, Munich and Vienna. Space-to-time conversion was applied to assemble all data in the same time-height sections by assuming stationarity of the storm. The temporal resolution places our analysis at the equivalent transition from α to β scale. After interpolation to a fixed grid other parameters were derived, in particular the vertical velocity which was computed using a method developed by the author (1985).

3. Results

The continuity equation $(\delta\rho)/(\delta t) = -\nabla(\rho\vec{v})$ relates spatial variations of the wind and density field to density changes. We first consider the order of magnitude of the terms in

$$g\frac{\delta\rho}{\delta t} = -g\nabla(\rho\vec{v}_h) - g\frac{\delta(\rho w)}{\delta z} \qquad (4)$$

0.5×10^{-1} 0.5×10^{1} 0.5×10^{1} $(Pa\times m^{-1}/(3h))$

where the second line indicates the mean of the absolute values. It is obvious that the two terms on the right side of (4) nearly cancel each other. The time-height sections reveal more detail in proving that in the frontal regions the vertical mass divergence was stronger than the horizontal contribution, whereas elsewhere the horizontal mass divergence prevailed somewhat.
Splitting equation (4) into

$$g\frac{\delta\rho}{\delta t} = -g\rho\nabla\vec{v}_h - g\rho\frac{\delta w}{\delta z} - gw\frac{\delta\rho}{\delta z} - g\vec{v}_h\nabla\rho \qquad (5)$$

0.5×10^{-1} 0.5×10^{1} 0.5×10^{1} 0.7×10^{0} 0.7×10^{-1}

we find likewise horizontal and vertical wind divergence, which were the dominating contributors, nearly cancelled each other. The data show that above 4 km horizontal wind divergence was somewhat preponderating, whereas below that height vertical divergence prevailed. This is not surprising. From equation (5) we conclude that the 3-dimensional wind divergence must have the same magnitude as the vertical density transport $-gw((\delta\rho)/(\delta z))$ and that both quantities nearly cancel each other. This implies that $\nabla\vec{v}$ is proportional to w. Since at the flat ground the vertical velocity vanishes and thus in the low levels horizontal divergence and vertical velocity are correlated, it follows that there usually $|(\delta w)/(\delta z)| > |\nabla\vec{v}_h|$ is fulfilled. The residual of $-g\rho\nabla\vec{v}$ and $-gw((\delta\rho)/(\delta z))$, which can be written $g((\delta\rho)/(\delta t)) + (g\vec{v}_h\nabla\rho)$, had the same magnitude as $-(g\vec{v}_h\nabla\rho)$ but usually possessed the oposite sign. However, $((\delta\rho)/(\delta t)) + (\vec{v}_h\nabla\rho)$ and $-\vec{v}_h\nabla\rho$ did not cancel. Both were closely correlated with a correlation coefficient of -0.76, which indicates that the effect of horizontal density advection on density change was often nearly counterbalanced by the other processes, the resulting density change in general being somewhat less pronounced than one would expect from advection alone. Nevertheless $(\delta\rho)/(\delta t)$ and $-\vec{v}_h\nabla\rho$ were correlated with 0.52, which proves that in our case horizontal density advection explains a fair portion of the temporal density change.

4. Additional Remarks

The relative airflow associated with the system has been described by Ragette (1984) using the terminology which had been employed by Kreitzberg (1968) and Browning and Harrold (1970). More recently, Carlson's (1980) analyses yielded a conceptual model of warm and cold conveyor-belt, which has been accepted as representative for most mid-latitude cyclones. In the light of his findings we shall pay special attention to the cold conveyor-belt, which manifests itself in our analyses as a flow of moist cool air descending from ahead of the storm towards the warm front, thereupon reaching the discontinuity and turning right beneath it towards the left side of the system. In contrast the warm conveyor-belt ascended above the warm front, approaching the cyclone from the right side, then flowing more or less parallel to the following surface cold front, at higher altitude with the increasing wind turning anticyclonically into the direction of storm motion, since the upper through was still wide and open. Carlson (1980) used isentropic analyses to demonstrate that in the low levels, where a closed depression or narrow trough has developed, the cold conveyor-belt eventually turns cyclonically around the depression, its associated low cloud appearing in the rear of the system from underneath of the high cloud canopy of the warm conveyor-belt, there forming a characteristic cloud feature which had been named "com-

ma". Carlson's concept of the cold conveyor-belt evidently represents an early stage of cyclone development, when the upper trough is still wide. Once the closed low extends to greater height, which is generally the case in a more advanced stage of cyclone development, also the warm air will circle cyclonically around the depression, which then corresponds more to the classical concept of an occlusion.

From the field of potential wet-bulb temperature we find that the same θ_w-values of 8 to 9 °C which occured in the cold conveyor-belt below the warm front reappeared above the cold frontal surface between 3 and 6 km. This suggests that indeed the cold conveyor-belt had turned around the low. Since the air in the storm's rear, which was saturated from almost 2 to 6 km - comprising the low and mid-level cloud of the comma - descended towards the right side of the system, we conclude that the air circling around the low had undergone at least some ascent on the system's left flank. Examining the airflow at 500 mb we find that the upper winds south of the surface low centre were considerably stronger than the storm's propagational speed, whereas north of it the winds soon became less intense than that velocity. In terms of relative flow this, too, substantiates the view that the cold conveyor-belt, while turning around the low, may have ascended to an altitude of 6 km. Dry air descending from high levels into the warm sector was responsible for the breaking of the cloud reported from several stations. This upper cold front or surge of potentially cold air may be called a dry intrusion (Carlson, 1980). It is usually best developed in so-called split fronts when an upper cold front precedes the surface cold front. Summarizing this information we arrive at an extended conceptual model of the relative airflow presented in Fig. 1 which complements the earlier sketch shown by the author (Ragette, 1984).

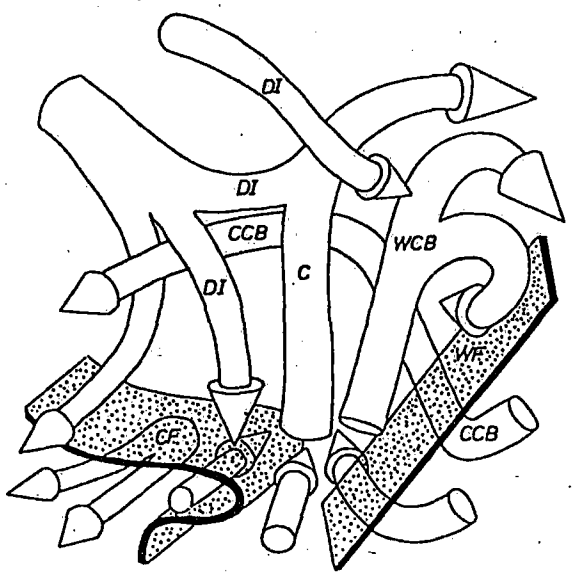

Fig. 1: Conceptual model of relative airflow with main features of storm of October 20, 1974. WF = warm front, CF = cold front, WCB = warm conveyor-belt, CCB = cold conveyor-belt, C = main cold-frontal updraft, DI = dry intrusion.

5. References

Browning, K.A., Harrold, T.W., 1970: Air motion and precipitation growth at a cold front. Quart. J. Roy Meteor. Soc., 96, 369 - 389.

Carlson, T.N., 1980: Airflow through midlatitude cyclones and the comma cloud pattern. Mon. Wea. Rev., 108, 1498 - 1509.

Kreitzberg, C.W., 1968: The mesoscale wind field in an occlusion. J. Appl. Meteor., 9, 417 - 432.

Pichler, H., 1984: Dynamik der Atmosphäre. Mannheim: Bibliographisches Institut, 456 pp.

Ragette, G., 1984: Analysis of a frontal system over Central Europe. Beitr. Phys. Atmosph., 57, 447 - 462.

Ragette, G., 1985: A new method of determining vertical velocities from serial radiosonde data. Arch. Met. Geoph. Biocl. Ser. A, 34, 159 - 166.

Section 4:

Planetary Boundary Layer Processes and Issues of Air Quality and Air Pollution

On the Influence of the Physico–Chemical Properties of Aerosols on the Life Cycle of Radiation Fogs

Andreas Bott

Institute for Atmospheric Physics, University of Mainz, F.R.G.

Abstract

A one dimensional radiation fog model with detailed microphysics is presented. Aerosols and cloud droplets are treated in a joint two dimensional size distribution. Radiative fluxes are calculated as functions of the radiative properties of the time dependend particle spectra. Radiative effects are considered in the droplet growth equation. Three numerical sensitivity studies are performed to investigate the impact of the different physico–chemical properties of urban, rural and maritime aerosols on fog formation. Numerical results elucidate that depending on the utilized aerosol models the resulting fog events are completely different. This holds in particular for the times of fog formation and dissipation as well as for the liquid water content and the supersaturations within the fogs.

Model description

A one dimensional radiation fog model is presented which includes a detailed description of the interaction between atmospheric radiative transfer and fog microphysics. Aerosol particles and fog droplets are treated in a joint two dimensional size distribution with a direct description of the activation of aerosols. The particle spectra are subdivided into 40 aerosol and 30 water classes yielding 1200 particles with different total radius and different radius of their dry aerosol nucleus. For each of the 40 aerosol classes a separate droplet growth equation is solved. This is done with a newly developed semi Lagrangian advection scheme. Atmospheric radiative fluxes are calculated using time dependend attenuation parameters of aerosols and fog droplets as function of the actual particle size distributions. Furthermore, the radiatively induced droplet growth is considered in the model calculations.

Turbulence ist simulated utilizing the 2.5 level model of Mellor and Yamada (1982). The interaction between the atmosphere and the soil is calculated with the soil model of Pielke (1984).

Numerical sensitivity studies are performed for three different aerosol models which are typical for urban, rural and maritime environments. These models differ in the total number concentrations as well as in the chemical composition of the aerosols yielding different radiative absorption and scattering properties. The rural aerosol is assumed to be composed of $(NH_4)_2SO_4$ and dust like material, whereby the mass fraction of dust is linearly increasing from 10% for $a = 0.01\mu$m to 50% for $a = 1\mu$m. The urban aerosol is a mixture of 80% rural aerosol and 20% soot, while the ocean aerosol consists of pure $(NH_4)_2SO_4$ for $a \leq 0.5\mu$m and pure NaCl for large aerosols. A detailed model description is given in Bott et al. (1990).

Numerical results

Three numerical sensitivity studies have been performed for a mitlatitude atmospheric situation in October typical for fog formation. These simulations only differ in the use of the urban, the rural and the maritime aerosol model. Numerical results elucidate that the thermodynamical and microphysical structures of the fog events are strongly controlled by the physico–chemical properties of the utilized aerosol models.

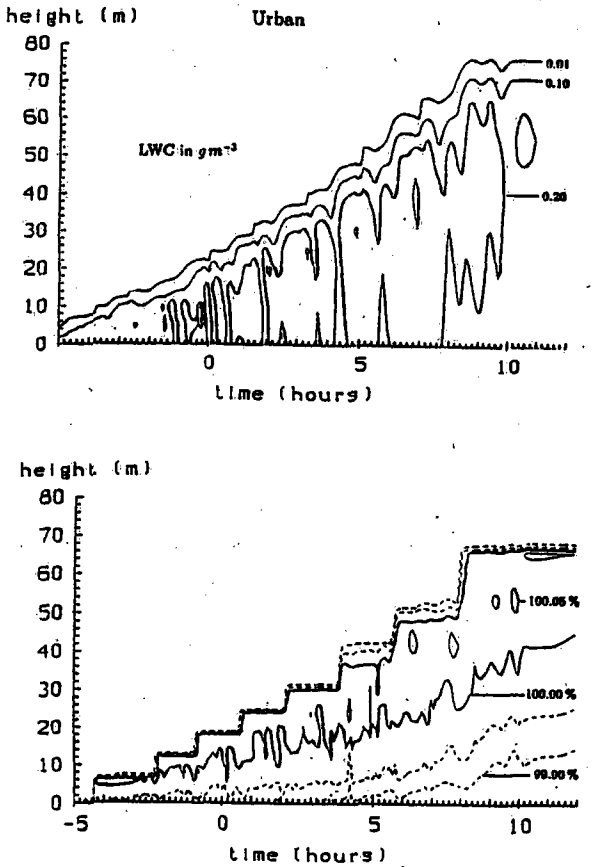

Figure 1

Figures 1—3 depict for the three model runs the liquid water content m_w and the supersaturations as functions of time and height. Due to the strong absorption of solar radiation by the soot containing urban aerosol particles, in this case the atmosphere remains colder than in the rural and maritime situation. Hence, the urban fog forms relatively early at 18:30h local time and does not disappear until to the end of the model simulations.

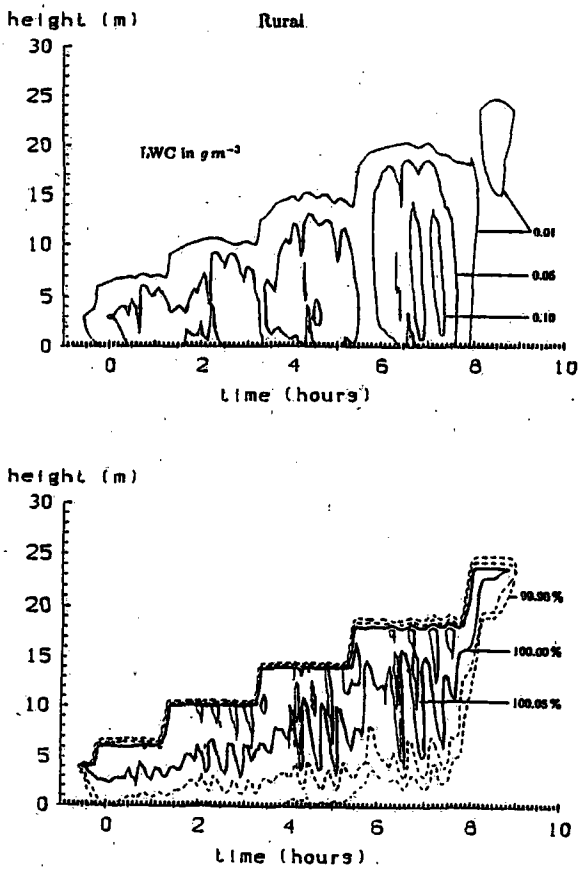

Figure 2

Between 19h and 8h the top of the fog grows nearly linearly in time up to its final height of 80m. The liquid water content is relatively high with peak values of more than 0.3 g/m^3. Due to the very large aerosol concentrations of more than 53000 particles per cm^3 there are always enough cloud condensation nuclei available

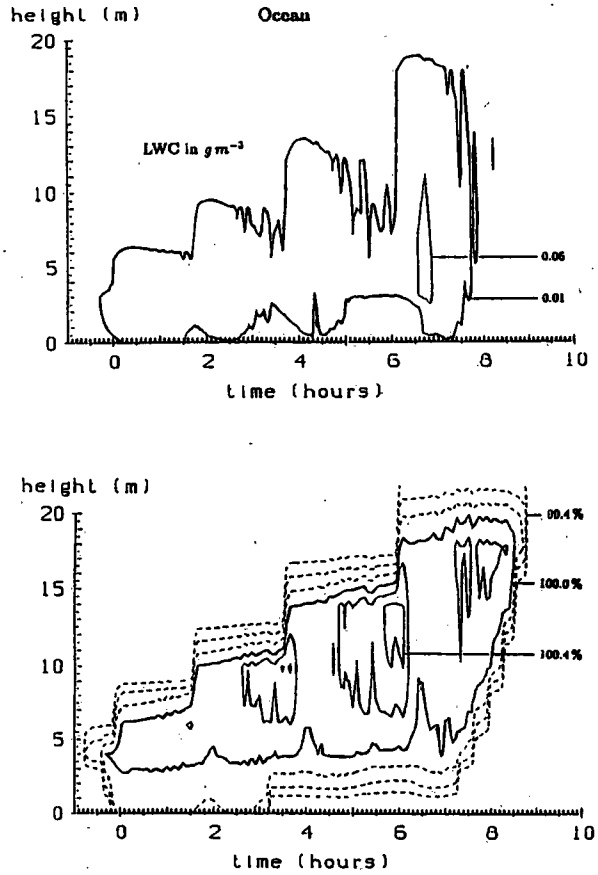

Figure 3

which become activated and then consume the excessive water vapor. Hence, the calculated supersaturations are relatively low with peak values of 0.05% only sometimes occuring in some upper fog layers.

Rural fog formation begins at 23:30h. At 9h of the following day the fog is dissipated by the incoming solar radiation and the resulting enhanced heat fluxes from the ground. The top of the fog grows not higher than 25m with maxima of m_w of 0.1 g/m^3. Now the calculated supersaturations are higher than in the urban model run because the total number concentration of aerosols is only given by 3890 particles per cm^3. Peak values of more than 0.05% are observed throughout the entire fog episode.

The ocean model run yields the weakest fog. Although times of fog formation and dissipation are similar to the rural simulation, the calculated liquid water contents are very low with a maximum value of 0.05 g/m^3 occuring at 7h of the second day. On the other hand, the supersaturations are very high with peak values exceeding 0.4%. This behavior is explained by the fact that the maritime aerosol model consists of only 105 particles per cm^3.

In each model run the lowest fog layers are subsaturated, although the fogs continue persist with liquid water contents sometimes exceeding 0.2 g/m^3. The reason for this is that with increasing top of the fogs the lowest layers become more and more radiatively shielded by the fog aloft so that the cooling rates are decreasing there. In addition to this, after the inclusion of the radiation term in the droplet growth equation the fog droplets may continue to grow even in slightly subsaturated environments.

The calculated particle spectra show the typical bimodal form separating the unactivated aerosols from the activated fog droplets. The minimum is found at $r \approx 5\mu$m and the local maximum of the droplet spectra is given at $r \approx 12\mu$m. The spectral distributions of the water masses are given by a relatively narrow unimodal curve with maximum at $r \approx 10\mu$m, while the aerosol masses have the same bimodal shape as the particle distributions. For future inclusions of chemical reactions in the liquid phase it is important to note that in the activated part of the curves the aerosol

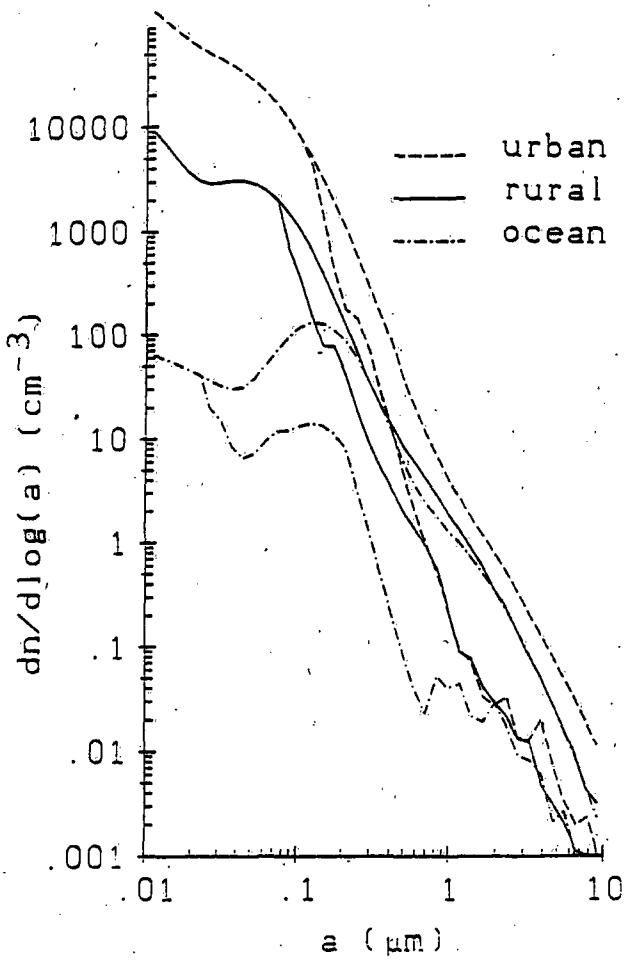

Figure 4

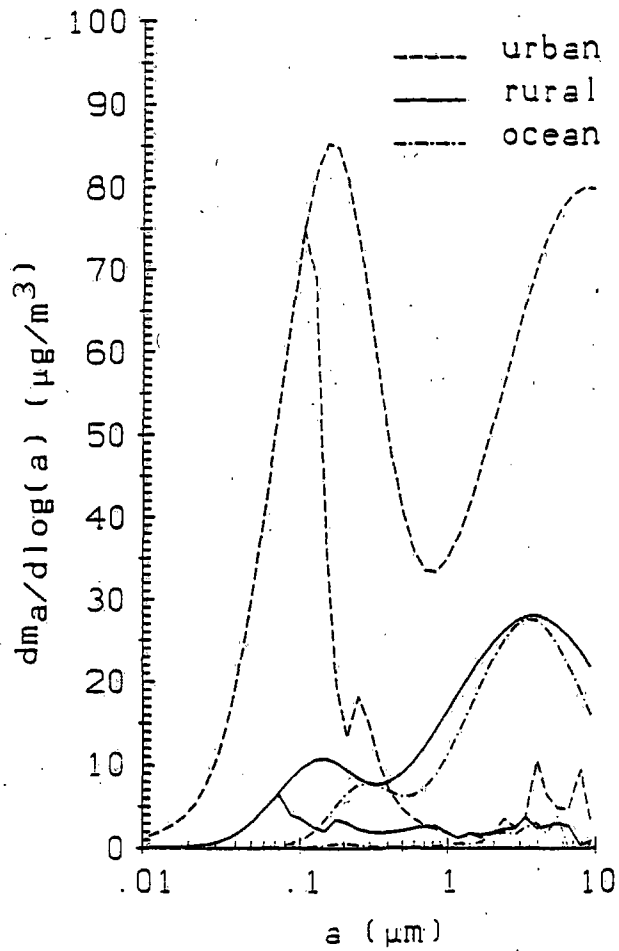

Figure 5

mass is very inhomogenously distributed. Hence, chemical reactions should be treated in spectral form as function of the droplet size.

Figure 4 shows for the three simulations the particle distributions before fog formation (upper curves) and at 9h of the second day (lower curves). In each model run the main differences are found in the large particle range where the number concentrations have decreased by several orders of magnitude. Figure 5 depicting the corresponding mass distributions, illustrates that the largest aerosol particles are almost completely washed out by the fogs.

References

Bott et al., 1990: Accepted for publication in J. Atmos. Sciences.

Mellor and Yamada, 1982: J. Geoph. Res., 851—875.

Pielke, 1984: Mesoscale Meteorological Modelling. Academic Press, 612pp.

THE GRAND MESA EXPERIMENT: A STUDY OF DRAINAGE FLOW STRUCTURE AND EVOLUTION WITHIN AN INCLINED BASIN

Dominique Ruffieux

NOAA/ERL/Wave Propagation Laboratory and Cooperative Institute for Research in Environmental Sciences
Boulder, Colorado 80303 USA

Clark W. King

NOAA/ERL/Wave Propagation Laboratory
Boulder, Colorado 80303 USA

ABSTRACT

Scientists from the Wave Propagation Laboratory studied the initiation and evolution of drainage flows within a large basin located in western Colorado, using both in situ and remote sensing instruments.

The paper describes the use of monostatic sodar data to classify the drainage flows according to their evolution and structure throughout the night. These data provided a seasonal climatology of the drainage flows within the region for the two-year measurement period. The drainage classifications are compared with the synoptic meteorology.

The paper next describes the spatial variability of the initiation of the drainage. A numerical model simulating the surface energy budget for the entire region shows that the orientation of the slopes is predominant in the timing of the formation of the drainage in the basin. A local surface cooling due to an early shadowing can produce downslope winds although the major part of the basin remains under the upslope regime.

1. Introduction

For the past 11 years, the Atmospheric Studies in Complex Terrain (ASCOT) program has carried out a series of field experiments designed to develop and test better models of transport and diffusion of pollutants in complex terrain. As part of this program, WPL operated an experiment site, the Big 10 Ranch, located in a steeply-inclined basin on the north face of the Grand Mesa (Fig. 1) in western Colorado. At this site, a monostatic sodar operated continuously from July 1988 through June 1990. Also, from December 1988 through November 1989, LLNL operated five 18-m meteorological towers at the sites indicated by asterisks on Fig. 1.

In this paper, data from the meteorological network are used for presenting simulations of the surface energy budget. Data from the monostatic sodar are used for classifying the types of drainage flow within the basin.

2. Drainage flow characteristics obtained from monostatic sodar data

2.1 Classifications using monostatic sodar data

Since 1979, WPL has used monostatic sodars to observe the initiation, evolution, and breakup of drainage winds as well as their interaction with other mesoscale flows. Sodars have an advantage over meteorological towers for such studies because they show the complete evolution of the drainage throughout its depth from onset near radiational sunset to cessation near radiational sunrise.

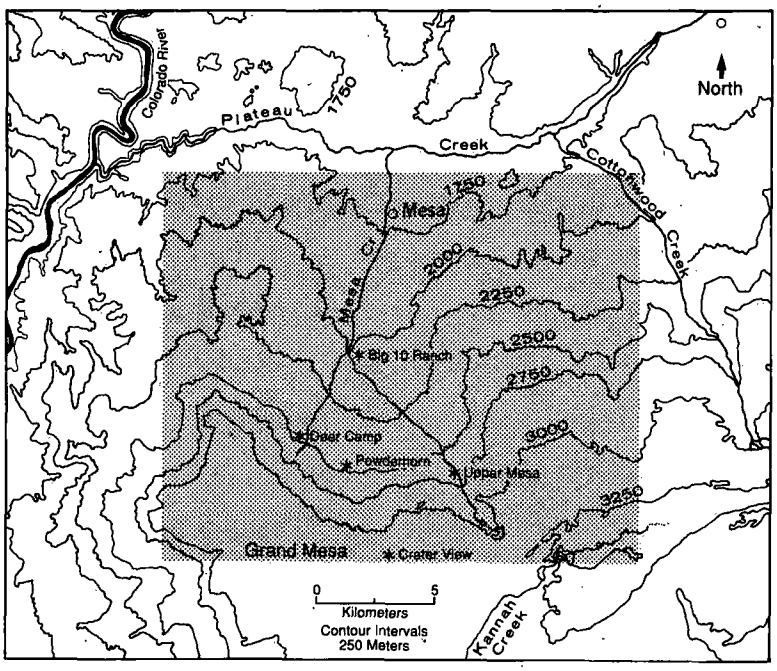

Figure 1. Topography of ASCOT study area in western Colorado. The shaded region corresponds to the topographical grid used in the simulations.

The sodar data obtained from the Big 10 Ranch were examined for each night over the 2-year period (July 1988 through June 1990); data were available for 79% of the nights. The analysis of monostatic sodar data is strictly qualitative. From the entire data set, it became obvious that the drainage fell into three fairly distinct categories: continuous drainage, discontinuous drainage, and no drainage. The criteria used to define these categories follow.

- Continuous drainage: at least 6 hours of drainage from onset to cessation. It includes steady, uninterrupted drainage from onset to cessation, steady drainage temporarily interrupted by disturbances, steady drainage transforming into disturbed drainage, and disturbed drainage transforming into steady drainage. A meteorological tower at the Big 10 Ranch showed relatively small standard deviations of the horizontal wind direction (σ_θ) during steady drainage periods. During disturbed periods, the drainage continued although speeds decreased and σ_θ values increased significantly.
- Discontinuous drainage: continuously disturbed drainage, intermittent drainage, and drainage winds which begin near radiational sunset but are destroyed by a disturbance. Possible sources of these disturbances include frontal passages, an increase in cloud cover, or the descent of strong ambient winds to the surface.
- No drainage: all flows that did not meet the criteria for the previous two categories.

Using the three drainage classifications we examined their monthly frequency distribution (Fig. 2). The results show June, November,

and December with the highest percentages of continuous drainage cases, recording 72%, 65%, and 66%, respectively. These 3 months also recorded the lowest monthly precipitation totals for the 2-year study period, each averaging less than 5 mm of precipitation for the month. March, recording the lowest frequency of continuous drainage and highest frequency of no drainage cases, also recorded the largest monthly average precipitation (34 mm). The large decrease in the frequency of continuous drainage cases from June to July and August appears to be associated with the climate of the region. While June is typically the driest month of the year in western Colorado, July and August are typically moist as a result of the seasonal monsoonal flow of moisture from the south. Since drainage winds are driven by radiative cooling at the surface, the presence of moisture and clouds will inhibit this cooling and decrease the frequency of continuous drainage cases.

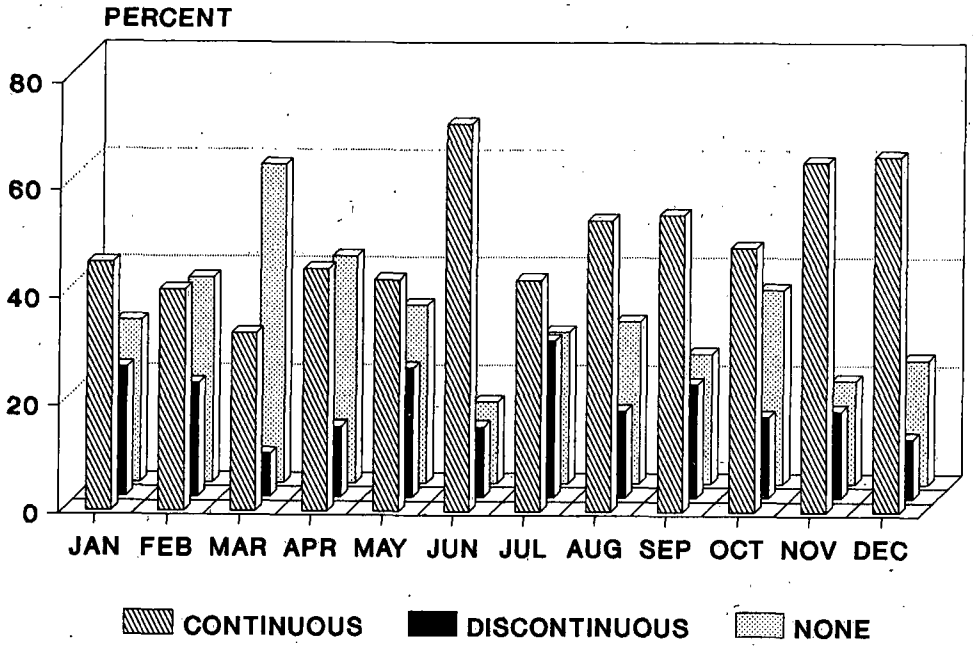

Figure 2. Monthly frequency distribution of drainage classifications from monostatic sodar data obtained at the Big 10 Ranch over a two-year period.

2.2 Relationship between drainage classifications and synoptic weather patterns

During the 2 years that the monostatic sodar operated at the Big 10 Ranch, nearly 70% of the nights experienced some drainage flow. As discussed previously, the structure and evolution of these flows differed greatly from night to night, ranging from steady, uninterrupted flows to intermittent flows. An examination of both the surface and 500-mb synoptic maps for periods with drainage winds revealed no distinct weather pattern for any particular type of drainage flow. Thus, predicting the drainage structure using the synoptic weather charts would be extremely difficult. The synoptic charts did reveal, however, that distinct synoptic patterns do exist for the no drainage cases. For the 2 years, 31% of the nights experienced no drainage. Of these no drainage cases, 95% can be explained by either a front approaching or passing through western Colorado, the passage of a 500-mb trough, or the presence of

monsoonal moisture. Nearly two-thirds of the cases were associated with surface fronts while nearly all of the no drainage cases during July and August were associated with the presence of monsoonal moisture.

3. Initiation of drainage, variability in space and time

3.1. Surface energy budget simulation

Wind data from the meteorological towers shows that the drainage flows did not all start at the same time within the basin. The shift in wind directions, from up- to downslope winds, can occur much earlier in the afternoon at some locations. This phenomenon seemed to be related to an early shadowing effect of the northeast-facing slopes. To study the variability in space and time of the initiation of the drainage flows we used a simplified surface energy budget simulation (Ruffieux, 1990). From a 72-m resolution grid of the area, the model calculates the value of sensible heat according to the different fluxes coming in and out of the cell. In the absence of synoptic perturbations and with light winds, this value of sensible heat is representative of the cooling of the cell.

3.2. Initiation of drainage at Deer Camp and the Big 10 Ranch

To illustrate the importance of the orientation of the slopes we chose a steady, uninterrupted drainage event (described in section 2.1). On 21 November 1989, the drainage began at 1330 MST at Deer Camp and 1610 MST at the Big 10 Ranch. Figure 3 shows the results of the computation of sensible heat for these two transition times.

The simulation of 1610 MST (Fig. 3c) illustrates a general cooling of almost all the basin. When the downslope flow starts at the Big 10 Ranch, the entire basin is already in a drainage situation (negative value of sensible heat flux). If we make the same simulation, but for 1330 MST, the results are much different (Fig. 3b). We have only a local cooling of some slopes in the southwest part of the basin. The shadowing effect due to the orientation of this part of the basin produces the early shift of the wind directions recorded by the Deer Camp tower. At this time, the energy available for heating exceeds 190 watts/m^2 at Big 10 Ranch.

With undisturbed synoptic conditions and clear sky, the local particularities (slope and orientation) strongly influence the spatial and temporal formation of drainage flows in different sections within the Grand Mesa Basin.

4. Conclusions

This study shows that a classification scheme of drainage winds is possible using remote sensing instruments. Monostatic sodars probe the entire vertical extent of deep drainages to heights unattainable with ordinary meteorological towers. This information can be valuable for studying transport and diffusion of pollutants in complex terrain.

A monthly frequency distribution of drainage categories showed June, November, and December with the highest percentages of continuous drainage cases. March recorded the lowest frequency of continuous drainage cases and the highest frequency of no drainage cases. A comparison of the drainage classifications with synoptic-scale meteorological parameters has shown that the only dependable predictor of whether or not drainage will occur lies in the accurate prediction of the position and strength of synoptic-scale disturbances approaching western Colorado.

Simulations of sensible heat fluxes over the entire basin showed a strong relationship between drainage wind onset and local intensities of downward short wave radiation. An early initiation of a local drainage situation can be induced by the shadowing of northeast-facing slopes, while the rest of the region is still in upslope wind conditions. Further work needs to be done on the effect of the orientation of the basin (at different scales) and on simulating the effect of the presence of snow on the initiation and evolution of the drainage winds.

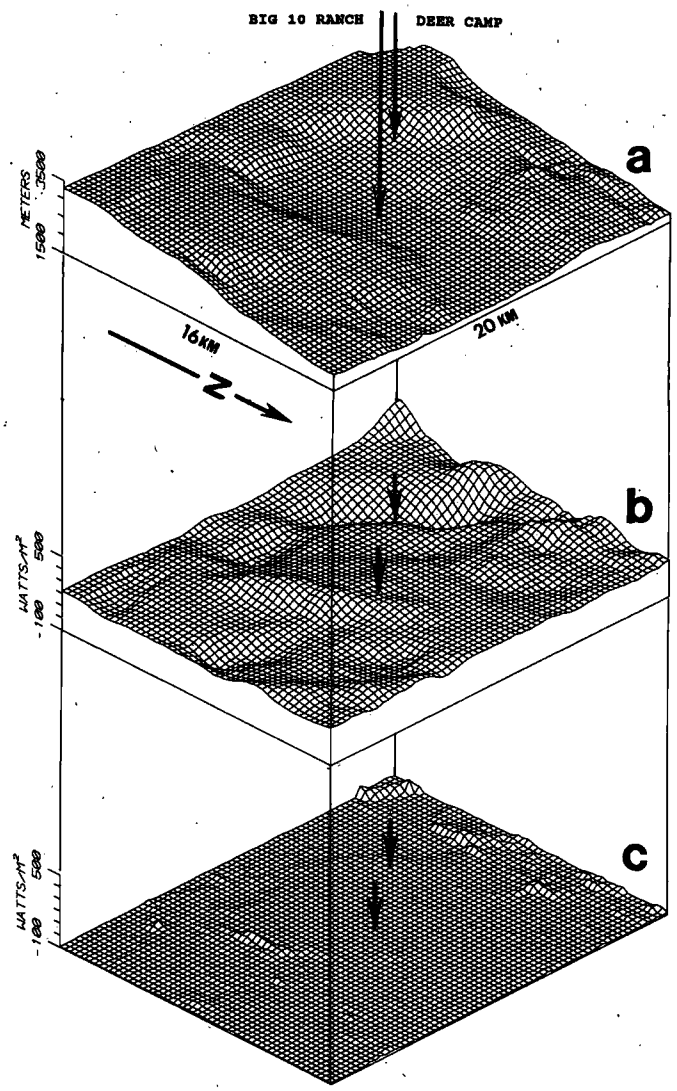

Figure 3. Model simulation of sensible heat flux on 21 November 1989. The arrows point to the two locations of measurement used in the model.
(a) 3-D view of the topography.
(b) Simulation for 1330 MST.
(c) Simulation for 1610 MST.

REFERENCES

Ruffieux, D., 1990: Evolution of the surface energy budget in complex terrain and its effect on the initiation of an inversion layer near the ground. Fifth Conference on Mountain Meteorology, 25-26 June 1990, Boulder, CO, Amer. Meteorol. Soc., Boston, MA, 255-259.

ACKNOWLEDGEMENTS

This study was supported in part by the U.S. Department of Energy ASCOT program and the Swiss National Science Foundation.

The calculation of back-trajectories with a mass-consistant diagnostic model over the Swiss Middleland

Urs Neu

Institute of Geography, University of Berne, Hallerstr. 12

1. Introduction / Summary

During the last 10 years about 20 automatic stations have been in operation over the Swiss Alpine Foreland (Swiss Middleland). Every 10 minutes they measure all important meteorological parameters. The aim of the presented model (called WITRA) is to use this data as a basis for the calculation of (back-)trajectories over complex terrain. WITRA interpolates a three-dimensional wind field out of the measured data and the radio-sonde profile of Payerne. By a mathematical method based on the variational analysis the windfield is slightly adjusted in a least-square sense in order to get it free of divergence, i.e. mass-consistant. Within the same step, the complex terrain and its effects on the wind are taken into account.

The most important problems of the method are:
1. the accuracy of the measured data (i.e. representation of the regional windfield);
2. the extrapolation of the wind data (usually measured at 10 m above ground level) to the top of the surface layer (represented by the lowest layer of the model) and
3. the vertical extrapolation of wind data in the eastern part of the model area (due to the lack of profile or higher-level measurements in this region).

This list shows that in the model the interpolation/extrapolation has the biggest influence on the resulting wind field. The mathematical adjustment only causes important changes near the surface.

2. Model description

2.1. The diagnostic non-divergent wind field

The application of the variational analysis method to meteorological problems was first described by Sasaki (1958). Later several applications concerning the calculation of diagnostic wind fields were made (Sherman 1978, Moussiopoulos and Flassak 1986, Ross et al. 1988). The now presented model follows more or less the description of the MATHEW model (Sherman 1978), except for a few changes.

The variational analysis theory defines an integral function whose extremal solution minimizes the differences between interpolated and adjusted values. In this specific case, the function used is

where u_o, v_o, w_o are the "observed" (i.e. interpolated) velocity components, u,v,w the adjusted ones, α_i are weighting factors and Φ is the Lagrange multiplier.
From the associated Euler-Lagrange equations whose solution minimizes equation (1) the equation for Φ is derived. The boundary conditions are definded as $\Phi \cdot du/dx=0$ for the boundary perpendicular to the x-direction, $\Phi \cdot dv/dy=0$ and $\Phi \cdot dw/dz=0$ for the boundary perpendicular to the y- and z-direction, respectively. As the spatial variation of the Lagrange multiplier gives the intensity of the adjustment at a certain point, there are two possibilities to satisfy these boundary conditions: Either to set $\Phi=0$ for open or "flow-through" boundaries or to set $d\Phi/dn=0$, i.e. the derivation of Φ perpendicular to the boundary is zero, which means no change of the flow through the boundary.

For the **computational formulation** the equation for Φ is approximated by a finite difference form at every point of a regular grid system, the boundary conditions at the boundary points inclusive.
The entire system of differential equations (one for each grid point within the boundaries and above the surface of the complex terrain) is solved simultaneously by a method developped by the Numerical Algorithms Group (NAG 1987). With the so derived values of Φ the adjusted velocities are calculated.
The model is working with a carthesian coordinate system because there would be difficulties with (the today normally used) terrain-following coordinates when the terrain is higher than the top of the calculated layer at certain locations. This is the case in the Swiss Middleland with the Alps on one side and the Jura mountains on the other side.

For the **interpolation** only meteorological stations are used, where there are no locally disturbing effects in the neighbourhood.
Many of the stations are more or less influenced by the terrain, a fact that can hardly be avoided over complex terrain, but often these effects are representative for a whole region (e.g. Altdorf in the Reuss-Valley). The extent of the area represented by a certain station is of course a question of the density of measuring points.
The acceleration of wind speed over a building in an open countryside is taken into account by a slightly diminution of wind speed for measuring points on buildings.
The wind speed, usually measured 10 m above ground, is extrapolated to the lowest model layer at 100 m above ground by using a power-law profile

$$u(z) = u_1 \cdot (z/z_1)^p$$

where $u(z)$ is the wind speed at hight z, u_1 the speed at the measuring hight z_1. The exponent p is estimated from the three-level tower data of the meteo-tower (110 m high) at Gösgen.
In a first step a horizontal wind field at the lowest level using stations below 700 m a.s.l. and a horizontal field at the top of the Planetary Boundary Layer taking mountain stations and data from the radio-sonde profile at Payerne are interpolated and extrapolated.
Data of mountain areas are difficult to handle because there are often strong influences of terrain induced winds like slope or valley winds. There is only one really "good" mountain-top station in the region in question with forest on all slopes around reducing the thermal effects (on the Napf).
For each grid point the velocity components are interpolated using the three nearest measuring points weighted by the square of the inverse distance between the grid point and the measurement.
Vertical interpolation between "top field" and "bottom field" is made by adjusting the profile to the radio-sonde profile of Payerne, diminishing the adjustment with increasing distance between the grid point and Payerne. For points far away from Payerne or with mountains in between, interpolation is linear.
The interpolated wind field is adjusted in the above described way. Vertical wind speeds are only induced due to the constraint of non-divergence by the mathematical adjustment. Since the lack of vertical wind speed data is usual, the initial values are set to zero.

2.2. Model area

The model area of about 90 x 220 km² contains the Planetary Boundary Layer over the area between the Alps and the Jura mountains. Grid resolution is about 1,5 km in the horizontal and 100 m in the vertical direction.

2.3. Trajectories

To determine the trajectories a wind field is calculated every hour. At the points of interest the velocity components are linearly interpolated between the grid points. The time step is variable.
First, the velocity components u_o, v_o, w_o are calculated at the time and place of start. Then a first approximation of the point after one time step is determined by

$$P_1(x_1, y_1, z_1) = (x_o + u_o \Delta t, y_o + v_o \Delta t, z_o + w_o \Delta t).$$

Afterwards the velocity components u_1, v_1, w_1 at point P_1 at time $t+\Delta t$ are calculated and the second approximation P_2 of the point in question is given by

$$P_2(x_2,y_2,z_2)=(x_o+u_o\frac{\Delta t}{2}+u_1\frac{\Delta t}{2}\ ,y_o+v_o\frac{\Delta t}{2}+v_1\frac{\Delta t}{2}\ ,z_o+w_o\frac{\Delta t}{2}+w_1\frac{\Delta t}{2}\ )$$

This step is repeated so that

$$P_n(x_n,y_n,z_n)=(x_o+u_o\frac{\Delta t}{2}+u_{n-1}\frac{\Delta t}{2}\ ,y_o+v_o\frac{\Delta t}{2}+v_{n-1}\frac{\Delta t}{2}\ ,z_o+w_o\frac{\Delta t}{2}+w_{n-1}\frac{\Delta t}{2}\ )$$

until $(x_n-x_{n-1})^2+(y_n-y_{n-1})^2+(z_n-z_{n-1})^2$ is smaller than a fixed convergence criteria. P_n is then taken as the new starting point for the next time step. This method was proposed by Pettersen (1956).
If the point is between the lowest model layer and the terrain surface, the interpolation is made by using the already mentionned power-law profile.
To determine back-trajectories, the negative values of the velocity components (e.g. $-u_o, -v_o, -w_o$ instead of u_o, v_o, w_o) are used in the same way to calculate the point at time $t-\Delta t$, $t-2\Delta t$, etc.

2.4. Restrictions on model applications

At the moment the application of WITRA is restricted to winter time boundary layer with poor convection, i.e. with a temperature inversion, a closed cloud layer and wind speeds greater than 2 m/s. The meteo-tower data show that at wind speeds below 2 m/s the data at 110 m a.g.l. and 10 m a.g.l are almost independent. This means that it is not possible to calculate the wind above the surface layer from 10 m data. In addition, the spatial changes of wind speed and direction are so big in situations with weak wind that the interpolation of point measurements cannot give accurate results.
To calculate wind fields in the Convective Boundary Layer, measurements of vertical wind speed would be necessary. And it wouldn't be possible anymore to neglect turbulence.

2.5. References

Pettersen, S., 1956: Weather analysis and forecasting. 2nd ed. vol.I. McGraw-Hill, New York, 488 pp.

Sasaki, Y., 1958: An objective analysis based on the variational method. *J. Meteor. Soc. Japan*, 36, 77-88.

Sherman, C.A., 1978: A mass-consistent model for wind fields over complex terrain. *J. Appl. Meteor.*, 17, 312-319.

Statistical study of the trajectories of air masses in Alpine area

Villone B. (*), Anfossi D.(*), Cassardo C. (**)

(*) Istituto di Cosmogeofisica , CNR, Torino

(**) Istituto di Fisica Generale dell' Universita' di Torino

1) Introduction

In this work we shall examine the statistics over five years of the air masses arriving to three sites of the Alps.
Among the aims of this study there is to find out the relative contribution to the deposited compounds of:
a) sources located below or above the P.B.L;
b) local or remoted sources;
Moreover , we shall examine the statistics of air masses arriving to an alpine location separating between all the days of the period considered and only rainy days.

2) Trajectory climatology calculation

Our method of air masses trajectories computation considers the motion of the centre of mass only, thus disregarding the real dimension of the mass itself and the diffusion processes.
The ECMWF three-dimensional wind analysis are the data input to our model. The grid resolution of the input data is 1.875X1.875 deg.
The interpolated values of u, v, ω are utilized to move the air mass at each time step Δt.
The wind data set at our disposal covered only a limited area (34.5 N - 51.0N, 0 - 21E). Considering that our analysis was devoted to Northern Italy, this fact limited the length of our trajectories to about 500 km.
Our program computes a series of backward trajectories arriving to a given receptor two times in a day.
A circle of given radius, centered on the receptor, is considered. The circle is divided into eight sectors and the analysis is carried out counting how many trajectories crossed each sector and

computing their average travel times. The present analysis distinguishes the four seasons.
The vertical distribution of the trajectories crossing heights, both at each sector and at the whole circle, is evaluated.

3. Application of the method

We applicated this method to Plateau Rosa (3500 m a.s.l., 45.56N, 7.42E), to the Careser glacier (3000 m a.s.l., 46.25N, 10.30E) and to the Brenner Pass (47N,11.30E).
At Brenner Pass we calculated also the statistics for only rainy days.

4. Results

There is a predominance as expected of trajectories from the western sectors. Also contribution from other sectors is present. Slight differences among the sites occur; a not relevant seasonal variability is present.
A general result is that the probability for a trajectory to be originating from P.B.L. is low. The sectors of which the majority of them arrive are S
and SE. Seasonal differences occur.
The vertical distribution indicate that a big part of trajectories considered on the distances considered are nearly isobaric, depending also on the sectors considered.
For Brenner Pass the difference between all the days and only rainy days is examined . For rainy dais the biggest contribution is from SW.
Other particularities on the differences between both the statistics are
considered.

5) Conclusions

By this way is possible to characterize meteorologically sites of interest.
One must use this results carefully taking account of the resolution of the ECMWF wind analysis used in this statistical study.

LA CLIMATOLOGIE DE LA DISPERSION ATMOSPHÉRIQUE EN PAYS MONTAGNEUX

Ph. Tercier, Dr. P. Viatte, P. Jeannet, J.M. Comment
Institut Suisse de Météorologie (ISM)

ABSTRACT : The new Swiss legislation on the protection of the environment sanctions the cantons' request for an impact study, before permitting the construction of new installations or the improvment of existing ones. The principal meteorological input data of the local scale atmospheric dispersion models is the windrose with respect to the atmospheric stability near the ground. This product is part of the climatology of the atmospheric dispersion. The goal of the project ist to give an adequate method to establish this meteorological input using the most widely measured parameters of the Swiss Meteorological Institute's ANETZ network.

RESUME : La nouvelle législation suisse sur la protection de l'environnement accrédite les cantons à exiger une étude d'impact pour l'autorisation de nouvelles installations ou pour l'assainissement d'anciennes installations. La donnée d'entrée météorologique principale aux modèles de dispersion atmosphérique à l'échelle locale est la rose des vents en fonction de la stabilité atmosphérique près du sol. Ce produit s'inscrit dans la climatologie de la dispersion atmosphérique. Le but du projet est d'élaborer une méthode pour déterminer cette donnée météorologique permettant d'utiliser des paramètres mesurés à toutes les stations du réseau ANETZ de l'ISM.

1. Introduction

Plusieurs schémas existent pour établir une climatologie de la dispersion atmosphérique: Pasquill, Turner, Cramer, Slade, Klug–Manier ou Vogt–Polster, etc.. Comme la stabilité atmosphérique correspond à une intensité de turbulence, les schémas utilisent communément un paramètre thermique dont l'influence est corrigée par la vitesse du vent près du sol. Le bilan de rayonnement et le gradient de température sont de bons indices de la stabilité atmosphérique. Ces mesures étant peu répandues, parce que difficile à réaliser, les auteurs des années 60 ont appliqué la nébulosité et la hauteur du soleil comme substitut. Le plan d'observation de la nébulosité du réseau ANETZ de l' ISM est limité. Une substitution de la nébulosité doit donc être recherchée tout en veillant à utiliser des paramètres météorologiques mesurés toutes les heures à toutes les stations ANETZ.

La plupart des schémas ont été ajustés pour des régions relativement plates. Il faut donc tester leur validité ou reconnaître leur sensibilité pour une région montagneuse comme la Suisse, le Plateau suisse compris.

Le schéma de Polster (1969) est issu d'une étude de corrélation entre les schémas "synoptiques", la mesure du gradient thermique vertical mesuré sur une base de 100 m et le bilan de rayonnement. A ce titre, les mesures météorologiques des sites de centrales nucléaires suisses, effectuées sur de hauts mâts, représentent une bonne base de référence pour une étude de corrélation avec les mesures ANETZ.

Nous présentons donc 10 variantes de schémas pour déterminer les classes de dispersion **à partir de données météorologiques horaires.** Certaines de ces variantes sont très semblables, ne se distinguant que sur la période "nuit", resp. "jour" de la journée.

Cette étude en est à son premier stade. Les résultats actuels n'ont donc pas un caractère définitif. Ils permettent toutefois d'entrevoir quelques possibilités intéressantes.

2. Réseau de mesures météorologiques ANETZ

La mise en route du réseau de mesures automatiques ANETZ a débuté vers la fin des années 70 de sorte que l'on dispose actuellement de plus ou moins dix ans de mesures horaires pour près de 50 stations (stations de montagne non comprises) permettant ainsi d'établir une statistique de référence. Les paramètres utiles sont la vitesse et la direction du vent, le rayonnement global et les précipitations, la température à 2 m et à 5 cm/sol et l'humidité relative. La nébulosité, le type et la hauteur des nuages sont limités à 8 observations par jour (jour et nuit) pour une dizaine de stations seulement, et à 6, voire 3 observations par jour (jour seulement) pour les autres stations. La création de séries horaires à partir des 8 observations est encore possible par interpolation temporelle.

3. Classes de stabilité (ou de dispersion) atmosphérique,

L'état de stabilité atmosphérique près du sol est souvent désigné par les lettres A à G ou 1 à 7. Il est bien caractérisé par le comportement d'un panache de fumée.

1	A	très instable	a) forte instabilité (typique
2	B	instable	d'une belle journée d'été, avec vent faible et convection
3	C	légèrement inst.	b) gradient adiabatique
4	D	neutre	(par vent modéré à fort, ou couverture nuageuse compacte)
5	E	légèrement stable	c) inversion au sol dépassant
6	F	stable	la hauteur du panache (par
7	G	très stable	nuit claire, avec vent faible)

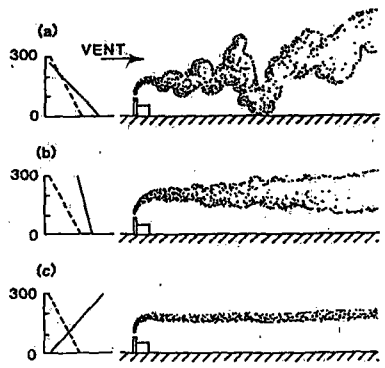

Pour limiter le nombre de cas à calculer dans une prévision des immissions, on peut dans certains cas appliquer la réduction suivante:

instable:A,B neutre : C,D stable : E,F,G

4. Variantes des schémas de détermination des classes de dispersion

Dix méthodes (ou modules) ont été programmées en fonction des mesures, dont-on dispose actuellement dans notre banque de données TIDOMES. La liste suivante précise les paramètres météorologiques horaires utilisés par les différentes méthodes, s'ils sont mesurés, voire s'ils peuvent être calculés sur la base du réseau ANETZ ou non.

Vitesse du vent	u	ANETZ
Gradient de température 110-10 m/sol	GRD	
Bilan de rayonnement mesuré	Q	
Bilan de rayonnement calculé	Q( )	
Indice de bilan de rayonnement	NRI( )	
Rayonnement global mesuré	K^+	ANETZ
Différence de température 2 m - 5 cm	DT	ANETZ
Couverture nuageuse totale	N	ANETZ
Couverture nuageuse totale calculée (Albisser)	N_{Alb}	ANETZ
Couverture nuages moyens	N_m	ANETZ
Hauteur des nuages moyens	H_m	ANETZ
Hauteur du soleil	H_s	

La méthode d'Albisser (1987) permet d'estimer la couverture nuageuse totale à l'aide de la différence de température 2m-5cm sur sol, de l'humidité relative, des précipitations et de la vitesse du vent. Dans le cas de 8 observations par jour de la nébulosité,

la série horaire est établie par interpolation temporelle. Le Tableau suivant donne un aperçu générale des relations paramétriques des différentes méthodes.

module	PARAMETRES jour	PARAMETRES nuit	limite jour–nuit	schéma de référence
1	u, GRD	u, GRD		Polster
2	u, Q	u, Q		Polster
4	u, Q (K^+) corrél. 1)	u, DT	$K^+ \leq 5$ W/m^2	Polster
5	u, Q (K^+) corrél. 1)	u, N_{Alb}	$K^+ \leq 5$ W/m^2	Polster–Turner
6	u, Q (K^+) corrél. 1)	u, N	$K^+ \leq 5$ W/m^2	Polster–Turner
7	u, Q (K^+, N) Wamser 2)	u, N	$K^+ \leq 5$ W/m^2	Polster–Turner
8	u, NRI (H_s, N)	u, NRI (N)	$H_s = 0°$	Turner simpl.
9	u, N	u, N	$H_s = 0°$ + ad. 3)	TALuft simpl.
10	u, NRI (H_s, N,N_m,H_m)	u, NRI (N,N_m,H_m)	$H_s = 0°$	Turner complet
11	u, N, N_m	u, N, N_m	$H_s = 0°$ + ad. 3)	TALuft complet

1) selon corrélation entre mesure du bilan de rayonnement et du rayonnement global 2) selon relation de Wamser (1980)
3) Il s'agit d'adaptations diverses en fonction de l'époque de l'année.

Commentaires :

- le gradient de température et le bilan de rayonnement mesurés ont l'avantage de fonctionner pour le jour et pour la nuit sans adaptation spécifique. Toutefois pour le module 1, on ne dispose que de mesures faites sur les sites de centrales nucléaires (Gösgen, Leibstadt, Beznau, Mühleberg pour le site étudié de Kaiseraugst près de Bâle) et pour le module 2, des mesures faites à Payerne.
- Les modules 4 et 5 disposent des mesures horaires présentes à toutes les stations ANETZ.
- Limite jour–nuit par le rayonnement global : dès le lever du soleil quelque soit la nébulosité, le rayonnement global horaire dépasse 5 W/m^2.
- La comparaison des modules 4, 5 et 6 n'est effective que pour la nuit. alors que celle des modules 6, 7 et 9 ne l'est que pour le jour.
- Les modules 8 et 9 n'utilisent que la couverture nuageuse totale et sont une simplification des schémas originaux (module 10 et 11). Les modules 9 et 11 (TALuft) restent néanmoins très semblables, ce qui n'est pas le cas des modules 8 et 10. Les schémas 8 à 11 distinguent 7 classes de stabilité. Une réduction à 6 classes est opérée par assimilation de la classe 7 à la 6.
- A titre d'exemple de schéma de classification, celui de Polster (GRD) est présenté ci–après avec la correspondance entre les classes du gradient de température 110–10m et celles du bilan de rayonnement exprimé dans 2 unités différentes.

K/100m	≤ – 1.5	–1.4 –1.2	–1.1 –0.9	–0.8 –0.7	–0.6 –0.0	+0.1 +2.0	≥ +2.0
cal/cm^2/min	> 0.60	0.60 0.35	0.34 0.16	0.15 0.09	0.08 –0.01	–0.02 –0.04	≤ –0.05
W/m^2	> 419	419 244	243 112	111 63	62 –7	–6 –27	≤ –28
0.0 0.9	A	A	B	C	D* 1)	G 3)	G 3)
1.0 1.9	A	B	B	C	D* 2)	G 3)	G 3)
2.0 2.9	A	B	C	D	D	E	F
3.0 4.9	B	B	C	D	D	D	E
5.0 6.9	C	C	D	D	D	D	E
≥ 7.0 m/s	D	D	D	D	D	D	D

modifications ISM–ENV : 1) D* --> E 2) D* --> D 3) G --> F

5. Premiers résultats

Le module 1 (Polster, gradient de température) est appliqué depuis des années sur les mesures du site de la centrale nucléaire de Goesgen, situé au centre du Plateau suisse. Les répartitions annuelles figurent ci–contre. Le Plateau suisse

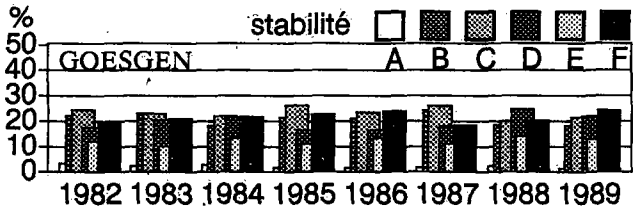

pouvant être assimilé à une très large vallée entre le Jura et les Alpes, les conditions de lac d'air froid maintiennent une proportion élevée des classes stables (E et F). Les répartitions ne varient pas fortement d'une année à l'autre.

La comparaison des méthodes (modules) élaborées s 'est faite sur l'année 1989 (déc.88 à nov.89). Les fréquences annuelles des classes de dispersion pour un choix de stations ANETZ figurent ci-dessous. En outre les corrélations ont été calculées entre les séries des différentes méthodes. On peut résumer ces premiers résultats comme suit :

- Le bilan de rayonnement (2) et la méthode TALuft (9 et 11) favorisent les classes stables (E+F) au détriment de la classe neutre (C+D), alors que la classe neutre prédomine avec le schéma de Turner (8 et 10). La classe très instable (A) est quasi inexistante avec le schéma Turner. Dans un relief comme celui de la Suisse, les brises, resp. les vents de vallée, d'origine thermique se maintiennent généralement au-dessus de 1 m/s. Conformément à l'attente, toutes les méthodes indiquent une plus grande part de situations stables dans les vallées (Sion et Locarno-Magadino) que sur le Plateau suisse (Genève, Payerne, Wynau et Zurich).
- La substitution du bilan de rayonnement par le rayonnement global n'est possible que pour le jour. Les corrélations établies entre les méthodes 2 et 4 (Payerne) laissent envisager une utilisation de la température mesurée à 2m et 5cm pour déterminer la stabilité nocturne. Puisque nous ne disposons pas de coefficients de dispersion établis en relation avec les paramètres météorologiques envisagés comme c'est le cas pour les schémas TALuft et Turner, il s'agira donc de maximiser les corrélations par adaptation des classes de valeurs entre le schéma approprié aux mesures ANETZ et l'un des 2 (ou les 2) schémas TALuft et Turner. Actuellement, on obtient entre le module 4 et celui de Turner (10), resp. celui de TALuft (11) une corrélation de 0.61 resp. 0.72 sur les cas de nuit.

Fréquences annuelles des classes de dispersion pour les modules 2 4 5 6 7 8 9 10 11

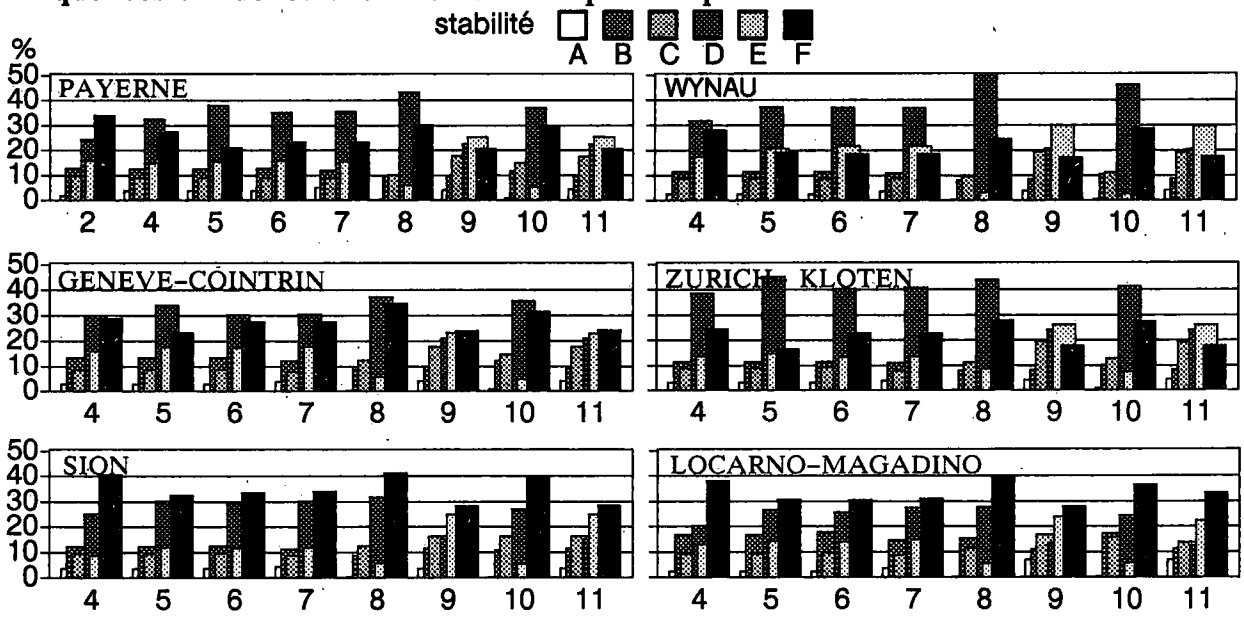

6. Références

Polster, G., 1969: Erfahrungen mit Strahlungs-, Temperaturgradient- und Windmessungen als Bestimmungsgrössen der Diffusionskategorien. Meteor. Rdsch., 22, 170-175.

Albisser, P. 1983: Abschätzung des nächtlichen Gesamtbewölkung mit Hilfe von ASTA-Daten. Rap. de travail de l'ISM No 116

Wamser, C., Schröter, J., 1980: Ein neues Ausbreitungskriterium. Meteor. Rdsch. 33

Section 6:

Examination of Short- and Longterm Variations of Climate and the Climatic Elements

LUFTTEMPERATURSCHWANKUNGEN OSTALPINER STATIONEN VON 1775-1989

Reinhard Böhm

Zentralanstalt für Meteorologie und Geodynamik, Wien, Österreich

Summary: Temperature variations on east-alpine observatories from 1775 to 1989.

The paper shows time series of 20 east-alpine temperature observing stations mainly situated in higher altitudes. Correlations between single stations are rather high (between 0.7 and 0.95) a fact which made it possible to obtain a representative spatial mean over all stations. The smoothed curve of the annual means shows high temperatures at the beginning (1775-1825) then a cooling of -1.1°C to two minima at 1840 and 1880 and in the following an increase to a maximum at 1950 of again +1.1°C. Since 1950 a slight decrease of -0.2°C has taken place.

Um einen Beitrag zu der aktuellen Frage der anthropogenen oder natürlichen Klimaschwankungen zu leisten, wurde im österreichischen Klimadienst damit begonnen, lange Zeitreihen von Lufttemperaturdaten kritisch zu sichten, zu korrigieren, zu reduzieren und statistisch zu bearbeiten. Zur Zeit liegen 20 fertig bearbeitete Reihen von ostalpinen Stationen vor, wobei zunächst in erster Linie Höhenstationen herangezogen wurden. Die in der Folge besprochenen Ergebnisse beruhen auf den gereinigten, einheitlich auf 24-stündige Mittel gebrachten Monats-, Jahreszeiten- und Jahresmitteldaten der in Abb. 1 gezeigten Stationen.

Ebenfalls in Abb. 1 dargestellt sind die Korrelationskoeffizienten der Jahresmittel aller Stationen mit dem zentral gelegenen Sonnblickobservatorium. Die hohen Werte von 0.7 bis über 0.9 lassen die Möglichkeit der Erarbeitung von räumlich gemittelten Trendkurven erkennen.

Bei der Reduktion und Homogenisierung der Datenreihen erwies sich der relative Homogenitätstest nach CRADDOCK als sehr brauchbar, der - in Verbindung mit einer genauen Aufarbeitung des Stationsarchivs - eine einwandfreie Festlegung der Homogenitätssprünge erlaubte. Diese wurden sodann durch Differenzenanpassung mit Daten von Nachbarstationen beseitigt. Abb. 2 zeigt einige Beispiele für die Anwendung des Craddock-Tests.

Infolge der hohen Korrelationen zwischen weiter entfernten oder auch von Stationen unterschiedlicher Lage konnte der Versuch unternommen werden, Mittelwerte aller Stationen zu bilden und diese räumlich gemittelten Zeitreihen zu analysieren, also eine repräsentative "Ostalpenkurve" zu erarbeiten. Abb. 3 zeigt das Ergebnis für die Jahresmittel, Abb. 4 die analogen Verläufe für die vier Jahreszeiten. Zur Glättung wurde ein Gauß'scher Tiefpaßfilter mit einer Filterweite von 20 Jahren verwendet. Ohne auf feinere Details eingehen zu können, sei auf den Anstieg der gefilterten Jahresmitteltemperaturen der Ostalpen von den Minima um 1840 und 1880 zum Maximum des 20. Jahrhunderts um 1950 von +1.1°C hingewiesen. Dieses Maximum liegt allerdings nicht höher als zwei Maxima um 1795 und 1820. Die Ostalpenkurve zeigt somit sehr gut den weltweit diskutierten steigenden Trend vom 19. zum 20. Jahrhundert, der allerdings durch zwei Tatsachen relativiert wird. Einerseits ist nach 1950 ein rückläufiger Trend von -0.2°C zu bemerken und andererseits zeigt die längere Ostalpenkurve - im Vergleich zu den verschiedenen globalen Kurven, die üblicherweise etwa zur Zeit des letzten markanten Minimums beginnen - in der langen Zeitspanne von 1775 bis 1825 ähnlich hohe bis leicht höhere Temperaturen als das aktuelle Maximum des 20. Jahrhunderts.

Die ostalpine Temperaturkurve der letzten 215 Jahre macht deutlich, daß bei der Verwendung von kürzeren Reihen - die zufällig (oder bewußt ?) zur Zeit eines Minimums beginnen - zur Untermauerung oder gar zum Beweis für einen evt. bereits wirksamen CO_2-Effekt zumindest größte Vorsicht am Platz ist, da man bei dem im 20. Jahrhundert beobachtbaren Maximum nicht von einem solitären Ereignis sprechen kann, da ähnlich hohe Lufttemperaturen bereits in instrumenteller Zeit beobachtet worden sind, und darüberhinaus etwa in den Ostalpen ein einheitlicher Trend zu nach 1950 wieder zurückgehenden Temperaturen beobachtbar ist.

Abb. 1:

MEßNETZ FÜR DIE ANALYSE DER OSTALPINEN LUFTTEMPERATURSCHWANKUNGEN

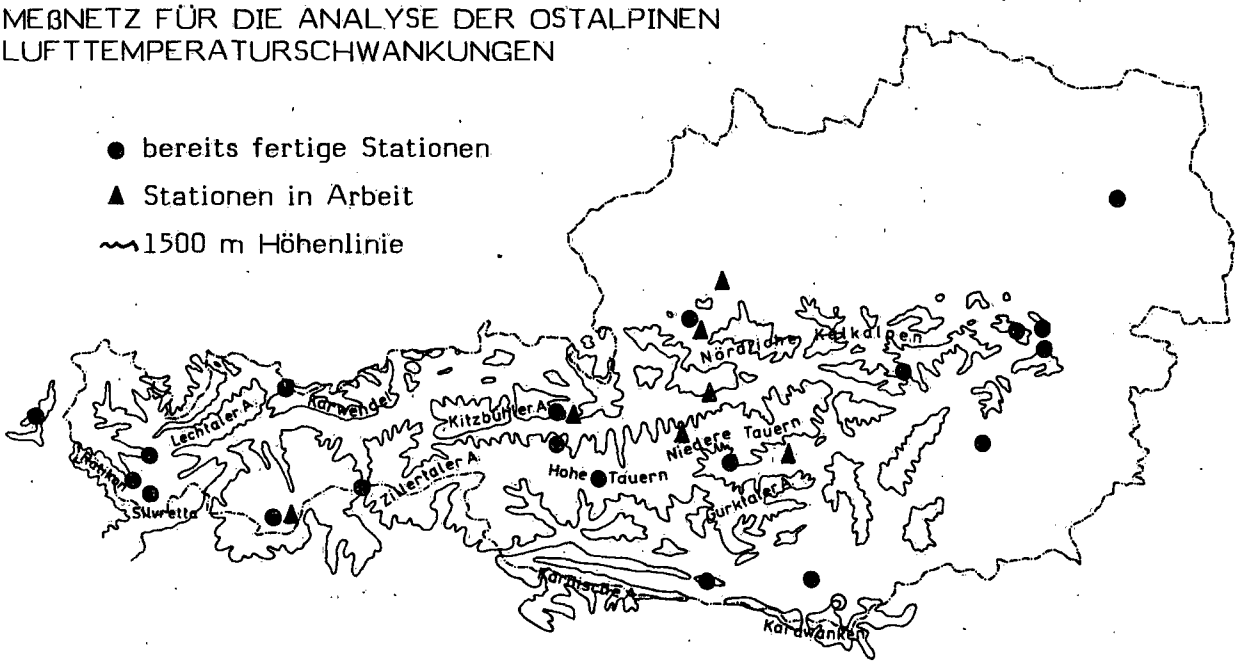

				Korrelation mit Sonnblick
3 106 m	SONNBLICK	1887-1989	Λ	1.00
2 962 m	ZUGSPITZE	1901-1989	Λ	0.96
2 500 m	SÄNTIS	1864-1989	Λ	0.94
2 140 m	DOBRATSCH-OBIR	1851-1989	Λ	0.94
2 036 m	MOOSERBODEN	1915-1989	∪	0.81
1 976 m	SCHMITTENHÖHE	1880-1989	Λ	0.95
1 908 m	VENT	1851-1989	∪	0.80
1 803 m	RAX	1878-1989	Λ	0.85
1 618 m	FEUERKOGEL	1930-1989	Λ	0.90
1 583 m	GALTÜR	1896-1989	∪	0.88
1 436 m	SCHÖCKL	1901-1989	Λ	0.87
1 372 m	BRENNER	1897-1989	X	0.71
1 270 m	LANGEN	1881-1989	/	0.79
1 227 m	PRÄBICHL	1897-1978	X	0.83
1 012 m	TAMSWEG	1919-1989		0.77
1 000 m	SEMMERING	1890-1989	X	0.76
980 m	GASCHURN	1885-1989	∪	0.79
486 m	REICHENAU	1865-1989	∪	0.69
447 m	KLAGENFURT	1851-1989	⌴	0.78
202 m	WIEN-HOHE WARTE	1775-1989	—	0.75

Λ Gipfellage ∪ Tallage / Hanglage X Paßlage ⌴ Beckenlage — Ebene

Abb. 2:
BEISPIELE FÜR DIE VERWENDUNG DES
RELATIVEN HOMOGENITÄTSTESTS NACH CRADDOCK
ALS ENTSCHEIDUNGSHILFE ZUR DATENPRÜFUNG UND REDUKTION

Lufttemperaturdaten - Jahresmittel in °C

Vergleich ZUGSPITZE - SONNBLICK

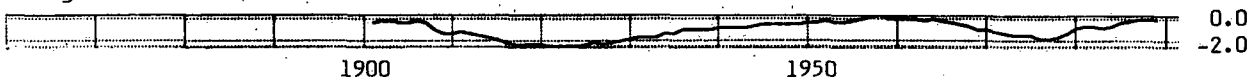

Vergleich ZUGSPITZE - SÄNTIS

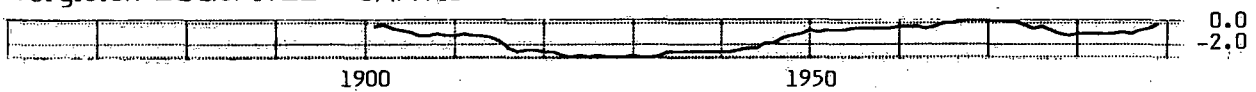

Vergleich SCHMITTENHÖHE - SONNBLICK, unreduziert

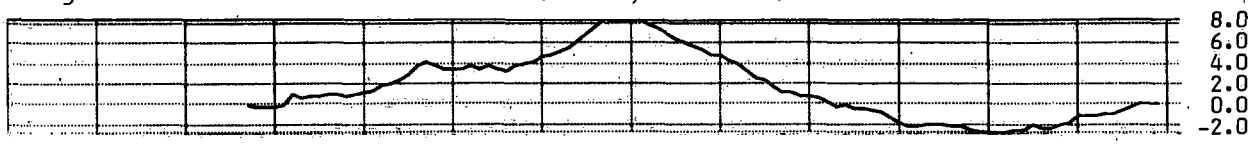

Vergleich SCHMITTENHÖHE - SONNBLICK, reduziert

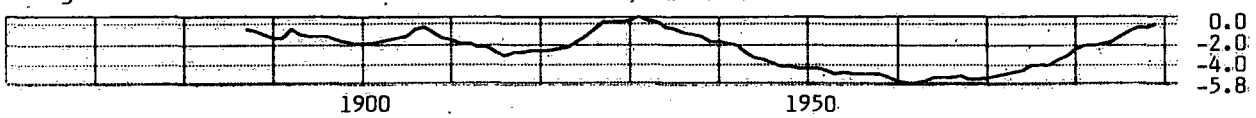

Vergleich GALTÜR - SÄNTIS, unreduziert

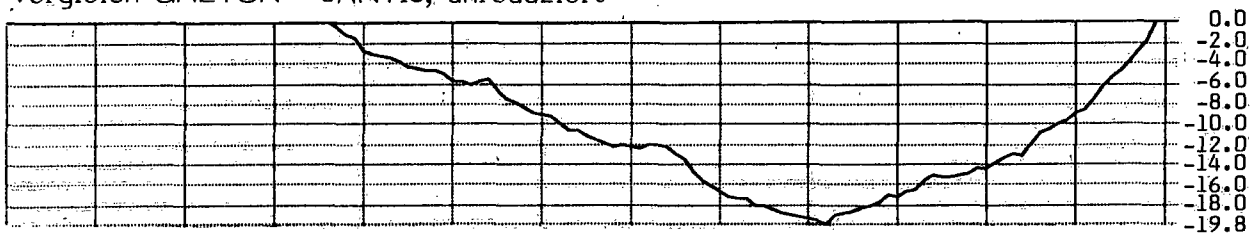

Vergleich GALTÜR - SÄNTIS, reduziert

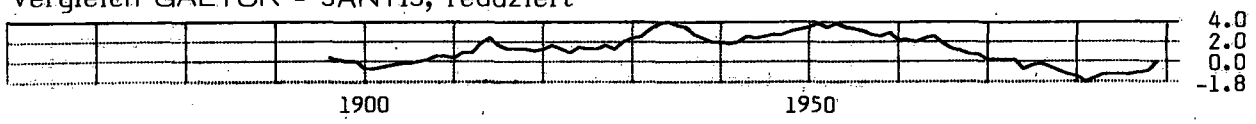

Vergleich REICHENAU/RAX - WIEN-HOHE WARTE, unreduziert

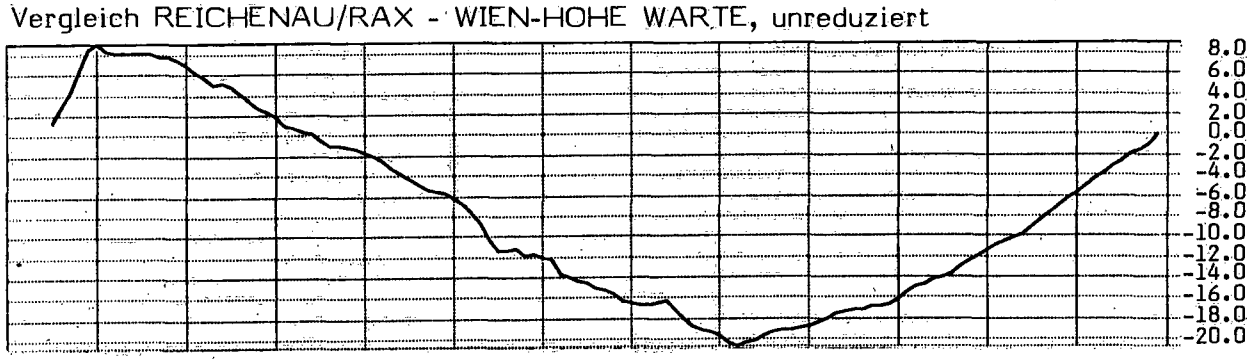

Vergleich REICHENAU/RAX - WIEN-HOHE WARTE, reduziert

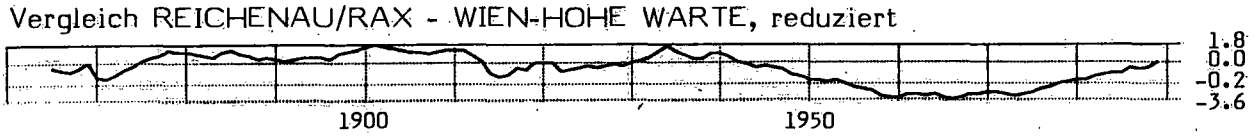

Abb. 3:
ZEITREIHENANALYSE DER OSTALPINEN LUFTTEMPERATURSCHWANKUNGEN
20 Stationen Analyse der Jahresmittelwerte

JAHRESMITTEL UND GEFILTERTER VERLAUF (Gauß'scher Tiefpaß, T * = 20 Jahre)
Relativwerte, bezogen auf das Mittel 1951-1980

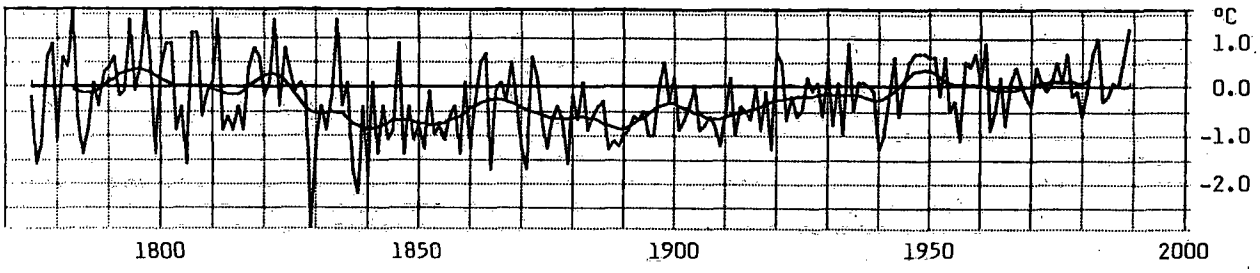

STANDARDABWEICHUNG DER EINZELSTATIONEN

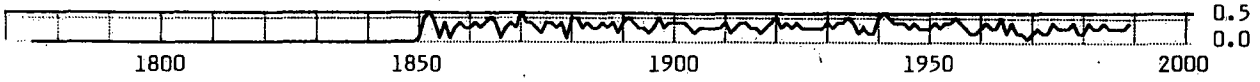

ZAHL DER VERWENDETEN STATIONEN

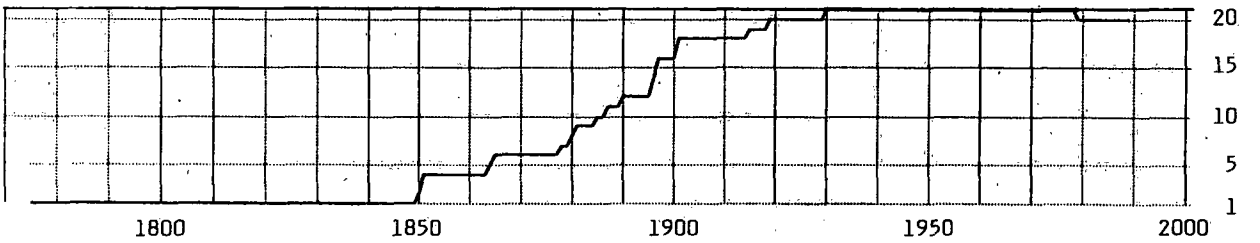

VARIANZ (20-jährig übergreifend)

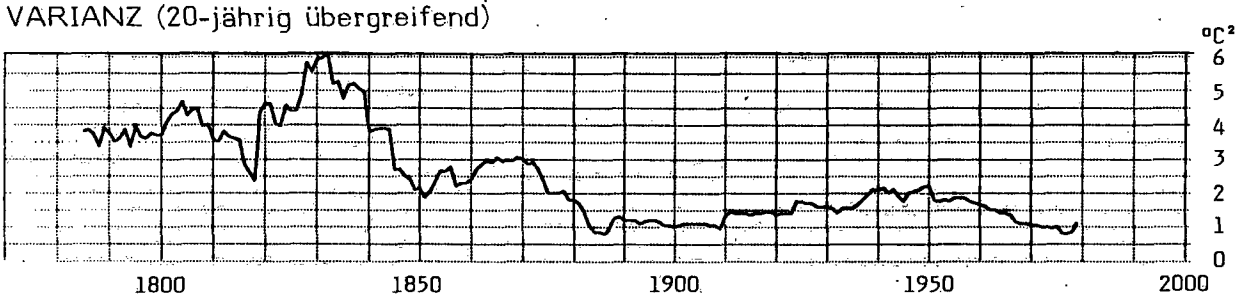

SCHIEFE (20-jährig übergreifend)

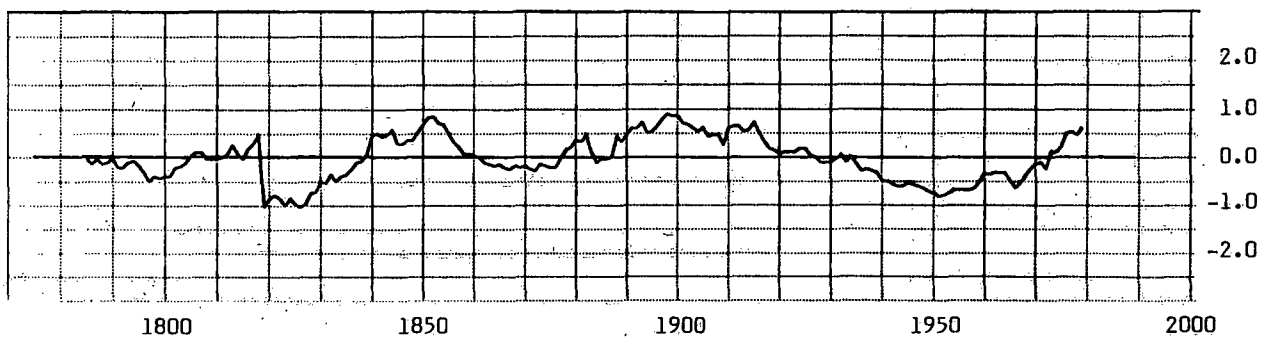

Abb. 4:
LUFTTEMPERATURSCHWANKUNGEN DER OSTALPEN - JAHRESZEITENANALYSE

Mittel aus 20 Stationen
Einzelwerte und gefilterter Verlauf (Gauß'scher Tiefpaß, T * = 20 Jahre)
Relativwerte, bezogen auf das Mittel 1951-1980

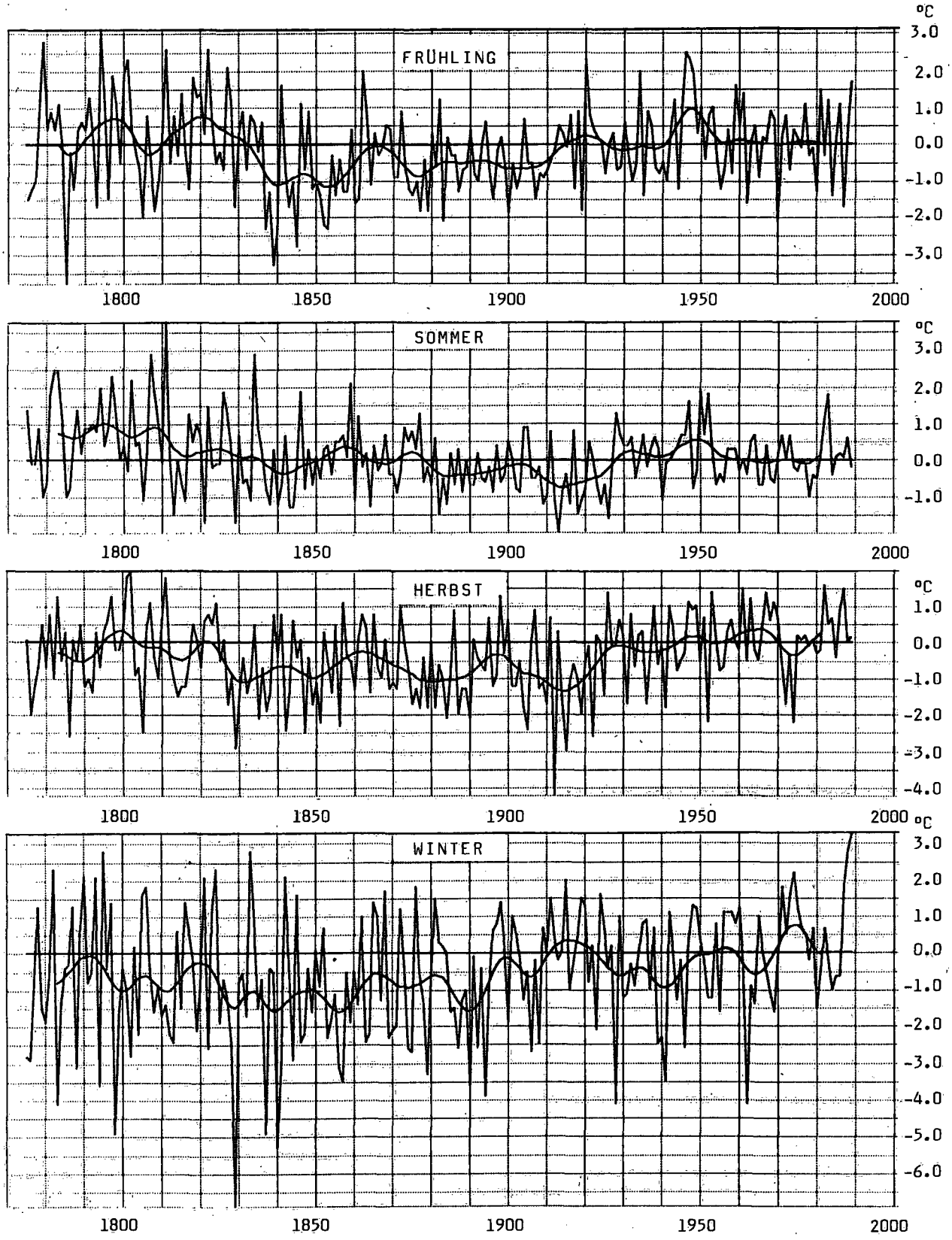

ZEITLICHE VARIATIONEN VON NIEDERSCHLAGSSUMMEN IN ALPINEN REGIONEN ÖSTERREICHS

Ingeborg Auer

Zentralanstalt für Meteorologie und Geodynamik, Wien, Österreich

Summary:

For the question of climatic change variabilities of precipitation have received far less attention than variations of temperature until now. Therefore in this paper the timeseries of precipitation records of stations above 1500 m should help to find out, whether there is a significant uniform trend in precipitation or not. For that the observations of about 120 precipitation stations have been taken into account, which partially reach back until 1876. As the record lenght of the available data sets differs much effort was needed to receive long-time homogeneous time series. For some locations in the Austrian Alps the reduction procedure was successful, so that a number of long timeseries can be presented here.

Zusammenfassung:

Beim Fragenkomplex der Klimaänderungen stehen zumeist Aussagen über langfristige Temperaturänderungen im Vordergrund, zeitliche Niederschlagsvariabilitäten bleiben meist im Hintergrund. Niederschlagstrendanalysen von Stationen über 1500 m Seehöhe sollen zur Klärung der Frage beitragen, ob ein eventuell vorhandener Niederschlagstrend innerhalb Österreichs auch einheitlich verlief. Zu diesem Zweck werden die Niederschlagsbeobachtungen von ca. 120 Meßstellen herangezogen, die vereinzelt bis 1876 zurückreichen. Auf Grund starker Stationsnetzfluktuationen nimmt das Homogenisieren des Datenmaterials großen Zeitaufwand in Anspruch. Für einige Orte war die Reduktionsprozedur bereits erfolgreich, sodaß schon einige Ergebnisse vorgestellt werden können.

Brauchbare Niederschlagsmessungen an österreichischen Höhenstationen liegen ab 1876 vereinzelt vor. Eine deutliche Verbesserung dieses Zustandes trat ab 1926 ein, markante Verschlechterungen sind infolge des 2. Weltkrieges und im Dezennium 1971-1980 eingetreten. Für die Bearbeitung solcher langen Datensätze stellen die zwangsläufigen Homogenitätssprünge die größten Hindernisse dar. Zum Auffinden der Inhomogenitäten wurden neben den noch vorliegenden Dokumentationen über die Änderungen an den Stationen absolute (z.B. ABBE) und relative Homogenitätstests (z.B. CRADDOCK) vorgenommen, wobei der Craddock-Test die schärfsten Aussagen zum Erkennen des Zeitpunktes der Inhomogenität lieferte.
Erst nach eingehenden Prüfungs- und Reduktionsprozeduren ist es sinnvoll, lange Datenreihen statistisch zu bearbeiten und Trendanalysen durchzuführen. Dazu gehören absolute und relative Häufigkeitsverteilungen, Perzentildarstellungen, die Bestimmung der Mittel- und Extremwerte und statistische Maße wie Schiefe, Varianz, Autokorrelation etc. Etwaige Trends werden mit Hilfe eines Gauß-Tiefpaßfilterverfahrens aufgezeigt, wobei sich Filterweiten von 20 bzw. bei längeren Reihen von 30 Jahren bewährt haben. Die Angabe des Stationaritätsbereichs erlaubt Aussagen über die Signifikanz der in der Zeitreihe auftretenden Klimaschwankungen.
Bis dato sind 3 alpine Regionen nach diesem Verfahren untersucht worden, die Ergebnisse werden auszugsweise dargestellt. Daß in Österreich in den letzten Jahren kein einheitlicher Niederschlagstrend vorherrschend war, wird klar, vergleicht man die gezeigten Beispiele. Es ist geplant, die Untersuchungen fortzuführen, wobei durch die Ausweitung auf Tal- und Ebenenstationen und die dadurch erreichte höhere Meßnetzdichte, eine Abgrenzung der Regionen mit einheitlichem Trend abgesichert werden sollte.

REGION SÜDKÄRNTEN Erste verfügbare Daten stammen vom Hochobir (2044 m). Diese wurden bis 1929 auf den Standort Dobratsch (2140 m) reduziert, sodaß eine homogene Niederschlagsreihe ab 1879 für die Region Dobratsch zusammengestellt werden konnte. Die mit Hilfe 20-jähriger Tiefpaßfilterung ermittelte Jahresniederschlagssumme zeigt eine markante niederschlagsreiche Phase zwischen 1947 und 1968, wohingegen der Zeitraum bis etwa 1896 als zu trocken erscheint. Bei der jahreszeitlichen Aufsplitterung verlassen speziell die Winter- und Herbstniederschläge den Stationaritätsbereich. 21-jährig übergreifende Varianzen weisen den Zeitraum von etwa 1940 bis 1970 als besonders niederschlagsvariabel auf. Vergleiche mit anderen, allerdings kürzeren Datensätzen zweier in der Region Südkärnten gelegenen Stationen wurden durchgeführt.

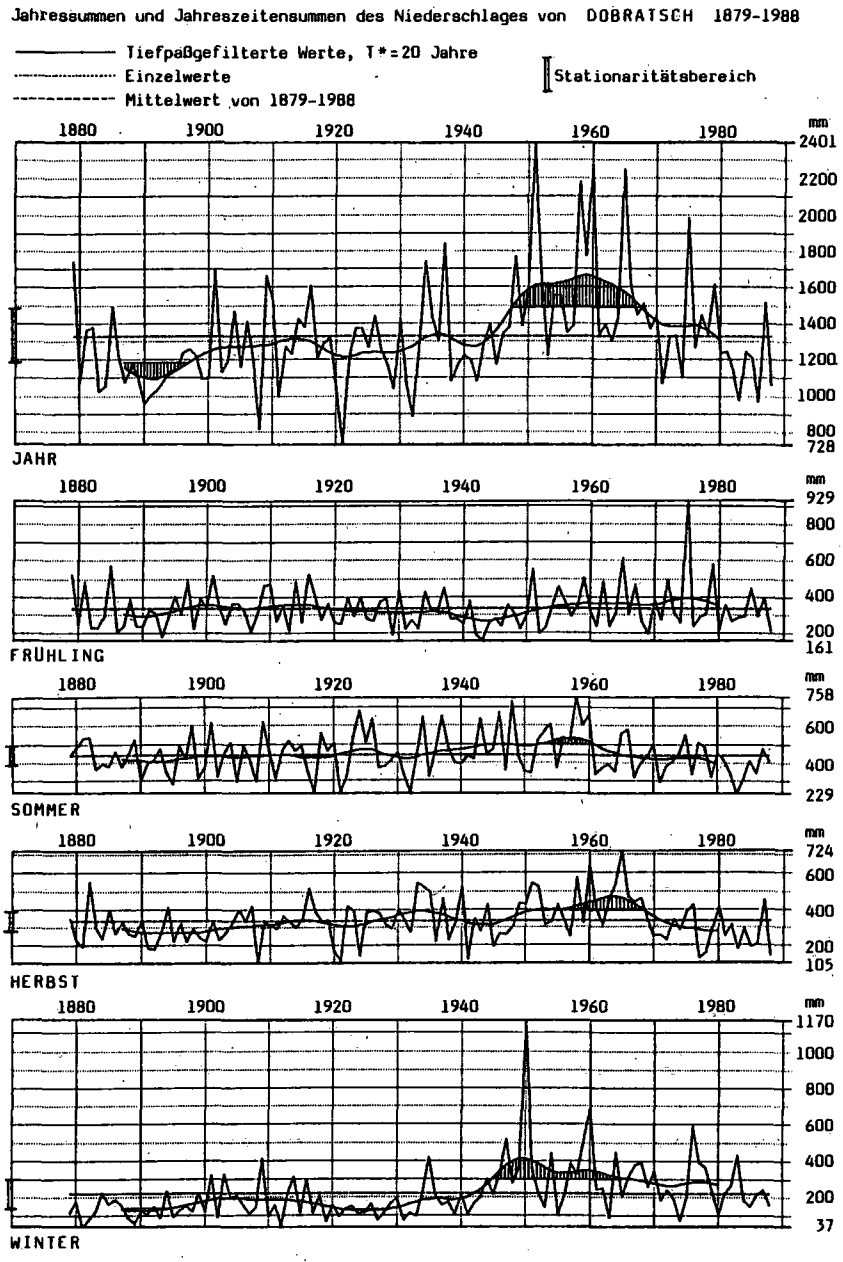

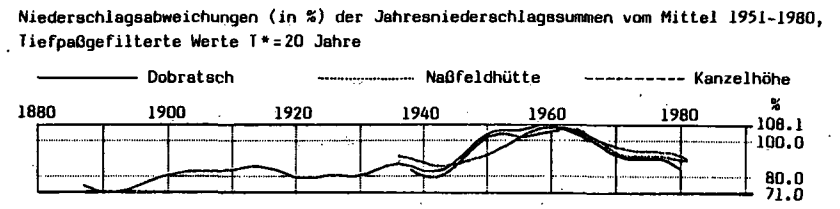

REGION ARLBERG

Die Beobachtungsreihe von Lech am Arlberg (1450 m) beginnt mit dem Jahr 1896. Die gefilterte Jahresniederschlagslinie zeigt 2 Minima um 1908 und um 1922, die stärkere Niederschlagszunahme ab 1960 läßt die gefilterte Jahreslinie um 1968 und ab 1976 den Stationaritätsbereich verlassen. Dem allmählichen Abklingen des Niederschlagsmaximums der Region Südkärnten steht also in diesem Gebiet eine Niederschlagszunahme gegenüber. Die 21-jährig übergreifende Varianz erreicht auch im Jahre 1971 ihren Höchstwert.

Jahressummen und Jahreszeitensummen des Niederschlages von LECH 1896-1989

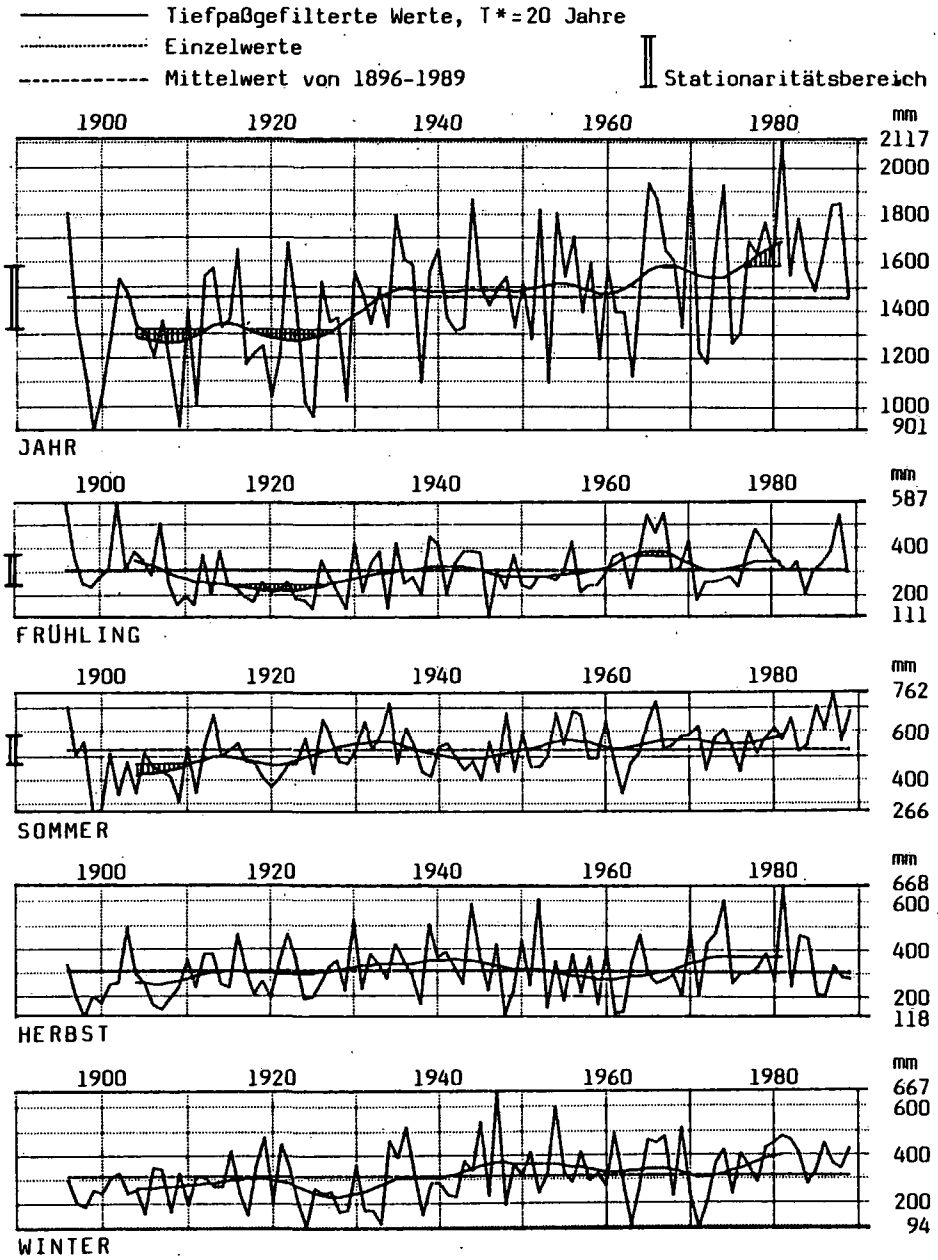

Niederschlagsabweichungen (in %) der Jahresniederschlagssummen vom Mittel 1951-1980, Tiefpaßgefilterte Werte T*=20 Jahre

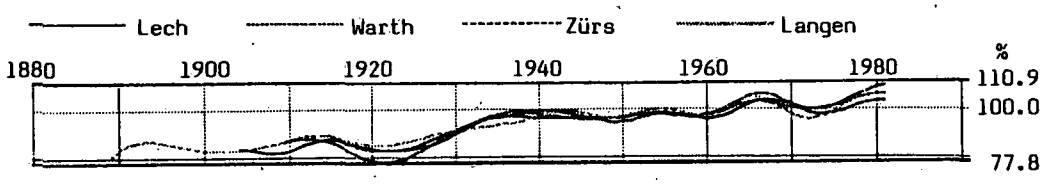

REGION HOHE TAUERN

Für die Hochgebirgsregion Hohe Tauern lieferten die Ombrometermessungen, die auf dem 3106 m hohen Sonnblickgipfel ab 1891 durchgeführt wurden, keine für Trendanalysen verwendbaren Daten. Daher wurde auf das Totalisatorenmeßnetz dieser Region zurückgegriffen, dessen Errichtung mit dem Jahr 1927 in Gang gesetzt wurde. Die zu bearbeitenden Datenreihen umfassen daher nur 63 Jahre. Beim 3076 m hochgelegenen horizontalen Totalisator wird eine markant zu niederschlagsreiche Phase von etwa 1958 bis 1968 klar erkennbar, die auch im Winter und Frühling aufscheint. Der Herbst zeigt ein Niederschlagsdefizit um 1970. Die 21-jährig übergreifenden Varianzen zeigen vom Tiefstwert um 1942 ein sprunghaftes Ansteigen mit einem Maximum um 1972. Mit den Vergleichstotalisatoren Rojacherhütte (2580 m), Radhaus (2117 m) Kolm-Saigurn (1600 m), Oberes Fleißkees (2808 m), Unteres Fleißkees (2558 m) und der Ombrometerstation Mooserboden (ab 1912) wurden Gebietsmittel errechnet, die im folgenden als Niederschlagsabweichungen zum 30-jährigen Mittel 1951-1980 dargestellt sind.

Jahressummen und Jahreszeitensummen des Niederschlages
Totalisator SONNBLICK (horizontal), 1927-1989

—— Tiefpaßgefilterte Werte, T*=20 Jahre
····· Einzelwerte
------ Mittelwert von 1927-1989
‖ Stationaritätsbereich

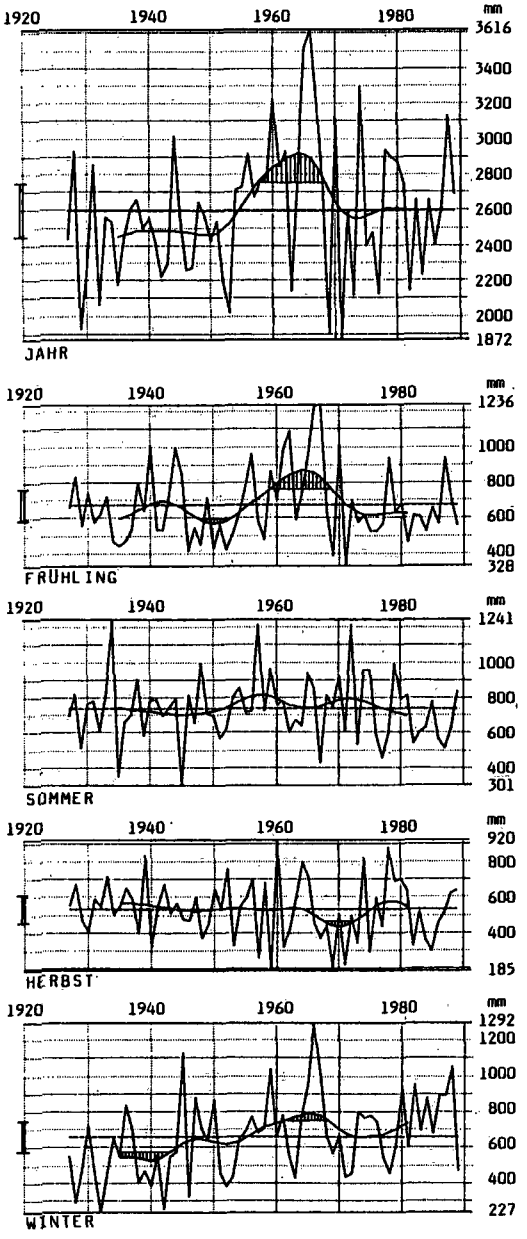

Niederschlagsabweichungen (in %) der Jahres- und Jahreszeitenniederschlagssummen vom Mittel 1951-1980 für die Region
HOHE TAUERN (Mittel aus 7 Stationen)
Tiefpaßgefilterte Werte, T*=20 Jahre
‖ Stationaritätsbereich

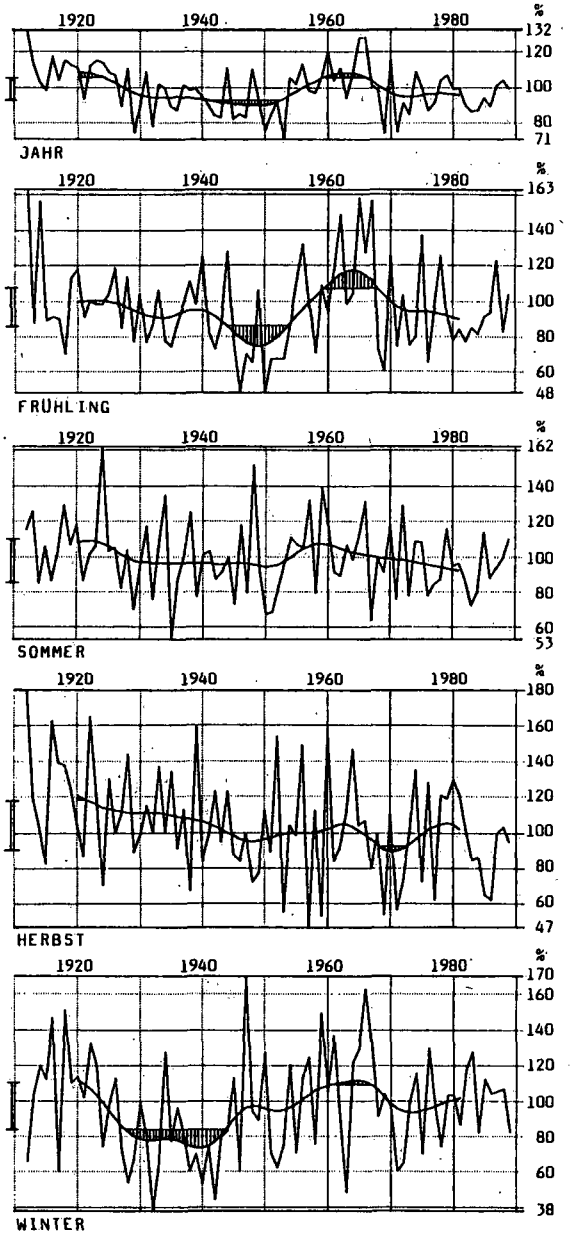

THE LAST CENTURY OZONE DATA MEASURED IN ZAGREB AND SOME ANALISES PROBLEMS

Inga Lisac

Geophysical Istitute,
Faculty of Natural Sciences and Mathematics,
University of Zagreb,
Horvatovac bb, 41001 Zagreb, Yugoslavia.

I n t r o d u c t i o n

Meteorological data files belonging to Zagreb-Grič Observatory have been in existance for 127 years and include 12-years of surface ozone data, measured at the end of the 19th century (1893-1900). Schoenbein's method with an 11-degree colorimetric scale was used and the measurements were taken twice a day.

Zagreb-Grič observatory ($45^0 49'$N, $15^0 59'$E, H_S=159 m NN) is situated in the centre of the city, on the edge of one of foothills of Medvednica, a mountain about 1000 m high, spreading N and NW from Zagreb. At the time when the ozone measurements were made, Zagreb had about 48 thousands inhabitants. There has been a decade of fast industrial growth, but the position of the meteorological observatory, situated on the Grič hill, was far enough from the industrial pollution and from any kind of intense traffic.

One of the aims of the data analysis disscussed here was to estimate the ozone concentration contained in the surface air layer over Zagreb before industrial development started, and to compare these results with those from the literature.

M e t h o d o f a n a l y s i s

The original data were primarily exposed to quality examination. In other words, Spearman's rank test and criteria following Helmert and Abbe were applied to check relative homogeneity accepting Vienna ozone data as standard. Moreover Landsberg and Jacobs criteria for the frequency distribution stability were used to check if the available lenghth of Zagreb data record were sufficient for statistical conclusions.

For conversion of the original data expressed in the Schoenbein 11-degree scale into absolute units, several different methods are known (Levy 1878, Linvill 1980, Lauscher 1983, 1984, 1988, Bojkov 1986, Volz and Kley 1988). These methods are linear over the whole Schoenbein scale or almost linear over the central part of the scale. But the calibration lines differ in slope towards the coordinate axes (Lisac and Grubišić 1990). Thus inspite of the fact that the relative variations of the data (for example the variatios of annual averages from year to year) do not depend on the conversion method used, the absolute values of the results may differ significantly. Therefore direct comparison of the results obtained by using different conversion methods, is not advisable.

The Zagreb data where converted into volume fractions (ppb) applying the regression equation according to R.Bojkov is:

$(O_3)/ppb = 3,4 + 4,6 * Sch$ where

$(O_3)/ppb$ is volume ozone fractions

Sch is the ozone value in the scale 0-10.

The equation calculates the volume fractions within 0-50 ppb range for the 11-degree Sch- scale. R.Bojkov derived the equation from the original Montouris regression equation (given by Levy) introducing a correction (farther in the text MRB) which makes the regression valid for 78% average relative humidity. He does not say how much the results may differ in cases when the relative humidity is not 78%. Therefore a comparison of results for different places with different relative humidity conditions may be problematic inspite of using the same calibration method, just because the relative humidity differences were neglected. The relative humidity lower then MRB considers it to be can make one to beleive that MRB supplies underestimated values obtained by the calibration procedure. This conclusion is derived from an early experience that at low humidity, the colour of a test paper is less intense, ispite of the possibility of a high ozone concentration in the air.

The average relative humidity in Zagreb was 72% during the time of ozone data sampling, what is 6% lower then MRB considers it to be. The average daily run of relative humidity during the same time interval gives the value of 78% for average night time (21-06h), 71% for the first part of a day (7-14h) and 68% for the entire day (7-20h) period. According to this, the day time Zagreb values might be underestimated, but it is hard to say how much.

Conclusions

The analysis of Zagreb surface ozone data, measured at the end of 19th century by Schoenbein's method and calibrating by MRB methode leads to the following conclusions :

1) The 12-year long data set (1893-1900) is sensitive to statistical quality tests (homogeneity and reliability of the set length). The first 4 year data set contains a large number of high scale values which decreases gradually during the initial period. The existence of such an the unexpectedly large number of high values in the very first data sample, together with its gradual decrease, is probably the result of improved measuring techniques. The first 4-year data set is therefoe excluded from the statistical parameters calculation. The deviation of the mean relative humidity in Zagreb from the reference value used in MRB (-6% in the annual mean, 0% during the night time and -20% during the day time) might make us to beleive that the day time values are underestimated particularly during the warm part of the year. The real amount of the underestimation level is not known.

2) Day and night data should be analysed separately, because of the different statistical character of daytime and night samples, as a result of the different nature of source and sink processes during the day and night (neglecting their influence on the measuring technique). In the course of a year, too, the processes manifest themselves differently in day and night samples, which is clearly reflected in the frequency distributions of the original data, compiled separately for every month.

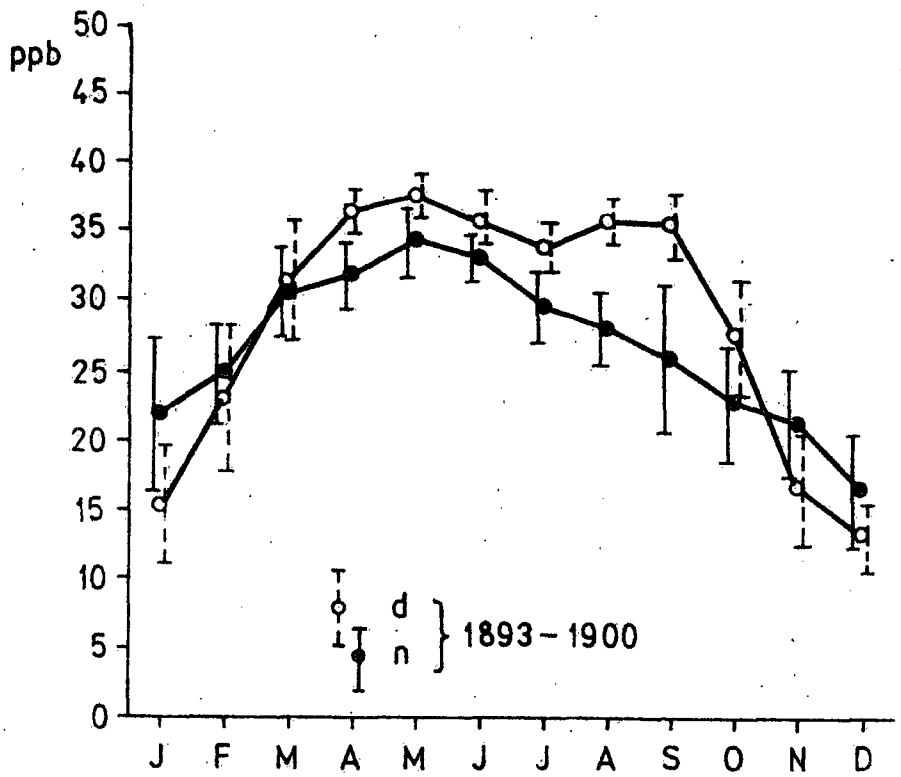

Fig.1. The annual run of volume ozone fractions (with standard deviation inside bars), Zagreb, 1893-1900.

3) The annual run of the daily data shows a primary maximum at the transition from spring to summer, and a secondary at the beginning of autumn. The annual run of night values is simpler and contains one maximum only, in the same part of the year as the primary maximum of daytime data. The midsummer decrease in the annual run of daily ozone data might be connected with destructive photochemical processes which become more intensive in rural areas, with increasing Sun height, and completely vanish during the night.

4) A comparison of Zagreb old ozone data averages (1893-1900, the time before intense industrial activity started) with present ozone measurements (1975) over the warm five- month period shows an increase of volume fraction from 36 to 67 ppb and from 30 to 56 ppb for day and night respectively. The result should be primarily treated as a fact, taking into account the reduced accuracy of absolute values as a result of the reduced precision of measuring techniques and dependence on the conversion method.

Acknowledgment

The research was partly supported by the Ruđer Bošković Institute, Zagreb, Croatia, Yugoslavia (whithin the EUROTRAC subproject "Ozone measurements during characteristic seasons and in selected sites of Yugoslavia") and partly by the Self-Manegement Community of Interest for Scientific Research (SIZ-Z), Zagreb, Croatia (subproject "Physical processes in the atmosphere and the sea").

L i t e r a t u r e

Bojkov R.D.(1986) Surface ozone during the second half of the ninetinth century, Jour.Climate and Appl.Meteorology, 25, 343-352.

Božićevic Z., V.Butković, T.Cvitaš, L.Klasinc (1978) Statistička obrada podataka fotokemijskog zagadjenja u Zagrebu, Kemija u industriji, 4, 177-181.

Božićevic Z., V.Butković, L.Klasinc (1978) Fotosmog u Zagrebu, Kemija u industriji, 6, 333-337.

Božićevic Z., L.Klasinc, T.Cvitaš, H.Guesten (1976), Photochemische Ozonbildung in der unteren Atmosphaere ueber den Stadt Zagreb, Staub- Reinhaltung der Luft, 36, Nr. 9, 363-394.

Cvitaš T., H.Guesten, L.Klasinc (1979) Statistical association of the photochemical ozone concentration in the lower atmosphere of Zagreb with meteorological variables, Staub- Reinhaltung der Luft, Nr.3, 92-95.

Lauscher F. (1983) Aus der Fruehzeit atmosphaerischen Ozonforschung, Wetter und Leben, 35, 69-80.

------- (1984) Ozon Beobachtungen in Wien von 1853-1981, Zusammenhaenge zwueschen Ozon und Wetterlagen, Arbeiten aus der Zentralanstalt fuer Meteorologie und Geodynamik, H 60, Publ. Nr 284,29.

------- (1988) Erkentnisse uber den Ozongehalt der Bodennahen Luft aus Messungen in Wien seit 1853, Arbeiten aus der Zentralanstalt fur Meteorologie und Geodynamik, H 70, Publ.Nr.290,10.

Levy,A.(1878) Analyse de l'air-Ozone, Annuaire de l'Observ. de Montsouris, 495- 4505.

Linvill,D.E., W.Y.Hooker, B.Olson (1980) Ozone in Michigan's environment 1876-1880, Monthly Weather Review, 108, 1883-1891.o

Lisac,I., V.Grubišić (1990) An analysis of surface ozone data measured at the end of the 19 century in Zagreb, in preparison for print in Atmospheric Environment Journal.

Singh,H.B., L.Ludwig, W.B.Johnson (1978) Tropospheric ozone concentrations and variabilities in clean remote atmospheres, Atmospheric Environment, 12, 2185-2196.

Volz,A., D.Kley (1988) Evaluation of the Montsouris series of ozone measurement made in the ninetinth century, Nature, Vol.332, 240-242.

Estimation of the snow cover in the Tatra Mountains and Podhale Region

Maria Klapowa

Institute of Meteorology and Water Management , Zakopane, Poland

In order to represent snow cover surface from point measurements several methods were in use. Relationship between distribution of the snow cover and different factors as topography, wind and others is widely recognized. But its estimation in the mountain area is very difficult. High irregularity of a snow cover surface occuring in mountain area is not sufficiently compensated by density of snow stations then research for an additional source of information on snow cover distribution is required.

The aim of this paper is to describe various methods of the estimation of snow pack parameters in the field.

At first basing on snow measurement at 250 pints in the Tatra Mountains lasting 10 years a map was prepared by the use of the very simple method of the isolines. This map shows a rough distribution of snow pack. But there can be distinguished two regions: the West and High Tatra Mountains where the snow cover is various decomposed. Its distribution is almost regularly in the West Tatra Mountain. While anomalies were found in the High Tatra Mountains. There are deflation and accumulation area in SW - NE zone according to the prevailing wind direction.

The analysis of the snow cover distribution on the profile from ridge to the feet of the Tatra Mountains have been done too. Accumulation of snow pack is higher about 30% at spring craters than at the ridge but there is lower by 16 - 19 % than on the forest border. In the forest snow cover is higher about 8 % and on the slope is about 28 % lower than in the river bed.

These results are not sufficient to estimate water storage in snow cover in the river basin.

For that reason a method of the deviation was applied to indicate water equivalent in snow cover. Strong relationship is between snow cover and altitude that can be called snow pack curve. Having this curve and a surface of the basin at the hypsometric zone we can calculate water storage in snow cover. On the base line relationship the regions of the Carpathian Mountains have been appointed. On either side of the regression line there can be found a field of points which was separated into 12 zones parallel to line regression. Width of the zone was defined by deviation which border values are + and - 0.5, + and - 1.0, + and - 1.5, + and - 2.0, + and - 2.5, + and - 3.0. These symbols were used to denote zones of similar snow cover depth in the Carpathian Mountains. But it was general view of the snow pack depth or water equivalent.

A statistical structure of the snow cover fields was also studied. The structure function was used which constitutes a mean square of the value difference for two successive points. According to Gandin the function is determined in the forms:

$$r_f(r_i, r_k) = [f(r_i) - f(r_k)]^2 \qquad (1)$$

where: r_i and r_k represent successive points (stations). From the definition of the structure function it follows: $r_f(r_i, r_k) > 0$. In this calculation there was found largely scatter of the points that indicated on the unhomogeneous field of the snow pack distribution.

Therefore a investigation enabling the estimation of snow pack parameters in field was continued by M. Klapowa and J. Parfiniewicz.

In this task the patrol records of the snow cover for 10 years were used in addition to data from standard stations. The area of upper river basin Dunajec confined with the profile Kowaniec was devided into 7 small or partial river basins and there was distinguished classes: nothern ones - covered with forests, southern ones - uncovered with forest. Method of field analysis through isotropic interpolation was applied, covering investigated area with the net of triangles, the peaks of which are the stations. Horizontal interpolation was supplemented with vertical interpolation the linear function of the height and the mean interpolation coefficients were calculated for each basin. The data for calculations were taken for several seasons from standard meteorological network and from field measurements. Statistical dependence on the elements f and altitude H from the interpolated values from the stations f and H and dependence on element deviations Δf and altitude deviations ΔH from the interpolated values from the station Δf and ΔH were calculated.

These relationships were expressed by the formula:

$$(f-\bar{f}) = r_{f,H}\frac{\sigma_f}{\sigma_H}(H-\bar{H}) \tag{2}$$

$$(\tilde{\Delta f}-\tilde{\bar{\Delta f}}) = r_{\tilde{\Delta f},\tilde{\Delta H}}\frac{\sigma_{\tilde{\Delta f}}}{\sigma_{\tilde{\Delta H}}}(\tilde{\Delta H}-\tilde{\bar{\Delta H}}) \tag{3}$$

where : $\tilde{\Delta f} = f-\tilde{f}$, $\tilde{\Delta H} = H-\tilde{H}$, symbol ~ indicates horizontal interpolation, σ_f = mean square element deviation f.

These procedures can give two possibilities:

a) The data from the stations can be conduced to any point of the elevation (vertical interpolation):

$$\hat{f}_H = f_i + r_{\Delta f,\Delta H}\frac{\sigma_{\Delta f}}{\sigma_{\Delta H}}(H-H_i-\overline{\Delta H}) + \overline{\Delta f} \tag{4}$$

where: for the i - standard station $\Delta f = f-f_i$, $\Delta H = H-H_i$, $\hat{f}_H$ value at any point of the elevation, f_i = measurement at the standard station. For the each stations the separated statistical research of the structure $(f_{pr} - f_i)$, $(H_{pr} - H_i)$, f_{pr}, H_{pr} of the measurement values at the point was carried out, using equation (4).

b) Horizontal interpolation of the value $\hat{f}_{iH}$ at any point of the basin can be done. The area of the small river basin was enclosed by the boundary of the "G". There were stable points: x_1, y_1, H_1; x_2, y_2, H_2; x_3, y_3, H_3 (coordinates and altitude) and data f_1, f_2, f_3 (snow pack depth or water storage). The value f_0 at any point having the coordinates and altitude x_0, y_0, H_0 is expressed by the function:

$$f_0 = L_1(f_1 f_2 f_3; x_0 y_0 H_0) \tag{5}$$

where L is linear transformation. Estimation of the average value f^G inside the "G" area is function f_1, f_2, f_3:

$$\hat{f}^G = L_2(f_1 f_2 f_3; G) \tag{6}$$

This function can be presented by formula:

$$\hat{f}^G = \frac{\iint_{xy\in G} f(x,y,H)\,dxdy}{\iint_{xy\in G} dxdy} = \frac{\iint_{xy\in G} L_1(f_1 f_2 f_3)\,dxdy}{S} = L_2(f_1 f_2 f_3) \tag{7}$$

where S = the river basin surface.

The method of the function L_1 and L_2 was worked out. Applying the equation 2 and 3 or 4 on the base f_1, f_2, f_3 for the river basin area f_0 can be presented by the formula:

$$f_0 = \tilde{f}_0 + A_{11}H_0 - A_{11}\tilde{H} + A_{12} \tag{8}$$

$$f_0 = A_{21}H + A_{22} \tag{9}$$

$$f_0 = \tilde{\hat{f}}_H = [\overline{f_i A_{31,i}(H-H_1)} + A_{32,i}] \tag{10}$$

where:

$$A_{11} = r_{\tilde{\Delta f},\tilde{\Delta H}}\frac{\sigma_{\tilde{\Delta f}}}{\sigma_{\tilde{\Delta H}}} \qquad A_{12} = \tilde{\bar{\Delta f}} - A_{11}\tilde{\bar{\Delta H}}$$

$$A_{21} = r_{f,H}\frac{\sigma_f}{\sigma_H} \qquad A_{22} = \bar{f} - A_{21}\bar{H}$$

$$A_{31,i} = r_{\Delta f \Delta H}\frac{\sigma_{\Delta f}}{\sigma_{\Delta H}} \qquad A_{32,i} = \overline{\Delta f} - A_{31,i}\Delta H$$

These equations and using ~ as a linear combination connected with x_0, y_0 and unconnected with H_0 (horizontal interpolation) can be described by forms:

$$f_0 = \sum_{i=1}^{3}\alpha_i f_i + A_{11}H_0 - A_{11}\sum_{i-1}^{3}\alpha_i H_i + A_{12} \tag{11}$$

$$f_0 = A_{21}H + A_{22} \tag{12}$$

$$f_0 = \sum_{i=1}^{3} \alpha_i [f_i + A_{31,i}(H_0 - H_i) + A_{32,i}] \tag{13}$$

where: α_i = weight of the horizontal interpolation for the i - station of the triangle. On the "G" area f_0 was integrated, for the formula (11):

$$\bar{f} = \iint_G f(x, yH)\, dxdy = \sum_{i=1}^{3} f_i \left[\iint_G \alpha_i (x, y)\, dxdy\right] + A_{11} \iint_G H(x, y)\, dxdy$$
$$- A_{11} \sum_{i=1}^{3} H_i \left[\iint_G \alpha_i (x, y)\, dxdy\right] + A_{12} dxdy \tag{14}$$

and for the form (12)

$$\bar{f} = A_{21} \iint H(x, y)\, dxdy + A_{22} \iint dxdy \tag{15}$$

and for the formula (13)

$$\bar{f} = \sum_{i=1}^{3} f_i \left[\iint_G \alpha_i (x, y)\, dxdy\right] + \sum_{i=1}^{3} A_{31,i} \left[\iint_G \alpha_1 (x, y) H(x, y)\, dxdy\right]$$
$$- \sum_{i=1}^{3} A_{31,i} H_i \left[\iint_G \alpha_i (x, y)\, dxdy\right] + \sum_{i=1}^{3} A_{32,i} \left[\iint_G \alpha_i (x, y)\, dxdy\right] \tag{16}$$

where $\bar{f}$ indicates integral magnitude f approximated by formula f_0 on the "G" area.
The following task was to calculate "the determined moments":

$$\iint \alpha_1 (x, y)\, dxdy \;,\; \iint \alpha_i (x, y)\, H(x, y)\, dxdy$$
$$\iint dxdy \;,\; \iint H(x, y)\, dxdy \tag{17}$$

On the base equations (14) and (15) values $\bar{f}$ were normalized on the area of the river basin:

$$\bar{f} = \sum_{i=1}^{3} f_i \frac{\iint \alpha_i (x, y)\, dxdy}{dxdy} + A_{11} \frac{\iint H(x, y)\, dxdy}{dxdy} - A_{11} \sum_{i=1}^{3} H_i \frac{\iint H(x, y)\, dxdy}{dxdy} + A_{12} \tag{18}$$

and

$$\bar{f} = A_{21} \frac{\iint H(x, y)\, dxdy}{\iint dxdy} + A_{22} \tag{19}$$

where $\bar{f}$ = average value of the snow cover parameter for this basin.
To calculate regression connections of the types (2-4) or moments (17) a procedure of the linear interpolation was used. The field $f(x,y)$ for the 3 stations was approximated through the surface:

$$f(x, y) = Ax + By + C \tag{20}$$

where:

$$A = [(f_1 - f_3)(y_2 - y_3) - (f_2 - f_3)(y_1 - y_3)] / W$$

$$B = -[(f_1 - f_3)(x_2 - x_3) - (f_2 - f_3)(x_1 - x_3)] / W$$

$$C = f_3 - Ax_3 - By_3$$

$$W = [(x_1 - x_3)(y_2 - y_3) - (x_2 - x_3)(y_1 - y_3)]$$

The interpolation procedure of the parameters x, y enables to calculated element $f(x,y)$ if there were data (x_1,y_1) (x_2,y_2) (x_3,y_3). To calculated moments $\iint \alpha_1 (x, y)\, dxdy$ it is necessary that to present value $f(x,y)$ as:

$$f(x, y) = \alpha_1 (x, y) f_1 + \alpha_2 (x, y) f_2 + \alpha_3 (x, y) f_3 \tag{21}$$

To obtain $\alpha_i (x, y)$ there was taken:

$$\alpha = [(y_2 - y_3)(x - x_3)] / W - [(x_2 - x_3)(y - y_3)] / W$$

$$\alpha = [(y_1 - y_3)(x - x_3)] / W - [(x_1 - x_3)(y - y_3)] / W$$

$$\alpha = [(y_1 - y_3) - (y_2 - y_3)(x - x_3)] / W + [(x_2 - x_3) - (x_1 - x_3)(y - y_3)] / W + 1$$

For the majority stations it is possible to applicated of the interpolation weights which sum is equal 1:

$$\sum_{i=1}^{N} \alpha_i \mu_{ij} = \mu_{i_0}\ ,\ j = 1 - N\ ,\ \sum_{i=1}^{N} \alpha_i = 1 \tag{22}$$

where μ_{ij} - are correlation coefficients for the homogeneous and isotropic field. It means that the geometrical scheme of the stations is in the relation to interpolation point.
Applying numerical integration the moments (17) can be expressed as double sums:

$$\sum_K \sum_L \alpha_i (x, y)\, DS_{KL}\ ,\ \sum_K \sum_L \alpha_i (x, y)\, H (x, y)\, DS_{KL}$$

$$\sum_K \sum_L H (x, y)\, DS_{KL}\ ,\ \sum_K \sum_L DS_{KL} \tag{23}$$

To estimate the surface there is required matrix $DS_{KL} = (dxdy)_{KL}$ where KL - integration net. On the base of the formula (22) there was calculated interpolation average weight, denoted as a influence of the i - standard station on the given point. Therefore the suitable markes were introduced:

$$\alpha_i = \frac{\iint \alpha_i (x, y)\, dxdy}{\iint dxdy} \tag{24}$$

To estimate average height of the given area was used form:

$$\overline{H} = \frac{\iint H (x, y)\, dxdy}{\iint dxdy}$$

and average surface:

$$\overline{DS} = \iint dxdy = \sum_x \sum_y DSxy \ \text{km}^2$$

By means of this model the estimation of the snow pack parameter in the upper river basin Dunajec was worked out (Tatra Mountains and Podhale Region). For the Podhale region the results are believed to be better than for the Tatra Mountains. This is because of the Tatra Mountains are distinguishable from whole Carpathian range owing to their altitude and relief. Well there snow cover variability can be largely noticed. As well as the stations are unequal decomposed in this field. While in the Podhale Region the stations create equal branch triangles in this model.
For all that calculations confirm this method is better than the ones hitherto applied.

Chairmen Reports

Berichte der Chairmen

Overview of Section 1
Observational Methods and Instrument Technology

S. Palmieri* and J. Joss**

*Dept. of Physics, Univ. of Rome,
**SMA, Osservatorio Ticinese, Locarno-Monti

Papers in this section dealt with the design and performance of both instruments and field programmes.

Results on the experience of designing and operating a network of automatic weather stations, specialized to forecast avalanches in Northern Italy, were presented by Cagnati and Luchetta (Centro Sperimentale di Arabba).

From a comparison of satellite data with ground truth Grassl and Jahnen concluded that the correction of the atmosphere's influence is a prerequisite for making full use of satellite data for remote sensing of the earth surface. With the help of the spectral properties of water, an individual atmospheric correction for every single scene is possible.

In an invited paper, Joss (Swiss Meteorological Institute) showed that good observations all year round and at a reasonable price can be made in Alpine terrain, but the instruments need to be designed and installed specifically for this particular application, taking into account effects caused by icing, lightning, wind and radiation. Also Joss and Pittini (Swiss Meteorological Institute) showed, based on the operational experience with the Swiss radars that precipitation can be reasonably estimated in an Alpine region, the main limitation originating from not "seeing" precipitation close to the ground.

Lamprecht and Merki (Paul Scherrer Institute, Villigen CH) showed results based on tracer experiments of TRANSALP in thermally induced up-valley winds in the prealpine valleys Blenio and Leventina. An astonishingly good agreement between measured and calculated ground level concentration was found.

The use of Doppler radar information for forecasting precipitation typical for an Alpine region, such as orographic rain, lee-phenomena, and local convection was illustrated by Land and Riedl (Deutscher Wetterdienst, Observatorium Hohenpeissenberg).

Mesinger (University of Belgrade) demonstrated convincingly that the "method of horizontal interpolation of the virtual temperature", for incorporation in the objective analyses scheme, is superior to the "standard method", using the surface temperature and an average gradient to reduce pressure to sea level.

As coordinator of POLLUMET, Neininger (LAPETH, Zurich) gave an overview on the program. Examples of NO_2 -measuring flights show pronounced mesoscale structures.

In a related study, Paffrath and Rösler (DLR Oberpfaffenhofen) discussed - and presented first results on - aircraft measurements to determine concentration distributions, transport, dispersion, origin, and transformation of pollutants to be investigated in POLLUMET, MEMOSA, and TRACT.

Direct measurements with SODAR of the exponent in the power law between windspeed and height were presented by Piringer (Zentralanstalt für Meteorologie, Wien); they show a surprisingly large dependence on the location and a larger range of variation than given in the literatur (e.g. Turner).

Scarchilli and Gorgucci (Istituto di Fisica dell' Atmosfera, Roma) discussed ways of correcting radar signal errors caused from propagation by estimating attenuation from measurments of the phase shift along the path.

In a similar vein Schmid et al. (LAPETH, Zürich) reported on the first tests with a new Doppler radar located at ETH. Encouraging results with respect to clutter suppression, detection of rotation features in severe storms, and wind profile measurements from clear air echoes were found.

T. Steiner (LAPETH, Zürich) presented results, and concluded that, the wind profiler used in his work is a suitable instrument for automatic and continuous observation of the wind field between 300 and 4500 m above ground.

Wege (Deutscher Wetterdienst, Observatorium Hohenpeissenberg) finds in the twenty year series an upward trend of the ozone concentration and a correlation with global radiation, vertical transport by convection, and a dependency on the wind direction.

Weihs (Universität für Bodenkultur, Wien) discussed results of two aerosol models as well as a comparison between Lowtran 6 and Lowtran 7 codes, the second one including effects of multiple scattering.

Overview of Section 2
Weather Prediction: Analysis and Forecasting of Synoptic and Mesoscale Systems

F. Mesinger* and G. Gensler**

*Institute of Meteorology , University of Belgrade,
**Zürich, Switzerland

This was one of the best supported Sections of the meeting, the topics of the papers spanning a wide spectrum of issues related to weather forecasting in mountainous regions.

The review paper in this section was given by J. Kuettner and it had the provocative title "What did we learn from ALPEX?" He considered three particular phenomena: - Lee cyclogenesis, flow splitting and upstream blocking and the Bora.
He noted that in all three cases the good results were due to:

(1) an excellent data set (one of the best)
(2) the stimulating effect of such an international program on the scientific community's interest in the field of mountain, meteorology and theory.

1. Lee cyclogenesis

The work of Pichler and Steinacker (Atlas of eight lee cyclogeneses during ALPEX IOP and analyses of 40 cyclones during the ALPEX year) is the most comprehensive analysis of lee cyclones so far. They distinguish two types: "Vorderseiten"- and "Überströmungs"-type.

One of the main results is the dynamic mechanism of lee cyclogenesis which is a coupling between an upper PV center that approaches the Alps and a lower one that forms on the lee side (Bleck, Tafferner, McGuinley). It is the same mechanism postulated by Hoskins et al. and is found also in explosive cyclogenesis events over the American east coast (Uccelini).

New theories have been developed (e.g. Speranza et al.; Pierrehumbert; Smith) based on linear, quasi-geostrophic, baroclinic flow. As Egger has shown, they cannot explain the dynamic mechanism, probably because of its non-linear character.

2. Flow splitting, upstreamblocking, mountain drag

Long range aircraft flights during ALPEX showed clear indications of steady state flow splitting in layers below 3 km with no flowsplitting above (decoupled flow patterns). The upstream distance of decelerated flow equals the Rossby radius of deformation, approximately (Pierrehumbert). Mountain drag of the Alps was found to be of the order of 5 to 10×10^{11} N by several authors (Hafner and Smith; Davies and Philipps; Carissimo et al.). In contrast to earlier suggestions, wave drag has been found to be a large portion of total mountain drag (Clark et al.).

3. Bora

The first 3 D analysis of the classical Bora was accomplished by ALPEX aircraft over the Adriatic coast of Yugoslavia. It shows hydraulic like flow (Smith) with severe turbulence in the hydraulic jump. Theoretical work (Klaus and Durran) suggests that there is no basic difference between the down slope winds of Foehn and Bora, despite of their temperature difference. Hydraulic theory using shallow water equations overestimates the wind velocity, as the effects of the upper stable layers, often containing breaking waves, are neglected. Bora research has stimulated world wide fundamental research in airflow over mountains.
Finally the role of the youngest generation participating in ALPEX was emphasized and the lesson learned from these types of cooperative, multinational field phases: Human relations are just as important as good science and technology.

Zhu Fukang and Li Shuhna of the Academy of Meteorological Science, Beijing, reported on their study of the energy budget over the Tibetan Plateau, based on the data of the Qinghai-Xizang Plateau Meteorological Experiment (QXPMEX) performed by China in May-August 1979. They have looked into the vertical profiles of total diabatic and latent heating, kinetic energy budget, and frequency and dynamics of "plateau lows", which

in summer appears to be a very frequent albeit shallow and short-lived phenomenon.

Their analysis reveals the dominance of sensible, in comparison to latent, heating in the lowest calculation layer over the plateau, while the opposite was true for the lowest layers of three neighboring regions Zhu and Li have considered. Latent heating however dominates in the upper troposphere over the plateau, as it does in two of the three neighboring regions.

Another Asian mountain wind system is the Altai-Sayan. It received attention in the paper by Lazic and Chen. Using the "eta" limited area model of the University of Belgrade and the U.S. National Meteorological Center they successfully simulated a case of the Altai-Sayan lee cyclogenesis. The simulations was more successful when the eta model was run in its normal eta coordinate mode, since then both the surface low as well as the mid-tropospheric cutoff were reproduced. The cutoff was not obtained when the model was run as a sigma system model, even though the model code and all its options other than the model coordinate, and the initial and boundary data were the same.

J. Rakovec and A. Poedos reported on their investigation on the meso-β and/or meso-γ structure of temperature field in complicated terrain. The results of the computations of autocovariance functions enable the use of optimum interpolation technique for the analysis, but some problems (inclusion of inversions and of the prevailing weather type) remain still unsolved.

The practical problem of calculating the lowering of cloud base due to orographic effects was considered by Krebs. A set of programmes have been developed that take into account some of the rain effects.

Binder presented the first results of a collaborative study between the German and Swiss weather services. A refined version of the DWD Europe model had been used with some notable success to examine the capability to predict rainfall in typical summer weather situation.

Geb provided a detailed synoptic-cum-mesoscale analysis of the frontal systems, air-masses and upper-level trough that together provided the ambient environment for the development of the destructive Munich Hail Storm (12.7.84). The combination of meso-scale internal forcing and orographic modification was shown to be a significant effect. In the subsequent discussion, attention was drawn to the feeding on of a rich moist airflow from the ITCZ directly to the Alpine region (8.7.84).

An overview of the eight ALPEX Lee-cyclogenesis events was given by Pichler. His presentation was based upon the comprehensive "ALPEX ATLAS" recently published by the University of Innsbruck. The various computed fields enable an interesting perspective to be obtained upon the various developments.

In a presentation on the use of satellite and NWP model output data to identify and diagnose synoptic and mesoscale systems Mahringer detailed some of the procedures that are employed by the weather service in Vienna.

Overview of Section 3
Diagnosis and Interpretation of Mesoscale Systems and Local Phenomena

Helmut Pichler * and Heinz Wanner**

*Institut für Meteorologie und Geophysik, Universität Innsbruck
**Geographisches Institut, Universität Bern

Die Abhandlungen unserer Sektion können drei Themenkreisen zugeordnet werden:

Bora

Die Untersuchungen der Bora wurden durch die aus den Flugexperimenten der ALPEX-SOP gewonnenen Daten gewaltig stimuliert. Die erste Phase der nachfolgenden Studien stand im Zeichen der Arbeiten um Ron Smith, welcher mit der Anwendung der hydraulischen Theorie die Grundlage zur theoretischen Erklärung des Phänomens Bora (vor allem im zweidimensionalen Fall) legte.

Die Präsentationen zur Bora wurden erfreulicherweise von der grossen Vertretung Jugoslawiens bestritten (Übersichtsreferat: V. Jurcec). Dabei zeigte sich eine ähnliche Entwicklung der Erkenntnisse wie seinerzeit beim Föhn: Nach den erheblichen Fortschritten bei der Erklärung der zweidimensionalen Struktur der Bora konzentrierten sich die Arbeiten dieses Mal auf dreidimensionale Analysen und stellten wie beim Föhn erhebliche regionale Differenzen fest (Abnahme von Andauer und Häufigkeit von Norden nach Süden).

Ein Hauptaugenmerk wurde auch auf die Modulation der Bora durch die real herrschende synoptische Wetterlage gerichtet. Dabei zeigte sich erneut, wie stark die Entstehung der Bora vom "Orographic Blocking" auf der Alpennordseite abhängt. Das Problem der Boraprognose kann jedoch noch nicht als gelöst betrachtet werden. Immerhin hat Z. Petkovsek die Temperaturdifferenz zwischen der advehierten Kaltluft und der warmen Luft über der Nordadria und die "Lapse Rate" innerhalb dieser warmen Luftmasse als Grundlagen für das Nowcasting der Bora-Windgeschwindigkeiten genannt.

Erfreulicherweise soll das jugoslawisch-amerikanische Boraprojekt durch Modellstudien (u.a. Anwendung des Mesingerschen "Step Mountain Model") und klimatologische Untersuchungen fortgesetzt werden. Eine ähnliche Wiedergeburt würde auch der Föhnforschung gut anstehen, welche an dieser Tagung bloss mit zwei Postern (C. Gandino, U. Zbigniew) vertreten war.

Temperature stratification and local airflow over complex terrain

Eine grössere Zahl von Postern und Vorträgen befasste sich mit den lokal- bis regionalskaligen Temperatur- und Stromfeldern. Die aus zahlreichen Feldexperimenten gewonnenen Daten lassen heute aufgrund ihrer feineren Auflösung auch über komplexer Topographie ein fundiertes Studium der Prozesse zu. Als wertvoll erwies sich dabei auch der Vergleich von Profilen aus dem Hügel- oder Gebirgsraum mit der freien Atmosphäre über einer Ebene (H. Richner, B. Neininger). Ein grosser Fortschritt ist im experimentellen Bereich zukünftig durch den Einsatz der Profilertechnik zu erwarten.

Die steigenden Computerkapazitäten erlauben heute die Entwicklung von "Limited Area Models" mit genügender raumzeitlicher Auflösung. Sowohl aus dem experimentellen Bereich als auch von der Modellseite her wurden schöne Beispiele zur dynamischen Erklärung von Lokalströmungen vorgelegt (A. Sturman, E. Mursch-Radlgruber, L. Gutmann, J. Roads). Zu erwähnen bleibt auch der fundierte Beitrag von S. Emeis zur Parametrisierung des "Pressure Drags".

Nicht zuletzt im Hinblick auf den Einsatz von Klimamodellen dürfte der Kopplung ökologischer Methoden mit experimentellen Messungen in Zukunft eine grössere Bedeutung zukommen (Beitrag G. Wooldridge).

Orographic influence on fronts and precipitation

Bis vor zirka 10 Jahren wurde das Phänomen der Front ausschliesslich auf dem synoptischen Scale betrachtet. Die dadurch bedingte Zweidimensionalität der Betrachtungsweise führte auch zu einer weitgehenden Übereinstimmung bezüglich der Frontendefinition. In diesem Skalenbereich sind die an einer Front (besser: Frontbereich) auftretenden Diskontinuitäten im Temperatur-, Wind- und Feuchtefeld untereinander nicht auflösbar. Mit dem Übergang zur mesoskaligen Frontenanalyse und insbesondere über komplexer Topographie, hat sich die Situation drastisch geändert. Anstelle einer einzigen Frontlinie sind verschiedene "Linien" analysierbar, die sich

auf die vorhin erwähnten Diskontinuitäten beziehen und untereinander auflösbar sind. Dazu kommt noch, dass das Frontenphänomen dreidimensional betrachtet werden muss. Dies ist nicht zuletzt auch deshalb notwendig, weil der Frontalbereich im Gebirgsraum kaum zusammenhängend ist und oft am Gebirge abreisst. R. Steinacker ist es gelungen, diese regionalen Strukturen objektiv (durch Verbesserung der bisherigen Methoden) zu analysieren und frontale Doppelstrukturen im Temperaturfeld herauszuarbeiten. Vielversprechende Resultate dürften in Zukunft auch aus der Verbindung theroretischer Arbeiten (z.B. von H.C. Davies) mit numerischen Simulationen (Beitrag A. Tafferner) und neuen Experimenten bzw. synoptischen Analysen (Beitrag M. Kurz) zu erwarten sein.

Im Hinblick auf die beschränkten Kenntnisse bezüglich der Auslösung orographischer Niederschläge ist der von M. Kerschbaum vorgeschlagene analytische Modellansatz zu begrüssen.

Es bleibt ein letzter Eindruck: Sowohl im experimentellen als auch im Modellbereich werden grosse Anstrengungen unternommen. Noch viel zu wenig wird jedoch eine Verbindung dieser beiden fundamentalen Arbeitsmethoden im Rahmen von Verifikations- bzw. Falsifikationsstudien angestrebt.

Overview of Section 4
Planetary Boundary Layer; Processes and Issues of Air Quality and Air Pollution

G. Wooldridge* and M. Roten**

*Rocky Mountain Forest and Experiment Station, Fort Collins USA
**Fac. des Sciences, Université de Fribourg

The introductory presentation focussed on gaseous pollutant behavior in the Northern Alps, i.e. on parametric representations, processes, distributions, and transport in mountainous terrain. The pertinent meteorological phenomena on the micro-, meso-, and macro-scales were identified as fronts, mountain-, plain regions, valley winds, blocking, stagnation, and dispersion. This discussion was complemented by a presentation describing trends of acid rain distribution with height and season in Italy - as they relate to meteorological situation and to trajectories near mountain slopes.

The development of the planetary boundary layer at a site next of the Continental Divide in Western Colorado, U.S.A., was shown to depend on the combinations of vertical fluxes of energy, on horizontal advection, and on subsidence. The analysis method used to demonstrate these processes increased our understanding of the contributions of their mechanisms to the vertical structure of the lower troposphere.

A spectrum of investigational techniques which are useful in predicting concentrations of pollutants in mountainous terrain was presented to the congress. They included several numerical models, a physical model, field investigations using surface instrumentation and soundings, a tracer study, and climatology. Each of them appears to have its special attributes. However, combinations which permit model verification and improvement prove to contribute most to the knowledge of circulation, transport, and dispersion which will lead to better predictions of surface concentrations, whether from persistent, long term releases or from sudden, catastrophic events.

The observational results indicate that we have more work ahead, using carefully designed experiments and models, to learn the important details of short- and long-range atmospheric transport. Trajectories respond to heating and cooling of mountain slope, valley channeling, and interaction with air flow at higher levels. These effects are not always properly predicted by numerical models.

Poster authors presented significant contributions in this section. Five posters placed their principal effort on interactions between meteorological parameters, turbulence, transport, and emissions of different pollutants in gaseous or solid form. Three working groups displayed the results of simulation models of atmospheric transport and diffusion and their possbile influences on the human milieu. Two groups presented themes particularly oriented towards meteorological problems by referencing field experiments to model results. The quality of the poster displays was generally good, making a valuable contribution to the avancement of atmospheric science.

Overview of Section 5
Surface Energy Exchanges related to Radiation and micro-physical Processes

A. Ohmura

Geographisches Institut, ETH Zürich

A distinctive feature of surface energy processes in mountainous regions is the spatial variation of the exchanges due to the altitudinal variations. These variations are manifested in the interaction of radiative processes with clouds, snow and ice, and they render montainous regions areas where the atmospheric heat budget plays a most significant role.

I. Dirmhirn gave a concise and apt review of historical development mainly in Switzerland and Austria, and examined the historical and present status of knowledge on radiation in the Alps. Consideration was given to the unresolved problems associated with 0_3, turbidity, and clouds. She saw a renewed necessity to improve the observing network of radiometry both in short- and longwave radiation because the satellite based estimations of surface radiation is incomplete. A continuing requirement in instrumental improvement of long-wave measurement and calibration requirements should be included. A new use of radiation is as a monitoring method of the changing environmental quality of the atmosphere (this is to be achieved mainly by high resolution spectral measurement).

Contributed papers that dealt with, and constitute significant advances to, our knowledge of energy exchanges were these of Mannstein and Haiden.
Mannstein presented a satellite-based method for the computation of sensible heat flux on mountain surface, which is increasingly important with increasing altitudes, making good use of the slope winds. Haiden's paper described models of cloud formation relating to the topography of the mountain and radiation. These two excellent works dealt with experimental and computational sectors.

Steady and concrete progress was reported by Blumthaler and Ambach. Their work is based on almost 10 years' hard won UV-data, and examines the altitude dependancy of the UV radiance in the Alps. Theoretical interpretation of this fact is still to be made, but this work is a very solid foundation.

Müller's paper on turbidity over the Alps is in harmony with the results that the turbidity during the last 80 years remained constant (Hoyt and Fröhlich, 1983) for Davos and by Rosen and Anglone (1984) for Table Mountain, Calif. and Mount Montezuma, Chile. Additional confirmation is always welcome.

A main outcome of section 5 was to note that in the field of radiation, there is a steady increase in high quality measurements. This is not the case in the non-radiative components, such as sensible and latent heat fluxes. There is also an increasing trend for model-oriented work. A most important modelling issue for the mesoscale and the Alps is the realistic formulation of the exchange coefficients. This aspect was not elaborated upon by the speakers in this section.

Despite the range of presentations, there remain several fundamental problems in the field of radiation and surface exchange, and the need for such projects as the Alpine-Traverse proposed as a part of the Swiss Climatic Programme is both evident and important.

Overview of the Section 6
Examination of short and longterm variations of climate and the climate elements
Untersuchung kurz- und langfristiger Änderungen des Klimas und der Klimaelemente

G. Fischer* and M. Schüepp**

*Universität Hamburg, Deutschland
**Wallisellen, Zürich

Dieser vielversprechenden Thematik waren nur acht Vorträge und sechs Poster gewidmet, was einer engen Auslegung durch das Programmkomitee zuzuschreiben ist, welches in dieser Sektion im wesentlichen nur Bearbeitungen langer Beobachtungsreihen im Alpinen Raum zuliess. Die Vortragenden verfolgten dabei allgemein die Zielsetzung, Anzeichen für Klimaänderungen zu finden. In dieser Hinsicht war der Befund von A. Bücher (J. Dessens) bemerkenswert, dass die mittlere Minimumtemperatur am Observatorium Midi-Pyrénées (2862 m Höhe) während des Zeitraums 1882-1970 um den Betrag von 0.82 Kelvin stetig zugenommen hat, während die Maximumtemperatur im wesentlichen konstant blieb. Aus einer ähnlichen, von A. Biancotti (L. Mercalli) durchgeführten, Analyse bezüglich der Station Gressoney-D'Ejola (1850 m Höhe) in Nordwest-Italien liess sich für die Periode 1927-89 ein solches Resultat jedoch nicht ablesen; in diesem Referat wurden auch die Niederschlagsverhältnisse an dieser Station behandelt. Eine umfangreiche und ausgefeilte Temperaturstatistik, beruhend auf Daten von 20 österreichischen Bergstationen seit 1850, wurde von R. Böhm vorgestellt; eine auf derselben Basis beruhende Niederschlagsstatistik hat I. Auer als Poster präsentiert. Temperaturreihen von vier bulgarischen Bergstationen wurden von A. Iotova (Ek. Koleva) für den Zeitraum 1930-88 unter besonderer Berücksichtigung der Variabilität diskutiert.

Als Poster haben I. Dagnino, G. Flocchini und G. Russo die Temperatur- und Niederschlagsbeobachtungen beschrieben, die seit 1830 von der Universität Genua durchgeführt werden, wobei auf die Besonderheiten der letzten Jahre (zu warm und zu trocken) hingewiesen wurde.

Die langjährigen Niederschläge an den Stationen Gr. St. Bernhard und Genf hat M. Schüepp untersucht, wobei die Homogenisierung der seit 1818 bzw. seit 1781 vorliegenden Messungen aufgrund wechselnder Aufstellung, Instrumentierung und personeller Besetzung im Vordergrund stand. Auf herausragende Ereignisse in den Niederschlagsverteilungen wurde aufmerksam gemacht.

Ueber die seit 1930 in der West-Schweiz aufgetretenen Trockenperioden referierte C. Aubert. Die Hagelniederschläge im serbischen Gebirge sowie im angrenzenden Flachland haben M. Curic (D. Janc) aufgrund der Daten von insgesamt 253 Schiessstationen während der Periode 1982-1988 und die Monate Mai-Oktober ausgewertet und die Resultate in einer ortsabhängigen Häufigkeitsstatistik dargestellt. Windbeobachtungen an der Radiosondenstation Payerne im Zeitraum 1981-1985 wurden von M. Furger herangezogen, um den Kanalisierungseffekt der Alpen unterhalb 500 hPa sichtbar zu machen.

In der Posterausstellung war ein recht umfänglicher klimatologischer Atlas der Schweiz, bearbeitet von W. Kirchhofer, zu sehen; weiter wurden dort Ozonmessungen in Zagreb von I. Lisac beschrieben. Auch theoretische Arbeiten fanden als Poster ihren Niederschlag; R. Sneyers, M. Vandiepenbeeck und R. Vanlierde stellten eine Normalkomponentenanalyse der Extremtemperaturen, gewonnen aus dem belgischen Beobachtungsnetz, vor, wobei es ihnen gelang, mit nur zwei Komponenten 99.9% der Varianz zu beschreiben. Baumringe hat P. Kahlig zu der Frage herangezogen, ob sich daraus Merkmale für ein chaotisches Verhalten des kurzfristigen Klimas ableiten lassen - das scheint jedoch nicht der Fall zu sein. Last not least behandelte ein Poster von M. Delmonte das mehr synoptische Thema, die Häufigkeit zyklonaler Wetterlagen über Nord-Italien.

Die Vorträge und Diskussionen in dieser Sektion haben die Notwendigkeit einer engeren Zusammenarbeit aller Alpenräume aufgezeigt, um das aktuelle Problem von anthropogen bedingten Klimaänderungen gegenüber der natürlichen Klimavariabilität mit mehr Aussicht auf Erfolg in Angriff nehmen zu können; ein intensiver Austausch von Daten und wissenschaftlichen Erkenntnissen, Vereinheitlichung von Auswertemethoden und finanzielle Förderung für die zügige Bearbeitung der vorliegenden Klimadaten erscheint wünschenswert.

Overview of Section 7
New Developments in the fields of Hydrometeorology, Snow- and Avalanche Research, Glaciology, and Biometeorology

H. Lang

Geographical Institute, ETH Zurich

General Comments

The topics in this section comprise several interdisciplinary fields. All of them have become quite important scientific and applied fields during the last decades, resulting at the same time in the establishment of their own scientific organisations and conferences. This may be at least one of the reasons why the representation of these fields within ITAM has obviously shown a decreasing trend.

On the other hand we have to be aware that in this conference many of the papers presented in the other sections were closely related to the topics of section 7, particularly to hydrometeorology (including hydrology). Two examples are "A parameterization of evaporation for use in land-surface atmosphere interaction modelling" by Mihailovic et al. in section 2 and " An analytical approach to orographic rain" by Kerschbaum in section 3. This underlines the fact that meteorology/climatology provides basic prerequisites to the science of the other fields like hydrology etc.

Overview	Presentations	
	Oral	Poster
Biometeorology	4	3
Hydrometeorology	5	4
Avalanche Research	-	1

Biometeorology

A very competent and up-to-date invited paper by Dr. Weihe provided an excellent outline on the aspects of human biometeorology in the Alps. A main point was that today the atmosphere is taken as part of the physical environment. The interest in the causal relationship between a single meteorological factor and its impact on the human body is fading. Complex ecological investigations deal now with the recent development of mass tourism, urbanization and affluent life styles. "The intense utilization of the European Alps is also of growing importance for the future anthropogenic modification of the regional Alpine climates".

The other papers of this subtopic dealt with classical questions like "Limits of cold stress in various climatic regions" by Zaninovic; here maritime, continental, and mountain conditions were compared, based on temperature, wind speed, and humidity as index of thermal comfort.

One paper by Pagliari dealt with the span of climate conditions for vineyards in Northern Italy; the influence of the hydrologic deficit on the qualitiy of vine is discussed particularly during the time when grapes are riping. It became obvious how difficult it is to describe climatic conditions on the basis of simple indices. Phenological topics were also discussed in a classical way.

Hydrometeorology

The papers under this subtopic dealt with the problems of precipitation in mountain regions which suffer to a great extent under serious difficulties of its measurement in high mountains.

The catastrophic flood events in Switzerland and Austria of the 1987 summer were the start for intensive studies on the depth-area-duration relationships and on the synoptic meteorological causes of high intensity precipitation, in particular rainfall; these studies are connected with statistical assessments. A much better understanding of the mechanisms and structure of extreme precipitation and flood events has now been achieved (Grebner and Richter). Another example of synoptic and mesoscale analysis of a heavy rainfall event in Yugoslavia was discussed by Capka. A descriptive slide report on 1987 floods was given by Schwarzl. Further papers were dedicated to average areal structures of mountain precipitation including vertical profiles and to the problem of estimating wind conditions during precipitation events as a parameter of the systematic error in precipitation measurement. Only one paper was presented which included all components of the hydrologi-

cal cycle and this was a study in the heavy glacierized Rhone basin (Bernath).

Snow and Avalanche Research

Lambert presented some results on risk cartography of avalanche phenomena which is very useful for planning purposes.

Final Comment

The papers as contributed to this section provided a valuable review of current research activities, some of them showing really very promising endeavours towards a better understanding of this corner of Alpine Climatology. Many people were missing and important subjects were not touched. One of the reasons being, without doubt, the inflation of meetings. The introduction of invited key speakers to this conference proved to be really successful and should be kept in mind for future ITAM's.

Scientific Programme / Vortragsprogramm

Programme Committee

Chairman: Prof. Huw C. Davies, ETH Zurich

Members: Dr. Jürg Joss, SMA, Locarno-Monti; Dr. Hans Richner, ETH Zurich; Prof. Herbert Lang, ETH Zurich; Prof. Michel Roten, University of Fribourg; Prof. Atsumu Ohmura, ETH Zurich; Prof. Heinz Wanner, University of Bern

Monday, September 17, 1990

0900 - 1000 **Official Opening of ITAM-90**
E. von Holzen, Mayor of Engelberg
Prof. G. O. P. Obasi, Secretary General, World Meteorological Organization
A. Höchli , Landesstatthalter, Kanton Obwalden
Dr. A. Junod, Director, Swiss Meteorological Institute
Dr. Th. Gutermann, Chairman Organizing Committee

Coffee Break

1030-1220 Davies Huw C. — Scientific Introduction

Section 1: Observational Methods and Instrument Technology

Chairmen: Sabino Palmieri, Jürg Joss

		Proceedings Volume	Page
Joss Jürg	Invited paper: The Challenge of Designing and Operating Ground Based Observational Instruments in Alpine Terrain	I	19
Cagnati Anselmo, Luchetta Alberto	Una rete di stazioni automatiche per la previsione delle valanghe	II	11
Mesinger Fedor	"Horizontal" Pressure Reduction to Sea Level	I	31
Wege Klaus, Vandersee Winfried	Ozonbeobachtungen am Nordrand der Alpen	I	36
Grassl Hartmut, Jahnen Waltraud	Correction of Atmospheric Masking as a Prerequisite of Ecological Mapping with Satellite Data	II	21

Lunch

Section 1 (Continued)

1345 - 1505 Paffrath Dieter, Rösler F. M.	Aircraft Measurements of Air Pollutants over the Alps	I	40
Neininger Bruno	POLLUMET (air-pollution and meteorology in Switzerland): Program and first results of the field-phase in summer 1990	I	44
Steiner Anton	Results from the Swiss Wind Profiler Experiment in 1989	I	45
Schmid Willi, Högl Donat, Syed N., Waldvogel Albert	A New Doppler Radar for Studies in Alpine Precipitation	I	49

Section 2: Weather Prediction: Analysis and Forecasting of Synoptic and Mesoscale Systems

Chairmen: Fedor Mesinger, Gian Gensler

1505 - 1535 Kuettner Joachim	Invited paper: What Did We Learn From ALPEX?	II	33

Coffee Break

1550 - 1730	Krebs Hans-Dietrich	Untergrenzen von Schichtwolken bei orographischer Hebung	I	80
	Rakovec Joze Poredos Ales	The Structure of Mesometeorological Fields in Mediterranean-Alpine Region	I	89
	Binder Peter Wacker Ulrike	Mesoscale Numerical Weather Prediction: Dependencies of Precipitation Simulations on Orography and Horizontal Resolution	I	115
	Geb Manfred	Unusual (sub-)Synoptic Features of the Weather Sequence July 11-13, 1984 (Munich Hailstorm)	I	124
1730 - 1900	**Poster Session 1**	Chairman: Huw C. Davies		
		Section 1:		
	Weihs Philipp	Verifizierung des Lowtran Codes durch Messungen	I	27
	Lehmann Martin	Measurements of Peroxides SO_2, NO_2 and O_3 with High Temporal Resolution at the Jungfraujoch		-
	Lang Peter Riedl Johann	Niederschlagsentwicklung über Süddeutschland anhand von Doppler-Radardaten	I	53
	Scarchilli Gianfranco Gorgucci Eugenio	A Correction Technique for C-Band Rainfall Rate Estimates by Means of Polarimetric Measurements	I	57
	Joss Jürg Pittini Araldo	Errors Involved in Using Radar Data to Estimate Precipitation in an Alpine Region	I	61
	Piringer Martin	Investigating atmospheric stability by Sodar	I	66
		Section 2:		
	Trüb Jürg	Orographic-Induced Flow Stagnation Viewed in an Isentropic Framework	I	76
	Sasaki Yoshi K. Zupanski Milija	Mechanism of Alpine Lee Cyclogenesis Revealed by Quasigeostrophic Variational Filter	I	85
	Ivancan-Picek Branka Tutis Vlasta	Investigations on the Mountain Drag of the Dinaric Alps from ALPEX Data	I	93
	Frei Christoph	On the North-South Asymmetry of the Alpine Diurnal Pressure Oscillation	I	98
	Ohmura Atsumu	On the Wind Profile over the Alps	I	102
	Böjti Béla Horváth Åkos	A Meso Scale Objective Analysis Procedure for Isallobars and Isobar Fields in the Stormwarning Service at Lake Balaton	I	106
	Frontero Paolo Lombroso Luca	Utilizzazione di alcune strutture dell' Osservatorio Geofisico dell' Università di Modena per previsioni meteorologiche locali	I	107
	Crespi M. Monai Marco	La previsione meteorologica per la montagna Veneta	I	111
	Lanzinger Andreas	Two case studies of Alpine lee cyclogenesis during ALPEX-SOP by numerical isentropic analysis	I	133
		Section 5:		
	Müller Walter	Radiation Extinction and Turbidity at Different Altitudes	I	295
	Siemer Andreas	The influence of liquid water transmission on the energy balance of a snow pack		-

Tuesday, September 18, 1990

Section 2 (Continued)

0830 - 0950	Pichler Helmut Lanzinger Andreas Steinacker Reinhold	On the Synoptics of Cyclogenesis during ALPEX-SOP	I	128
	Fukang Zhu Shuhua Li	The Relationship Between the Energy Budget over the Tibetan Plateau and the Plateau Low	I	129

	Mahringer Günter Zwatz-Meise Veronika	On the Analysis of Synoptic and Mesoscale Systems Using Satellite Images, Isentropic Analyses and Relative Flow Patterns	I	139
		Coffee Break		

Section 3: Diagnosis and Interpretation of Mesoscale Systems and Local Phenomena

Chairmen: Helmut Pichler
Heinz Wanner

1020 - 1110	Jurcec Vesna	Invited paper: The Current Status of Research on the Bora	I	144
	Bajic Alica	Application of Two-Layer Hydraulic Theory on the Severe Northern Adriatic Bora	I	148
1115 - 1245	**Poster Session 2**	Chairman: Thomas Gutermann		
		Section 3:		
	Vrhovec Tomaz	A Numerical Study of a Cold Air Lake Formation in an Alpine Basin	I	181
	Walker Andreas	Cold Airstream across the Brünig Pass (Central Switzerland)	I	186
	Richner Hans Berset Bernhard	The representativity of wind and temperature data from hilltops for the undisturbed atmosphere above an airport	I	187
	Neininger Bruno Gassner Martin	Comparison of inner-Alpine pTu-soundings at summer-nights with the soundings from Payerne and with ground stations (ANETZ)	I	192
	Gandino Claudio	The Decrease of the Vertical Thermal Gradient During the Foehn Winds at the Southern Foot of the Alps	I	199
	Ustrnul Zbigniew	Influence of Foehn Winds on Air Temperature and Humidity in the Polish Carpathians	I	202
	Fazlagic Slobodan Grubic Nebojsa	Investigation of Temperature Distribution in Sarajevo Valley		-
	Gelo Branko	Simulation of Orogenic Rainfall by a Mesoscale Model	I	216
	Malberg Horst	Orographic Effects on the Distribution of Precipitation in a Slightly Hilly Terrain	I	222
	Cantù Vittorio	Mario Bossolasco e i Congressi di Meteorologia alpina	I	236
		Section 4:		
	Eugster Werner Wanner Heinz Gälli Purghart Brigitte C.	Origin of Anthropogenic and Natural Trace Metals on Aerosol Particles Collected in the Bernese Prealps	I	243
	Schultz Eckhart Kamm M.	Grössendifferenzierende Partikeldepositionsmessungen an einem Bergstandort (Schauinsland) und in einer Grossstadt (Berlin)		-
	Flocchini Giuseppe Russo Giorgio	The SO_2 in the middle Polcevera Valley and the meteorological parameters	I	247
	Ruffieux Dominique King Clark W.	The Grand Mesa Experiment: The Study of Drainage Flow Structure and Evolution within an Inclined Basin	II	61
	Neu Urs	The calculation of back-trajectories with a mass-consistent diagnostic model over the Swiss Middleland	II	66
	Villone Barbara Anfossi Domenico Cassardo C.	Statistical study of the trajectories of air masses in Alpine area	II	70

	Palmieri Sabino Inghilesi Roberto	Acid Rain in Italy: Trends and Meteorological Aspects	I	241
	Mayr Georg McKee Thomas B.	Conserved Variable Analysis of PBL Evolution in the Colorado Rockies	I	253

Afternoon *Excursion to Mount Titlis*

Thursday, September 20, 1990

Section 4 (Continued)

0830 - 1010	Fallot Jean-Michel	Valley and mountain winds modelling in a prealpine complex topography: the Sarine valley in Gruyère	I	264
	Salerno Raffaele	Meteorological and Pollutant Dispersion Analysis about Experiments of Tracer Releases in South Alpine Valleys	I	270
	Gburcik Petar	Three-Dimensional Air-Stream above an Afforested Mountain in the Viciniti of a Strong Air-Pollution Source	I	275
	Werner Richard	Wetterlagen und Ozon eines alpinen Hangprofiles	I	279
	Seibert Peter Vergeiner Ignaz	Report on a Meteorological Study of the Potential Impact of Accidental Releases from the German Nuclear Reprocessing Plant Wackersdorf on Austria	I	283

Coffee Break

Section 5: Surface Energy Exchanges Related to Radiation and Microphysical Processes

Chairmen: Manfred Reinhardt
Atsumu Ohmura

1030 - 1220	Dirmhirn Inge	Invited paper: Roots and Present Problems of Alpine Radiation-Studies	I	290
	Blumthaler Mario Ambach W. Huber M.	Höheneffekt der solaren UV-Strahlung	I	291
	Mannstein Hermann	The Regional Variation of Sensible Heat Flux in the Alps Derived from AVHRR Data	I	298
	Haiden Thomas	An Analytical Model of Moisture Transport and Cumulus-Convection over Orography	I	305
	Song Zhengshan Ma Yimin Gao Dengyi	The Heat and Moisture Budgets over the Hengduan Mountains in China during the Summer of 1985	I	309

Lunch

Section 6: Examination of Short- and Longterm Variations of Climate and the Climatic Elements

Chairmen: Günter Fischer
Max Schüepp

1400 - 1600	Biancotti Augusto Mercalli Luca	Variazioni climatiche a breve termine (1927-89) a Gressoney (Italia Nord Occidentale), 1850 m slm	I	315
	Böhm Reinhard	Temperature Trends of High Altitude Stations in the Austrian Alps	I	322
	Furger Markus	Climatological Aspects of the Wind Fields over Payerne, Switzerland	I	330

	Schüepp Max	Die Niederschlagsmengen in den südwestlichen Walliseralpen im Verlauf der letzten 170 Jahre und ihre Abhängigkeit von den verschiedenen Witterungslagen	I	334
	Aubert Cyril	Périodes de sécheresse en Suisse Romande de 1931 à nos jours	I	337
	Bücher Alain Dessens J.	Un Siècle d'Observation de la Température en Altitude dans les Hautes-Pyrénées, France	I	342
		Coffee Break		
	Section 6 (Continued)			
1630 - 1710	Koleva Ek. Iotova Antoaneta	Air Temperature Variation in Upper Parts of Bulgarian Mountains	I	355
	Curic Mladjen Janc Dejan	Comparison between the areal characteristics of precipitation type from Cb in mountainous and flat land terrain	I	398
1710 - 1840	**Poster Session 3**	Chairman: Manfred Reinhardt		
		Section 6:		
	Dagnino Ignazio Flocchini Giuseppe Russo Giorgio	Sugli inverni eccezionalmente miti a Genova, Italia	I	318
	Auer Ingeborg	Zeitliche Variationen von Niederschlagssummen in alpinen Regionen Österreichs	II	84
	Kirchhofer Walter	Climatological Atlas of Switzerland	I	327
	Sneyers Raymond Vandiepenbeeck M. Vanlierde R.	Principal Component Analysis of Air Temperature in Belgium	I	351
	Lisac Inga	The Last Century Ozone Data Measured in Zagreb and some Analyses Problems	II	88
		Section 7:		
	Limanówka Danuta	Carpathian bioclimate for tourism and recreation	I	378
	Defila Claudio	Phänologische Beobachtungen in Engelberg, 1956-82	I	389
	Gao Dengyi	Influence of the dynamic and heating effects of mountains on the nature and mankind in China		
	Sevruk Boris Tettamanti R.	Estimation of wind speed during precipitation events	I	406
	Cebulak Elzbieta	Precipitation variability in the Polish Carpathians	I	410
	Capka Borivoj Gajic-Capka Marjana	Synoptic and Mesoscale Situation Causing Heavy Rainfall over Mount Medvednica on 3 to 4 July 1989	I	419
	Bernath Andre	Niederschlag, Verdunstung und Abfluss im Einzugsgebiet Gletsch	I	426
	Lambert Richard	Réflexion sur la représentation graphique des risques naturels prévisibles: Contribution à une nouvelle cartographie des avalanches	I	430

Friday, September 21, 1990

Section 6 (Continued)

0830 - 0920	Panel: Herbert Lang Max Schüepp Reinhold Steinacker	**Plenum Discussion:** **Key Questions in Alpine Climatology**	

Section 7: New Developments in the Fields of Hydrometeorology, Snow- and Avalanche Research, Glaciology, and Biometeorology

Chairmen: Dirmhirn Inge
Herbert Lang

0920 - 1010	Weihe Wolf H.	Invited paper: Aspects of Human Biometeorology in the Alps	I	363
	Zaninovic Ksenija	Limits of cold stress in various climatic regions	I	371
		Coffee Break		
	Section 7 (Continued)			
1040 - 1200	Pagliari Marcello	The Valleys of Vine: A Climatological Outline	I	385
	Grebner Dietmar Richter K. G.	Zum Aufbau einer Gebietsniederschlagsstatistik in der Schweiz	I	394
	Primault Bernard	Détermination du Début de la Période de Végétation par l'Evolution de la Température Comparée à Deux Phases Phénologiques	I	381
	Carniel Roberto Ceschia Mario Micheletti Stefano	Precipitation Distribution in Friuli-Venezia Giulia: Average Amounts and Cluster Analysis	I	402
		Lunch		
	Section 7 (Continued)			
1400 - 1500	Schwarzl Siegfried	Ursachen und Auswirkungen der Hochwasserkatastrophen in den Alpen (am Beispiel der Ereignisse 1987)	I	423
	Mihailescu Ion-Florin	Profils verticaux des précipitations atmosphériques dans la partie extérieure des Carpates orientales (Roumanie)	I	412
	Blumer Felix P. Spiess Roman	Investigations on the Altitudinal Dependence of Precipitation in the Swiss Alps	I	415
1500 - 1600	**Final Session and Official Closing of Conference**			

Contents Volume 1 / Inhaltsverzeichnis Band 1

List of Participants / Teilnehmerverzeichnis

Albisser	Peter		8044 Zürich
Anfossi	Domenico	Dr.	I-10133 Torino
Antor	Alfons	Dipl. Geologe	D-8080 Fürstenfeldbruck
Aubert	Cyril	Dipl. sc. nat.	1261 Borex
Auer	Ingeborg	Dr. phil.	A-1190 Wien
Bajic	Alica		YU-41000 Zagreb
Bauer	Helmut	Dr.	A-9010 Klagenfurt
Beck	Martin		8093 Zürich
Beniston	Martin	Dr.	3001 Bern
Bernath	Andre	Dr.	5600 Lenzburg
Berod	Dominique		1015 Lausanne
Biancotti	Augusto	Prof.	I-10125 Torino
Binder	Peter		8044 Zürich
Blumer	Felix P.		8057 Zürich
Blumthaler	Mario	Dr.	A-6020 Innsbruck
Böhm	Reinhard	Dr.	A-1190 Wien
Böttcher	Susanne		D-3016 Seelze 2
Bridge	G.		D-6100 Darmstadt
Britzkow	Klaus	Dipl. Met.	D-8959 Halblech
Brunner	Thomas		3012 Bern
Bücher	Alain		F-65200 Bagnères de Bigorre
Bumke	Karl		D-2300 Kiel 1
Burri	Klaus	Dipl. Geogr.	8702 Zollikon
Cagnati	Anselmo	Dr.	I-32020 Arabba (BL)
Cantù	Vittorio		I-00062 Bracciano - RM
Caparelli	Mario	Prof.	I-38040 Martignano (TN)
Capka	Borivoj		Yu-41000 Zagreb
Carboni	Gabriele		I-29100 Piacenza
Carniel	Roberto	Dr.	I-33100 Udine
Cartwright	Gordon D.		1202 Genève
Cavalli	Remo		6605 Locarno-Monti
Cebulak	Elzbieta	Dr.	PL-30215 Krakow
Ceschia	Mario	Prof.	I-33100 Udine
Courvoisier	Hans Wolfgang	Dr.	8044 Zürich
Curic	Mladjen	Prof.	YU-11000 Beograd
Damm	Albert	Oberbaurat	A-1014 Wien
Davies	Huw C.	Prof.	8093 Zürich
Davies	Rebecca		8914 Aeugst am Albis
Defila	Claudio		8044 Zürich
Dirmhirn	Inge	Prof.	A-1180 Wien
Dittmann	Ernst	Dr.	D-6050 Offenbach
Dreyer	Gudrun		D-8000 München 22
Drossmann	Thomas		D-2300 Kiel 1
Dünsing	Georg	Dr.	D-2000 Hamburg 36
Ehinger	Jaques		1817 Brent
Emeis	Stefan	Dr.	D-7500 Karlsruhe 1
Emery	Gaspard		8038 Zürich
Escher-Vetter	Heidi	Dr.	D-8000 München 2
Eugster	Werner		3012 Bern
Fallot	Jean Michel		1700 Fribourg
Fassbind	Stefan	Dipl. Geogr.	8057 Zürich
Fazlagic	Slobodan		YU-71000 Sarajewo
Filliger	Paul	Dr.	3003 Bern
Fischer	Günter	Prof.	D-2000 Hamburg 13
Flocchini	Giuseppe	Prof.	I-16135 Genova
Förster	Heidrun		3012 Bern
Frauchiger	H.		3007 Bern
Frei	Christoph		8093 Zürich
Frölich	Andreas		8093 Zürich
Frontero	Paolo		I-41100 Modena
Fukang	Zhu	Prof.	PRC-100081 Beijing
Furger	Markus	Dr.	5232 Villigen PSI

Gajic-Capka	Marjana		Yu-41000 Zagreb
Gandino	Claudio	Dr. Ing.	I-21020 Ispra (VA)
Gao	Dengyi	Prof.	PRC-100080 Beijing
Gasser	Oswald	Dr.	D-8946 Memmingerberg
Gburcik	Petar	Prof. Dr.	Yu-11000 Beograd
Geb	Manfred	Prof.	D-1000 Berlin 41
Gelo	Branko	Dr.	YU-41103 Zagreb
Gensler	Gian A.	Prof. Dr.	8053 Zürich
Ghelli	Anna		5232 Villigen
Gisler	Othmar	Dr.	8044 Zürich
Gorgucci	E.		I-00144 Roma
Grebner	Dietmar		8057 Zürich
Gremlich	Christina		8200 Schaffhausen
Grossklaus	Martin		D-2300 Kiel 1
Grubic	Nebojsa		YU-71000 Sarajewo
Gutermann	Thomas	Dr.	8044 Zürich
Gutman	Lev	Prof.	IL-84990 Sde-Boqer Campus
Haake	Borchert	Dipl. Met.	D-2800 Bremen 33
Häberli	Christian		5424 Unterehrendingen
Hächler	Patrick		8044 Zürich
Hager	Klaus		D-8902 Neusäss-Westheim
Haiden	Thomas	Dr.	A-1190 Wien
Haller	Guido		8044 Zürich
Hansen	Imke		D-2300 Kiel 1
Hantel	Michael	Prof.	A-1190 Wien
Harlfinger	Otmar	Dr.	A-1010 Wien
Holzner	Helga	Dipl. Met.	D-8000 München 2
Horvath	Akos		H-1525 Budapest
Ihly	Beat		3063 Ittigen
Iotova	Antoaneta		Sofia 1184
Ivancan-Picek	Branka		YU-41000 Zagreb
Jäger	Peter		8057 Zürich
Jahnen	Waltraud		D-2000 Hamburg 13
Jeannet	Pierre		1530 Payerne
Joss	Jürg	Dr.	6605 Locarno-Monti
Junod	Agnes		8044 Zürich
Junod	André	Dr.	8044 Zürich
Jurcec	Vesna	Dr.	YU-41000 Zagreb
Kähler	Claudia		D-2300 Kiel
Kaiser	August	Dr.	A-1190 Wien
Kaiser	Marion		D-7800 Freiburg
Kappenberger	Giovanni		6605 Locarno-Monti
Kerschbaum	Markus		A-1190 Wien
Kirchhofer	Walter	Dr.	8044 Zürich
Klante	Brigitte	Dipl. Met.	D-6500 Mainz
Krebs	Hans-Dietrich	Dipl. Met.	D-8080 Fürstenfeldbruck
Künzle	Thomas		3012 Bern
Kuettner	Joachim	Dr.	USA-Boulder, Colorado 80307
Kuhn	Walter	Prof.	8006 Zürich
Kunz	Arthur		8044 Zürich
Kurz	Manfred	Dipl. Met.	D-6050 Offenbach
Kusch	Wolfgang	Dipl. Met.	D-6050 Offenbach
Lambert	Richard	Dr.	F-74230 Thônes
Lang	Herbert	Prof.	8057 Zürich
Lang	Jürgen	Dip. Met.	D-6100 Darmstadt
Lanzinger	Andreas	Dr.	A-6020 Innsbruck
Lehmann	Martin		3012 Bern
Limanowka	Danuta	Dr.	PL-30215 Krakow
Lisac	Inga	Dr. Dipl. Ing.	YU-41103 Zagreb
Lombroso	Luca		I-41100 Modena
Luchetta	Alberto	Dr.	I-32020 Arabba BL
Lüthi	Daniel		8093 Zürich
Mahringer	Günter	Mag.	A-4063 Hörsching
Malberg	Horst	Prof.	D-1000 Berlin 41

Mannstein	Hermann	Dr.	D-8031 Wessling
Mast	Gebhard	Dipl. Met.	D-7024 Filderstadt
Maurer	Heinz		8044 Zürich
Mayr	Georg		USA-Fort Collins, CO 80523
Mercalli	Luca		I-10123 Torino
Merki	Gallus		5232 Villigen PSI
Mesinger	Fedor	Prof.	YU-11001 Belgrade
Micheletti	Stefano	Dr.	I-33100 Udine
Migliardi	Ernesto	Dr.	I-00143 Roma
Mihailescu	Ion-Florin	Dr.	R-8700 Constanta
Minetti	Giorgio		I-10134 Torino
Mitsumoto	Shigeki	Dr.	USA-Princeton
Monai	Marco	Dr.	I-35037 Teolo PD
Mong-Ming	Lu		5232 Villigen
Morgenthaler	Daniel		3013 Bern
Morscher	Peter		8044 Zürich
Mühlebach	Roland		8044 Zürich
Müller	Gerhard		8044 Zürich
Müller	Heinrich		8044 Zürich
Müller	Peter		8037 Zürich
Müller	Walter	Prof.	D-7000 Stuttgart 70
Mursch-Radlgruber	Erich	Dr.	A-1180 Wien
Neininger	Bruno	Dr.	8093 Zürich
Neu	Urs		3012 Bern
Obasi	G.O.P.	Prof.	1211 Geneva 20
Oeckel	Horst	Reg. Dir.	D-6000 Frankfurt 60
Oelke	Christoph	cand. rer. nat.	D-2300 Kiel
Ohmura	Atsumu	Prof.	8057 Zürich
Oswald	Paul	Dr.	8152 Opfikon
Paesler	Martin	Dipl. Met.	D-8900 Augsburg 21
Pätzold	Klaus	Dipl. Met.	D-6050 Offenbach
Paffrath	Dieter	Dr. rer. nat.	D-8031 Oberpfaffenhofen
Pagliari	Marcello	Ing.	I-00198 Roma
Palmeri	Fabio	Dr.	I-39100 Bolzano BZ
Palmieri	Sabino	Prof.	I-00144 Roma
Petkovsek	Zdravko	Prof.	YU-61111 Ljubljana p.p.64
Pfisterer	Wolfgang	Dipl. Met.	D-7000 Stuttgart 50
Pichler	Helmuth	Prof.	A-6020 Innsbruck
Pilger	Harald	Dr. phil.	A-8010 Graz
Piringer	Martin	Dr.	A-1190 Wien
Prenosil	Thomas	Dr.	D-5580 Traben-Trarbach
Primault	Bernard	Dr.	8053 Zürich
Pristov	Janko	Director	YU-61210 Ljubljana Sentuid
Ragette	Gerd	Dr.	A-1190 Wien
Rakovec	Joze	Prof.	YU-61111 Ljubljana
Ramseier	Bernhard		8093 Zürich
Rauh	Peter		8044 Zürich
Rebetez Beniston	Martine		1015 Lausanne
Reichmuth	Urs		8044 Zürich
Reinhardt	Manfred	Dr.	D-8031 Oberpfaffenhofen
Richner	Hans	Dr.	8093 Zürich
Riedl	Johann	Dipl. Ing.	D-8126 Hohenpeissenberg
Roads	John	Dr.	USA-La Jolla CA 92093
Rossetti	Roberto		I-27100 Pavia
Roten	Michel	Prof.	1700 Fribourg
Ruffieux	Dominique	Dr.	USA-Boulder CO 80303
Russo	Giorgio	Dr.	I-16132 Genova
Salerno	Raffaele	Dr.	I-20138 Milan
Sasaki	Yoshi		USA-Normann OK 73019
Scarchilli	Gianfranco		I-00144 Roma
Schacher	Felix		8044 Zürich
Schlegel	Max	Dipl. Met.	D-6050 Offenbach /M.
Schmid	Willi	Dr.	8093 Zürich
Schönemeyer	Thomas		D-8100 Garmisch-Partenkirchen

Schubert	Christina		D-2300 Kiel 1
Schubert	Klaus-Peter	Dipl. Met.	D-4300 Essen
Schubiger	Francis		8044 Zürich
Schüepp	Max	Prof.	8304 Wallisellen
Schuepbach	Evi		3012 Bern
Schultz	Eckhart		D-7800 Freiburg
Schwarzl	Siegfried	Prof.	A-1190 Wien
Schweizer	Jürg	Dr.	7260 Weissfluhjoch-Davos
Scioli	Piero	Dr. Ing.	I-21053 Castellanza VA
Sciortino	Domenico	Dr.	I-00144 Roma
Seibert	Peter	Dr.	A-1190 Wien
Sevruk	Boris	Dr.	8057 Zürich
Siemer	Andreas	Dipl. Met.	D-3000 Hannover 21
Simmen	Edith		8044 Zürich
Sneyers	Raymond	Dr. sc.	B-1180 Bruxelles
Song	Zhengshan	Prof.	PRC-Beijing Western suburb 100080
Spaar	Rosemarie		8044 Zürich
Spiess	Roman		8057 Zürich
Stankovic	Katarina		YU-41000 Zagreb
Steinacker	Reinhold	Dr.	A-6020 Innsbruck
Steiner	Anton		8093 Zürich
Stilke	Gerd	Prof.	D-2110 Buchholz
Strauss	Harald	Dipl. Met.	D-6972 Ramstein
Sturman	Andrew P.	Dr.	NZ-Christchurch 1
Suter	Hansruedi		6390 Engelberg
Tafferner	Arnold	Dr.	D-8000 München 2
Tercier	Philippe		1530 Payerne
Thiel	Dietmar	Dipl. Met.	DDR-1260 Strausberg
Thomas	Christian		D-2300 Kiel
Tognini	Evio		6605 Locarno-Monti
Trontelj	Miran	Dipl. Ing.	YU-61000 Ljubljana
Trüb	Jürg		8093 Zürich
Urbani	Stefano	Dr.	I-23032 Bormio SO
Ustrnul	Zbigniew	M. Sc.	PL-30215 Krakow
Valt	Mauro		I-32020 Arabba BL
Vergeiner	Ignaz	Doz. Dr.	A-6020 Innsbruck
Vissy	Karoly	Dep. Dir.	H-1016 Budapest
Vogt	Roland		4055 Basel
Volz	Richard	Dr.	3003 Bern
Vrhovec	Tomaz	Mag.	YU-61111 Ljubljana
Vucetic	Visnja		YU-41000 Zagreb
Wagner	Stephan		8092 Zürich
Walker	Andreas		8051 Zürich
Wanner	Heinz	Prof.	3012 Bern
Weber-Woywod	Marion	Dr.	8505 Pfyn
Wege	Klaus	Dr.	D-8126 Hohenpeissenberg
Weickmann	Ludwig	Dipl. Met.	D-8130 Starnberg
Weihe	Wolf	Dr.	8044 Zürich
Weihs	Philipp		A-1180 Wien
Weisel	Luzian	Dr.	D-7514 Eggenstein-Leopoldshafen 2
Werner	Richard	Dr.	A-6901 Bregenz
Wihl	Gunter	Dr.	A-1190 Wien
Wildberger	Liliane		8044 Zürich
Wooldridge	Gene	Prof.	USA-Fort Collins CO 80523
Wunderle	Stefan		D-7800 Freiburg
Zanella	Guglielmo	Prof.	I-43100 Parma
Zaninovic	Ksenija		YU-41000 Zagreb
Zanon	Giorgio		I-35123 Padova
Zupanski	Milija		Camp Springs, MD 20746
de Buman	Anne-Marie		1700 Fribourg
de Montmollin	Andre		8044 Zürich
de Morsier	Guy		8044 Zürich
x.Du	Xingyuan	Dr.	1211 Geneva 2

List of Authors / Autorenverzeichnis

Gälli Purghart	Brigitte C.			I	243
Gandino	Claudio	Dr. Ing., Centro di Ricerca Radioprotezione Via E. Fermi; I-21020 Ispra (VA)	Italia Tlx.380058EUR	I	199
		Tf.+39 332'789254 Tfx.+39 332789413			
Gao	Dengyi	Prof., Institute for Atmospheric Physics, Academia Sinica Zhong Guan Village; PRC-100080 Beijing Tel.202 5885	China Tlx.5000	I	309
Gassner	Martin			I	192
Gburcik	Petar	Prof. Dr., Institute of Sumarski fakultet u Beogadu Kneza Viseslava 1; Yu-11000 Beograd Tel.+38 149'893	Yugoslavia	I	275
Geb	Manfred	Prof., Freie Universität Berlin, Institut für Meteorologie Dietrich-Schäfer-Weg 6-10; D-1000 Berlin 41 Tel.+49 30 721'99'13 Tfx.+49 30 838'3844	BRD Tlx. 183'188	I	124
Gelo	Branko	Dr., Rep. Hydrometeor. Zavod SRH Gric 3; YU-41103 Zagreb Tel.+38 41'421'222 Tfx.+38 1138'412'787'03	Yugoslavia Tlx.21357 YU METEOR	I	216
Gensler	Gian A.	Prof. Dr. Zweiackerstrasse 38; 8053 Zürich Tel.01 53'31'41		Chairman II	99
Gorgucci	Eugenio	Istituto di Fisica dell'Atmosfera P. le Luigi Storzo 31; I-00144 Roma	Italia	I	57
Grassl	Hartmut			II	21
Grebner	Dietmar	Geographisches Institut ETH, Abteilung Hydrologie Winterthurerstrasse 190; 8057 Zürich Tel.01 257'52'33		I	394
Grubic	Nebojsa	Hydrometeorological Institute Hadzi Loje 8; YU-71000 Sarajewo Tel.+38 71 36-290, 214-766 Tfx.+38 71 217-148	Yugoslavia Tlx.41-516		-
Gutermann	Thomas	Dr., Schweizerische Meteorologische Anstalt Krähbühlstrasse 58; 8044 Zürich Tel.01'256'91'11 Tfx.01'256'92'78	Tlx.817373 METZH	Chairman II	4
Gutman	Lev N.	Prof., Ben Gurion University of the Negev IL-84990 Sde-Boqer Campus Tel.+39 436'79227 Tfx.+39 436'79319	Israel Tlx.PREVAL 440824	I	172
Haiden	Thomas	Dr., Institut für Meteorologie und Geophysik Hohe Warte 38; A-1190 Wien Tel.+43 1'364453'2910 Tfx.+43 512'507'2170	Österreich	I	305
Hammer	N.			I	367
Heitzmann	Peter	Dr. Landeshydrologie und Geologie; 3003 Bern		I	15
Högl	Donat			I	49
Holzner	Christoph			I	193
Horvath	Akos	Meteorological Service P.O.Box 38; H-1525 Budapest	Hungary	I	106
Huber	M.			I	291
Inghilesi	Roberto			I	241
Iotova	Antoaneta	Institute for Meteorology and Hydrology blvd "Lenin"66; Sofia 1184 Tel.72 22 71-262	Bulgaria	I	355
Ivancan-Picek	Branka	Hydrometeorological Institute of Croatia Gric 3; YU-41000 Zagreb Tel.+38 421'222 Tfx.+38 278'703	Yugoslavia Tlx.21356	I	93
Jahnen	Waltraud	Max-Planck-Institut für Meteorologie Bundesstrasse 55; D-2000 Hamburg 13 Tel.+49 40'411'73'205	BRD	II	21

Lazic	Lazar		I	134
Lehmann	Martin	Physikalisches Institut, Abt KUP, Universität Bern Sidlerstrasse 5; 3012 Bern Tel.031'65'85'29 Tfx.031'65'44'05		-
Limanowka	Danuta	Dr., Institute for Meteorology and Water Management ut. Borowego 14; PL-30215 Krakow Poland Tel.+ 22 60'33	I	378
Lisac	Inga	Dr. Dipl. Ing., Geofizicki Zavod SRH Gric 3; P.B. 3009; YU-41103 Zagreb Yugoslavia Tel.+41 420 222 Tlx.22575 GEOZAG-YU	II	88
Lombroso	Luca	Osservatorio Geofisico dell' Università Via Campi 213/a; I-41100 Modena Italia Tel.+39 59 370'703 Tfx.+39 59 373'180	I	107
Luchetta	Alberto	Dr., Centro Sperimentale Valanghe e Difesa Idrogeologica Via P.sso Campolongo 122; I-32020 Arabba BL Italia Tel. +39 436'79227 Tfx. +39 436'79319 Tlx. PREVAL 440824	II	11
Ma	Yimin		I	309
McGowan	Hamish A.		I	185
McKee	Thomas B.		I	253
Mahringer	Günter	Mag., Bundesamt für Zivilluftfahrt, Flugwetterdienst Linz A-4063 Hörsching Österreich Tel.+43 7221'72030 Tfx.+43 7221'73376	I	139
Malberg	Horst	Prof., Institut für Meteorologie, Uni Berlin Fachbereich Geowissenschaften WE 07 Dietrich-Schäferweg 6-10; D-1000 Berlin 41 BRD Tel.+49 30'83'85'825	I	222
Mannstein	Hermann	Dr., DLR, Institut für Physik der Atmosphäre D-8031 Wessling BRD Tel.+49 81'53'28503	I	298
Mayr	Georg	Department for Atmosperic Science, Colorado State University Foothills Campus; USA-Fort Collins, CO 80523 USA	I	253
Mercalli	Luca	Comitato Glaciologico Italiano Via Accademia delle Scienze 5; I-10123 Torino Italia Tfx.+39 11'836'485	I	315
Mesinger	Fedor	Prof., Institute for Meteorology, University of Belgrade Dobracina 16; YU-11001 Belgrade Yugoslavia Tel.+38 11'625'981 Tfx.+38 11'632'133	Chairman I II	31 99
Micheletti	Stefano	Dr., Istituto di Fisica dell'Università di Udine e Regionale dell'Agriculture Via Larga 36; I-33100 Udine Italia Tel.+39 432'504'832 Tfx.+39 432'50'6392	I	402
Mihailescu	Ion-Florin	Dr., The Research Station "Dobrudja" Bl.S 6, Sc.C, Apt 59, Et.4 Bdul. Al.Lapusneanu 183; R-8700 Constanta Romania Tel.916'55'260	I	412
Mihailovic	Dragutin T.		I	302
Monai	Marco	Dr., Centro Sperimentale per l'Idrologia e la Meteorologia v. Euganea 19; I-35037 Teolo PD Italia	I	111
Müller	Walter	Prof. Dr., Inst. 320, Universität Hohenheim D-7000 Stuttgart 70 BRD Tel.+49 711'459'2836 Tfx.+49 711'459'2785 Tlx.	I	295
Mursch-Radlgruber	Erich	Dr., Institut für Meteorologie, Klimatologie und Grundlagen der Physik Türkenschanzstrasse 18; A-1180 Wien Österreich Tel.+43 222 315'499/18 Tfx.+43 222 315'499/12	I I	177 260
Musselman	R.		I	173
Nebojsa	Grubic		I	346
Neininger	Bruno	Dr., Laboratorium für Atmosphärenphysik ETH-Hönggerberg; 8093 Zürich Tel.01 377'27'45 Tfx.01 371'18'64 Tlx. 823 480 EHEBCH	I I	44 192
Neu	Urs	Geographisches Institut der Universität Bern Hallerstrasse 12; 3012 Bern	I II	259 66

Nikolic	Ivan			I 120
Obasi	Godwin O.P.	Prof., Secretary-General P.O. Box 5; 1211 Geneva 20 Tel.022'7308'200 Tfx.022'734'23'76 Tlx.23260 OMMCH		II 7
Obrebska-Starkel	Barbara			I 375
Ohmura	Atsumu	Prof., Geographisches Institut der ETH-Irchel Winterthurerstrasse 190; 8057 Zürich Tel.01'257'52'20 Tfx.01'362'51'97 Tlx.815813AGGECH		Chairman I 102 II 104
Paffrath	Dieter	Dr.rer.nat., DLR, Institut für Physik der Atmosphäre Münchnerstrasse; D-8031 Oberpfaffenhofen BRD Tel. +49 8153 28'511 Tfx. +49 8153 28'243		I 40
Pagliari	Marcello	Ing., ENEL-DSR Via G.B. Martini 3; I-00198 Roma Italia Tel.+39 8509'8509 Tfx.+39 8509'2560		I 385
Palmieri	Sabino	Prof., Università "La Sapienza", Dipartimento di Fisica Roma via Quasimodo 65; I-0014 4 Roma Italia Tel.+39 650'02316		Chairman I 241 II 98
Perels	R.			I 260
Petkovsek	Zdravko	Prof. Dr., Dept. for Physics, Faculty of Sciences FNT Jadranska 19; YU-61111 Ljubljana p.p.64 Yugoslavia Tel.+38 61'332'611		I 156
Pichler	Helmuth	Prof., Inst. f. Meteorologie und Geophysik, Universität Innsbruck Innrain 52; A-6020 Innsbruck Österreich Tel.+43 512-507/2175 od.2171 Tfx.+43 512-507/2170		Chairman I 128 II 101
Piringer	Martin	Dr., Zentralanstalt für Meteorologie und Geodynamik Hohe Warte 38; A-1190 Wien Österreich Tel.+43 364'453'2405 Tfx.+43 369'12'33 Tlx.131837 a metw a		I 66
Pittini	Araldo			I 61
Poredos	Ales			I 89
Primault	Bernard	Dr. Witikonerstrasse 440; 8053 Zürich Tel. 01/53'45'59		I 381
Ragette	Gerd	Dr., Zentralanstalt für Meteorologie und Geodynamik Hohe Warte 38; A-1190 Wien Österreich Tel.+43 36'4455-2310		I 215 II 52
Rajkovic	B.			I 302
Rakovec	Joze	Prof. Dr., Univ. Ljubljana, Dept. Physics, Chair Meteorology Jadranska 19; P.O.B. 64; YU-61111 Ljubljana Yugoslavia Tel.+38 61'332'611 Tfx.+38 61'224'312 Tlx.31620 METLJ YU		I 89
Reinhardt	Manfred	Dr., Institut für Physik der Atmosphäre, DLR Post Wessling/Obb.; D-8031 Oberpfaffenhofen BRD Tel.+49 8153'28507 Tfx.+49 8153'28'243 Tlx.526 419 dvlop d		Chairman
Richner	Hans	Dr., Laboratorium für Atmosphärenphysik ETH-Hönggerberg; 8093 Zürich Tel.01'377'27'59 Tfx.01'371'18'64		I 187
Richter	K. G.			I 394
Riedl	Johann	Dipl. Ing., Deutscher Wetterdienst, Meteorologisches Observatorium Albin-Schwaigerweg 10; D-8126 Hohenpeissenberg BRD		I 53
Roads	John O.	Dr., Climate Research A-024, Scripps Inst.of Oceanography University of CA 92093; USA-La Jolla CA 92093 USA Tel.619'534'2099 Tfx.619'534'8561		I 197
Rösler	F. M.			I 40
Roten	Michel	Prof. Dr., Université de Fribourg, Fac. des Sciences 1700 Fribourg Tel. 027/25'32'64		Chairman II 103
Rudel	E.			I 367
Ruffieux	Dominique	Dr., CIRES-NOAA Broadway 325; Boulder CO 80303 USA Tel.303 497 5240 Tfx.303 497 6978		I 258 II 61

Russo	Giorgio	Dr., Università di Genova		I 247
		Via Benedetto XV, 5; I-16132 Genova	Italia	I 318
		Tel.010/353'80'82 Tfx.010/35'21'69	Tlx.271114 UNIVGE I	
Salerno	Raffaele	Dr., A.R.S. S.p.A.(ENI Group)		I 270
		Via Medici del Vascello 26; I-20138 Milan	Italia	
		Tel.+39 2'520'254'51 Tfx.+39 2'520254'23		
Sasaki	Yoshi	University of Oklahoma, School of Meteorology		I 85
		200 Felgar-Street; USA-Normann OK 73019	USA	
Scarchilli	Gianfranco	Istituto di Fisica dell'Atmosfera		I 57
		P. le Luigi Sturzo 31; I-00144 Roma	Italia	
Schmid	Willi	Dr., Laboratorium für Atmosphärenphysik		I 49
		ETH-Hönggerberg HPP; 8093 Zürich		
		Tel.01'377'36'25 Tfx.01'371'18'64		
Schüepp	Max	Prof.		Chairman
		Bürglistrasse 16; 8304 Wallisellen		I 334
		Tel.01'830'36'81		II 105
Schultz	Eckhart	Deutscher Wetterdienst; Zentrale Medizinmeteorologische Forschungsstelle		-
		Stefan Meier Str. 4; D-7800 Freiburg	BRD	
		Tel.+49 761 28'202 50		
Schwarzl	Siegfried	Prof. Dr., OMG-IFHP-FgW		I 423
		Krottenbachstrasse 29/5; A-1190 Wien	Österreich	
Seibert	Peter	Dr., Institut für Meteorologie und Geophysik		I 283
		Hohe Warte 38; A-1190 Wien	Österreich	
		Tel.+43 222'364'453'2410Tfx.+43 369'1233	Tlx. 131837 metur a	
Sevruk	Boris	Dr., Geographisches Institut ETH, Abteilung Hydrologie		I 406
		Winterthurerstrasse 190; 8057 Zürich		
		Tel.01'257'52'35 Tfx.01'362'51'97		
Shuhua	Li			I 129
Siemer	Andreas	Dipl. Met., Institut für Meteorologie und Klimatologie der Uni Hannover		-
		Herrenhäuserstrasse 2; D-3000 Hannover 21	BRD	
		Tel.+49 511'762'4416		
Slobodan	Fazlagic			I 346
Sneyers	Raymond	Dr. sc., Institut Royal Météorologique		I 351
		Av. Circulaire 3; B-1180 Bruxelles	Belgique	
		Tf.+32 2373'0622 Tfx.+32 2375'1259		
Song	Zhengshan	Prof., Institute for Atmospheric Physics, Academia Sinica		I 309
		Zhong Guan Cun; P.O.B. 2718; PRC-Beijing Western suburb 100080 China		
Spiess	Roman	Geographisches Institut ETH, Abteilung Hydrologie		I 415
		Winterthurerstrasse 190; 8057 Zürich		
		Tel.01 257'52'09 Tfx.01 362 51 97		
Stankovic	Katarina	Hydrometeorological Institute of Croatia		I 160
		Gric 3; YU-41000 Zagreb	Yugoslavia	
		Tel.+38 42'12'22 Tfx.+38 421'78'03	Tlx.21356 YU METEOR	
Steinacker	Reinhold	Dr., Institut für Meteorologie und Geophysik		I 128
		Innrain 52; A-6020 Innsbruck	Österreich	II 47
		Tel.+43 512'507'2171		
Steiner	Anton	Laboratorium für Atmosphärenphysik		I 45
		ETH-Hönggerberg HPP; 8093 Zürich		
		Tel.01'377'27'45 Tfx.01'371'18'64	Tlx. 823 480 EHEBCH	
Sturman	Andrew P.	Dr., Univ. of Canterbury, Dept. Geography		I 185
		NZ-Christchurch 1	New Zealand	
Syed	N.			I 49
Tafferner	Arnold	Dr., Institut für Theoretische Meteorologie		I 209
		Theresienstrasse 37; D-8000 München 2	BRD	
		Tel.+49 89-2394'4637		
Tercier	Philippe	Institut suisse de météorologie		I 274
		Station aérologique; 1530 Payerne		II 72
		Tel. 037/62'61'11 Tfx.037/61'11'94	Tlx.942'116	

Veröffentlichungen der Schweizerischen Meteorologischen Zentralanstalt
Publications de l'Institut Suisse de Météorologie Pubblicazioni della Centrale Meteorologica Svizzera

Nr. 1a Uttinger H., Die Niederschlagsstunden in Zürich.
22 Seiten, 1962

Nr. 1b Ambrosetti Fl., Die Niederschlagsstunden in Locarno-Monti.
12 Seiten, 1965

Nr. 2 Thams J.C., unter Mitarbeit von A. Aufdermaur, P. Schmid und E. Zenone.
Die Ergebnisse des Grossversuches III zur Bekämpfung des Hagels im Tessin in den Jahren 1957–1963.
32 Seiten, 1966 (vergriffen)

Nr. 3 Grütter M., Die bemerkenswertesten Niederschläge der Jahre 1948–1964 in der Schweiz.
20 Seiten, 1966

Nr. 4 Schram K. und Thams J.C., [Redaktion], 9. Internationale Tagung für Alpine Meteorologie in Brig und Zermatt, 14.–17. September 1966.
366 Seiten, 1967

Nr. 5 Ambrosetti Fl. und Thams J.C., Die direkte Sonnenstrahlung auf die Flächen eines nach Süden orientierten Würfels ohne Grundfläche in Locarno-Monti.
16 Seiten, 1967

Nr. 6 Schram K. und Thams J.C., Der Tagesgang der Abkühlungs- und Aufwärmungsgrösse in Locarno-Monti.
20 Seiten, 1968 (vergriffen)

Nr. 7 Ambrosetti Fl., Schram K. und Thams J.C., Die Intensität der direkten Sonnenstrahlung in verschiedenen Spektralbereichen in Locarno-Monti.
13 Seiten, 1968 (vergriffen)

Nr. 8 Uttinger H., Die Zahl der Tage mit Windspitzen von mindestens 20 Metern pro Sekunde in Zürich (1934–1967).
22 Seiten, 1968

Nr. 9 Mäder F., Untersuchung über die Windverhältnisse in Bodennähe bei verschiedenen Wetterlagen.
42 Seiten, 1968

Nr. 10 Schram K., Die Windverhältnisse in der bodennahen Luftschicht an einem Hang von etwa 25 Grad Neigung.
13 Seiten, 1968 (vergriffen)

Nr. 11 Schüepp M., Kalender der Wetter- und Witterungslagen von 1955 bis 1967.
44 Seiten, 1968 (vergriffen)

Nr. 12 Ackermann P., Die neue Radiosondenstation Payerne der Schweizerischen Meteorologischen Zentralanstalt.
36 Seiten, 1968 (vergriffen)

Nr. 13 Junod A., Contribution à la méthodologie granulométrique des aérosols amicroscopiques.
70 Seiten, 1969

Nr. 14 Joss J., Schram K., Thams J.C., Waldvogel A., Untersuchungen zur quantitativen Bestimmung von Niederschlagsmengen mittels Radar.
37 Seiten, 1969 (vergriffen)

Nr. 15 Courvoisier H.W., Die quantitative Niederschlagsprognose winterlicher zyklonaler Witterungslagen auf der Alpennordseite der Schweiz.
15 Seiten, 1970 (vergriffen)

Nr. 16 Schram Karin und Thams J.C., Die kurzwellige Globalstrahlung und die diffuse Himmelsstrahlung auf dem Flugplatz Zürich-Kloten.
18 Seiten, 1970

Nr. 17 Kasser P., Schram Karin und Thams J.C., Die Strahlungsverhältnisse im Gebiet der Baye de Montreux.
46 Seiten, 1970

Nr. 18 Gutermann Th., Vergleichende Untersuchungen zur Föhnhäufigkeit im Rheintal zwischen Chur und Bodensee.
68 Seiten, 1970

Nr. 19 Ginsburg Theo, Die statistische Auswertung von langjährigen Temperaturreihen.
42 Seiten, 1970

Nr. 20 Primault B., Du risque de gel et de sa prévision.
20 Seiten, 1971

Nr. 21 Piaget A., Utilisation de l'ozone atmosphérique comme traceur des échanges entre la troposphère et la stratosphère.
72 Seiten, 1971

Nr. 22 Zenone E., Die Gewitterverhältnisse in den südlichen Zentralalpen und Voralpen.
24 Seiten, 1971

Nr. 23 Kirchhofer W., Abgrenzung von Wetterlagen im zentralen Alpenraum.
72 Seiten, 1971

Nr. 24 Primault B., Le climat, élément du plan d'aménagement.
Das Klima, eine der Grundlagen der Landesplanung.
The climate as an element of the land management.
28 Seiten und eine Karte, 1971

Nr. 25 Fröhlich C. und Wierzejewski, Die verschiedenen Messverfahren zur Bestimmung der Strahlungsintensität mit dem Kompensationspyheliometer und die Entwicklung eines verbesserten Modells.
36 Seiten, 1972

Nr. 26 Bouët M., Le foehn du Valais.
12 Seiten, 1972

Nr. 27 Zenone E., Die Gewitterverhältnisse in den südlichen Zentralalpen und Voralpen
32 Seiten, 1972

Nr. 28 Catzeflis J., Primault B., Strehler H., Analyse de la pluviosité dans le Valais central.
15 Seiten, 1972

Nr. 29 Courvoisier H.W., Die Niederschlagswirksamkeit markanter, hochreichender Kaltlufteinbrüche im Sommer in der Schweiz.
11 Seiten, 1973

Nr. 30 Sevruk B., Erfahrungen mit Totalisatoren mit schiefen, geneigten und bodenebenen Auffangflächen im Einzugsgebiet der Baye de Montreux.
Einfluss der Temperatur auf die Messung des Niederschlages mit Totalisator.
44 Seiten, 1973

Nr. 31 Strehler H., Beziehung zwischen Witterung und Zuckerrübenmerkmalen im Spätsommer.
20 Seiten, 1975

Nr. 32 Courvoisier H.W., Katalog objektiv-statistischer Wetterprognosen für die Alpensüdseite und das Oberengadin.
24 Seiten, 1975

Nr. 33 Primault B., Essais d'évaluation climatologique du risque de gel.
28 Seiten, 1975

Nr. 34	Kirchhofer W.,	Stationsbezogene Wetterlagenklassifikation 50 Seiten, 1976
Nr. 35	Piaget A.,	L'évolution orageuse au nord des Alpes et la tornade du Jura vaudois du 26 août 1971 114 Seiten, 1976
Nr. 36	Bouët M.,	Contribution à l'étude de la variation diurne de pression en Suisse romande 23 Seiten, 1976
Nr. 37	Zenone E.,	Die Gewitterverhältnisse in den südlichen Zentralalpen und Voralpen 60 Seiten, 1976
Nr. 38	Primault B., Quiby J.,	Diagrammes psychrométriques différenciés en altitude 36 Seiten, 1977
Nr. 39	Courvoisier H.W.,	Katalog objektiv-statistischer Wetterprognosen für die Alpennordseite, das Wallis sowie Nord- und Mittelbünden 58 Seiten, 1978
Nr. 40	Gutermann Th., Mäder F. (Redaktion)	15. Internationale Tagung für alpine Meteorologie, Grindelwald 19.–23. September 1978, 332 Seiten, 1978 Tagungsbericht 1. Teil
Nr. 41	Gutermann Th., Mäder F. (Redaktion)	15. Internationale Tagung für alpine Meteorologie, Grindelwald 19.–23. September 1978, 1979 Tagungsbericht 2. Teil
Nr. 42	Courvoisier H.W.,	Starkniederschläge in der Schweiz in Abhängigkeit vom Druck-, Temperatur- und Feuchtefeld 59 Seiten, 1981
Nr. 43	Urfer Charlotte,	Mittlere Temperatur- und Windverteilung im Dischmatal bei Davos bei typischen sommerlichen Witterungslagen 32 Seiten, 1981
Nr. 44	J.-D. Altherr, M. Dupanloup, Y. Ganter, E. Junet,	Prévision objective des hauteurs de précipitations et de l'ensoleillement relatif au moyen de l'analyse discriminante 43 Seiten, 1982
Nr. 45	Courvoisier H. W.,	Abgeschlossene Höhentiefs und ihre Wetter- auswirkungen in der Schweiz 44 Seiten, 1984
Nr. 46	Perret R.,	Une classification des situations météorologiques à l'usage de la prévision 127 Seiten, 1987
Nr. 47	Courvoisier H.W.	Regionale Wetterauswirkung und Prognose von Staulagen in der Schweiz 22 Seiten, 1988
Nr. 48	Gutermann Th., Mäder F. (Redaktion)	21. Internationale Tagung für alpine Meteorologie, Engelberg 17.–21. September 1990, 437 Seiten 1990 Tagungsbericht 1. Teil
Nr. 49	Gutermann Th., Mäder F. (Redaktion)	21. Internationale Tagung für alpine Meteorologie, Engelberg 17.–21. September 1990, 135 Seiten, 1991 Tagungsbericht 2. Teil